Novel Nitric Oxide (NO)-Releasing Polymers and Their Biomedical Applications

by

Elizabeth J. Brisbois

A dissertation submitted in partial fulfillment
of the requirements for the degree of
Doctor of Philosophy
(Chemistry)
in the University of Michigan
2014

Doctoral Committee:

Professor Mark E. Meyerhoff, Chair
Professor Kristina Håkansson
Associate Professor Nicolai Lehnert
Professor Steven P. Schwendeman

2014

DEDICATION

This work is dedicated to my family.

Thank you for all your love and support!

ACKNOWLEDGEMENTS

During my graduate studies and research I have worked with a fabulous group of people that helped me make this dissertation work such a success. First, I would like to thank Dr. Mark Meyerhoff for being such a wonderful mentor and giving me the opportunity to work in his lab for my graduate studies. Over the past 5 years I have learned so much under his guidance; and I especially appreciate his continuous encouragement, insightful ideas, and excitement about science that helped keep me motivated throughout my graduate studies.

I would also like to thank the professors who served on my dissertation committee: Dr. Kristina Håkansson, Dr. Nicolai Lehnert, and Dr. Steven Schwendeman. I really have appreciated all of their helpful suggestions and recommendations on my various research projects, and especially the valuable time that each of them gave to be on my committee.

My research projects have been highly collaborative in nature, so I must give special thanks to all those worked with me to show the potential biomedical applications of these new materials. Many thanks to Dr. Robert Bartlett and his research team for providing their invaluable expertise and facilities (in the Extracorporeal Membrane Oxygenation (ECMO) lab at the University of Michigan Medical School) for the blood compatibility experiments. I am especially grateful to Dr. Hitesh Handa and Terry Major, who have given me so much valuable insight regarding polymer coatings development, blood-material interactions, and the rabbit model used for many of the experiments reported in this thesis. I also appreciate the assistance from Dr. Ryan Davis and Anna Jones who provided their superb surgical skills and care for the sheep during catheter testing. The collaboration with Dr. Stewart Wang and Jill Bayliss also provided

a great opportunity to test my new NO release materials in the mouse wound healing model. I would also like to thank Dr. Chuanwu Xi and Dr. Jianfeng Wu, from the School of Public Health, for their help and teaching me the basics of antimicrobial studies. The opportunity to work with these interdisciplinary teams has been one of the most valuable aspects of my graduate studies and truly helped make many of the projects described in this thesis so successful.

I would also like to extend thanks to all the past and present members in the Meyerhoff group for their helpful suggestions and support throughout my time as a graduate student: Anant Balijepalli, Andrea Bell, Dr. Wenyi Cai, Kyoung Ha Cha, Alessandro Colletta, Dr. Natalie Crist, Dr. Kebede Gemene, Dr. Lajos Höfler, Dr. Grace (Chuncui) Huang, Dr. Gary Jensen, Alex Ketchum, Dr. Dipankar Koley, Dr. Gergely Lautner, Dr. Kun Liu, Dr. Bo Peng, Hang Ren, Dr. Xuewei Wang, Yaqi Wo, Alex Wolf, Dr. Qinyi Yan, Dr. Jun Yang, Si Yang, Zheng Zheng, and Dr. Laura Zimmerman. It has been a pleasure working with this great group of people. It has also been a wonderful experience working with Yaqi Wo on new directions for the SNAP projects, as well as mentoring undergraduate researchers Jessica Brownstein, Tim Sippell, and Beth (McDonagh) Yuill on their various projects.

I also owe thanks to Drs. John and Kristy Jurchen who really started me on my path as a chemist. They have been some of the most enthusiastic teachers I have had and gave me a great chemistry foundation, instilled in me a passion for chemistry, and encouraged me to pursue a PhD.

Lastly, I would like to thank my family and friends, especially my parents, grandparents, my sister, and Aunt Janet, for all of their love, support, and encouragement during my graduate studies. I love you all and feel so blessed to always know that you are here for me. You all have been just a phone call away, providing ears to listen and an incredible support when I needed it. Thank you!

TABLE OF CONTENTS

LIST OF FIGURES

LIST OF TABLES

LIST OF ABBREVIATIONS

A. baumannii	*Acinetobacter baumannii*
A-V	Arteriovenous
Alb	Albumin
Amb	Ambient Light
BB	Bromothymol Blue
BG	Bromocresol Green
Cys	Cysteine
CysNO	*S*-nitrosocysteine
DBHD/N_2O_2	Diazeniumdiolated Dibuytylhexanediamine
DBHD	*N,N'*-Dibutyl-1,6-Hexanediamine
DMAc	*N,N*-Dimethylacetamide
DMHD/N_2O_2	Diazeniumdiolated *N,N'*-Dimethyl-1,6-Hexanediamine
DOS	Dioctyl Sebacate
EC	Endothelial Cells
ECC	Extracorporeal Circulation
ECLS	Extracorporeal Life Support
EDTA	Ethylenediaminetetraacetic Acid
EO	Ethylene Oxide
GPx	Glutathione Peroxidase
GSH	Glutathione
GSNO	*S*-Nitrosoglutathione
ICU	Intensive Care Unit
LB	Luria Bertani

LPEI/N_2O_2	Diazeniumdiolated Linear Polyethylenimine
MDI	Methylene Diphenyl Isocyanate
NAP	*N*-Acetyl-DL-Penicillamine
NO	Nitric Oxide
NOA	Nitric Oxide Analyzer
NOgen	NO-generating
NONOate	Diazeniumdiolate
NOrel	NO-releasing
NOS	Nitric Oxide Synthase
O^{2-}	Superoxide
$ONOO^-$	Peroxynitrite
PBS	Phosphate Buffered Saline
PDMS	Poly(dimethylsiloxane)
PEG	Poly(ethylene glycol)
PLGA	Poly(lactic-*co*-glycolic acid)
PPP	Platelet-Poor Plasma
PRP	Platelet-Rich Plasma
PVA	Poly(vinyl alcohol)
PVC	Poly(vinyl chloride)
RH	Relative Humidity
RSNO	*S*-nitrosothiol
RSSR	Disulfide
SeCA	Selenocystamine
SeDPA	3,3'-Diselenidedipropionic Acid
SNAC	*S*-nitroso-*N*-acetyl-*L*-cysteine
SNAP	*S*-Nitroso-*N*-acetylpenicillamine
SR	Silicone Rubber
TGF-β	Transforming Growth Factor Beta
THF	Tetrahydrofuran
vWF	von Willebrand Factor

ABSTRACT

Novel Nitric Oxide (NO)-Releasing Polymers and their Biomedical Applications

by

Elizabeth J. Brisbois

Chair: Mark E. Meyerhoff

Two common factors that can cause complications with indwelling biomedical devices are thrombus and infection. Nitric oxide (NO) is known to be a potent inhibitor of platelet activation and adhesion. Healthy endothelial cells exhibit a NO flux into the bloodstream of $0.5\sim4\times10^{-10}$ mol cm^{-2} min^{-1}. In addition, NO that is released within the sinus cavities and by neutrophils/macrophages functions as a potent natural antimicrobial agent. Therefore, polymer materials that release NO are expected to have similar anti-thrombotic and antimicrobial properties.

In this dissertation work, two novel approaches to achieving long-term NO release from polymers were studied and evaluated for their potential biomedical applications. In the first approach, *S*-nitroso-*N*-acetypenicillamine (SNAP)-doped polymers were studied for potential hemocompatibility. The SNAP-doped Elast-eon E2As (block copolymer of poly(dimethylsiloxane) and polyurethane) creates an inexpensive polymer that can locally deliver physiologically relevant levels of NO (via thermal and photochemical

reactions). SNAP was also found to be surprisingly stable in the E2As polymer during shelf-life stability and ethylene oxide sterilization studies. The SNAP/E2As polymer was coated on the inner walls of extracorporeal circulation (ECC) circuits and was found to preserve the platelet count at ~100% of baseline and reduce thrombus area after 4 h blood flow in a rabbit model. The SNAP/E2As polymer was also used to fabricate NO-releasing catheters that were implanted in sheep veins for 7 d. The SNAP/E2As catheters significantly reduced the amount of thrombus and bacterial adhesion (in comparison to E2As control catheters).

In the second approach, the NO release from diazeniumdiolated dibutylhexanediamine (DBHD/N_2O_2)-doped polymers was significantly improved using various poly(lactic-*co*-glycolic acid) (PLGA) additives. Using acid-capped PLGA additives was found to cause high initial bursts of NO, while using an ester-capped PLGA additive extended the NO release for up to 14 d. The pH changes corresponding to the NO release profiles from these films was visualized by doping films with pH indicator dyes. Poly(vinyl chloride)- and Elast-eon E2As were used as the base polymers for combined DBHD/N_2O_2 and PLGA coatings on the inner walls of ECC circuits. After 4 h of blood flow in a rabbit model, the E2As-based NOrel circuits preserved platelets at a higher level than PVC-based NOrel circuits (97% and 80% of baseline, respectively). This demonstrates that the inherent hemocompatibility properties of the base polymer can also influence the efficiency of the NO release coatings. A DBHD/N_2O_2-doped SG-80A polymer material was also studied and used to fabricate patches that were applied to scald burn wounds infected with *Acinetobacter baumannii*. The NO released from these patches applied to the wounds is shown to significantly reduce the *A. baumannii* infection after 24 h (~4 log reduction).

The results for both of types of NO-releasing polymers studied here demonstrated greatly enhanced biocompatibility properties, in terms of reducing thrombus and infection. These materials have the potential for improving the hemocompatibility of a wide variety of blood-contacting medical devices.

CHAPTER 1

Introduction: Recent Advances in Hemocompatible Polymers for Biomedical Applications

1.1 Introduction

1.1.1 Hemocompatibility of Common Blood-Contacting Devices

Blood-material interaction is critical to the success of implantable medical devices, including simple catheters, stents and grafts, insulation materials for electrical leads of pacemakers and defibrillators, and complex extracorporeal artificial organs, which are used in thousands of patients every day.[1] Polymers, including polyurethanes, silicone rubber, and poly(vinyl chloride), are used extensively in the healthcare industry to fabricate such biomedical devices. Among other complications, thrombosis is one of the primary problems associated with clinical application of blood-contacting materials, which can cause serious complications in patients and ultimately failure of the device's functionality.[2] Thrombus formation can lead to significant consequences such as complete obstruction of blood vessels in which stents are placed,[3] occlusion of catheters[4] and small diameter vascular grafts,[1] errant results from implantable chemical sensors,[1] embolic complications with artificial hearts,[5] and extensive blood damage and platelet consumption during extracorporeal membrane oxygenation.[5] Such complications can result in significantly increased medical costs, extended hospitalization, amputation, or increased morbidity. Despite a thorough understanding of the mechanisms of blood-surface interactions and decades of bioengineering research effort, the ideal non-thrombogenic prosthetic surface remains unidentified.[5]

Over the last 50 years, much has been learned about foreign surface-induced thrombosis and the attempt to prevent it with systemic anticoagulation and surface modifications. In a clinical setting, many of these devices require the use of systemic anticoagulation (e.g., heparin) to avoid device failure.[6] The long-term use of anticoagulants can also have adverse effects, including hemorrhage and thrombocytopenia.[7] Despite these complications, heparin is still used as the standard anticoagulation therapy for patients on extracorporeal circulation (ECC), but the use of heparin does not prevent platelet activation and consumption.

In this chapter, a review of some of the current and most promising strategies that have been used over the years to develop polymeric materials with improved hemocompatibility will be discussed, including highly hydrophilic or hydrophobic surfaces, albumin coated surfaces, zwitterionic polymers, attached endothelial cells, patterned surfaces, immobilized heparin, and nitric oxide (NO) release/generating surfaces. Some of the important techniques employed (using *in vitro* and *in vivo* models) to assess the hemocompatibility of any new material, including the measurement of platelet preservation, platelet and protein adhesion, the effect of flow rates on thrombosis, and the ultimate surface clot area, will also be reviewed.

1.1.2 Blood and the Coagulation Cascade

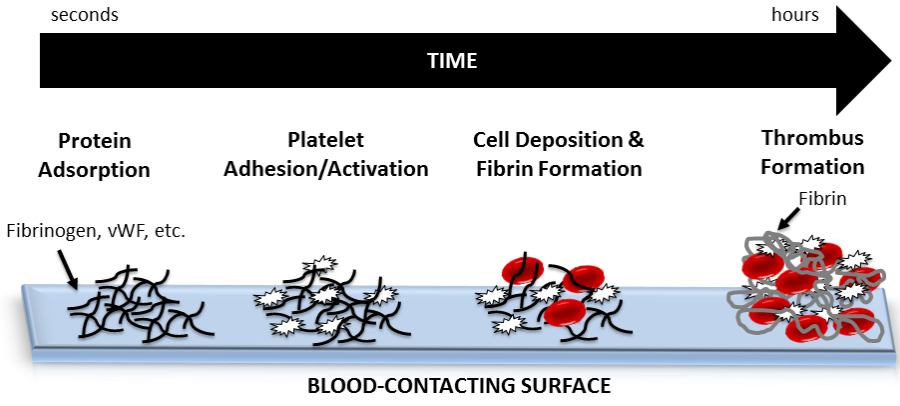

Figure 1.1. Sequence of events leading to thrombus formation on blood-contacting surfaces (e.g., implanted medical devices).

Biomaterial related thrombosis is a complex process, where the initial biological response when blood comes in contact with a foreign surface is protein adsorption, which

is followed by platelet adhesion and activation, leading to thrombus formation (**Figure 1.1).**[8] Plasma proteins adsorb onto the surface of the implanted device (e.g., fibrinogen, fibronectin, von Willebrand factor (vWF), etc.) within seconds. These proteins further interact with receptors on the plasma membranes of platelets and facilitate platelet adhesion on the surface.[9] Upon contact with the foreign surface and platelet activation, a conformational change occurs leading to the exposure of the glycoprotein GPIIb/IIIa receptor that binds platelets to fibrinogen.[3] Platelet activation also leads to conformation changes and the excretion of intracellular granulates containing agents (e.g., coagulation Factors V and VIII, adhesion molecules P-selectin and vWF, calcium ions, etc.) that further induce activation and aggregation of more platelets. This also activates the coagulation cascade, where a series of self-amplifying reactions triggered through surface contact (intrinsic pathway) or tissue factors (extrinsic pathway) ultimately converge at the final common pathway to form a thrombus (**Figure 1.2)**. Throughout the coagulation

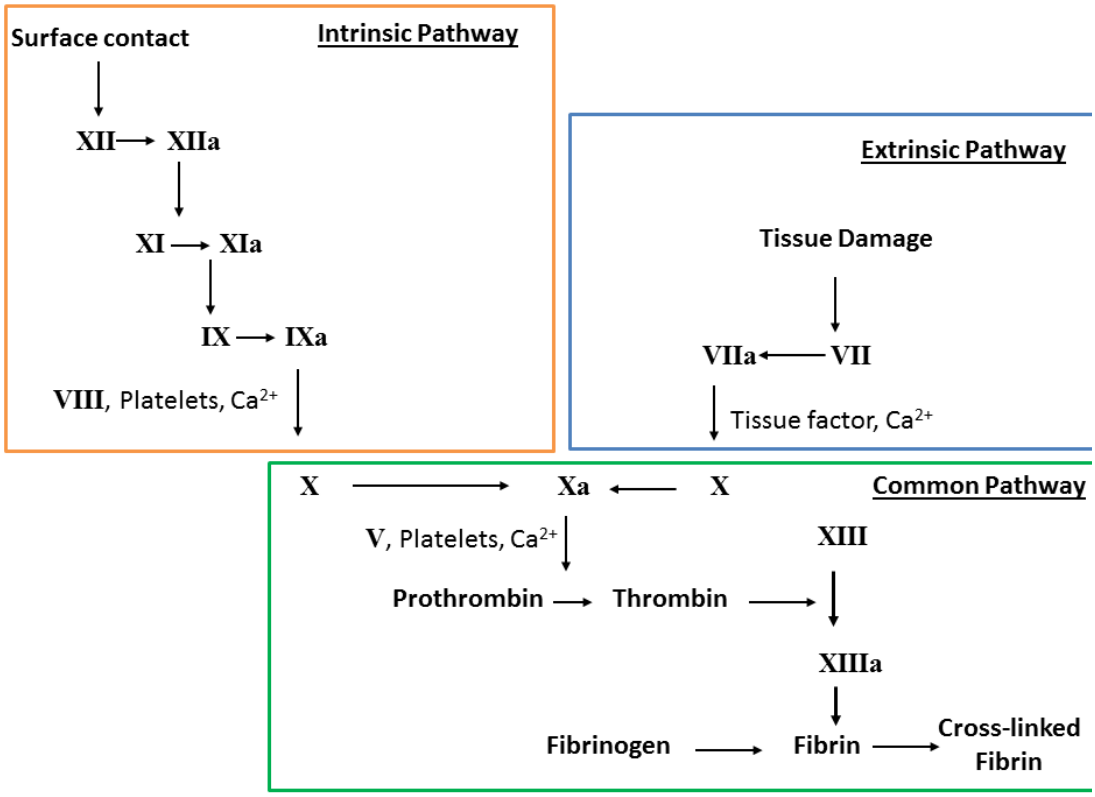

Figure 1.2. Simplified schematic of the coagulation cascade, where clotting is initiated by either surface contact (intrinsic) or tissue factors (extrinsic) and ultimately converges at the common pathway to form a thrombus.

cascade, the normally inactive factors become enzymatically activated (e.g., Factor X becomes Factor Xa) by surface contact or cleavage by other activated enzymes. This sequence allows for rapid activation of other clotting factors and amplification of the entire coagulation cascade. When blood comes in contact with a foreign surface (biomedical device) protein adsorption will trigger the first step of the intrinsic pathway, with activation Factor XII to Factor XIIa. The presence of Factor XIIa will lead to the activation of Factor XI and eventually lead to the activation of Factor X and formation of thrombin (Factor II) in the common pathway.[3] Thrombin converts fibrinogen into fibrin and also activates Factor XIII, which cross-links and stabilizes fibrin into an insoluble gel that traps platelets and red blood cells in a thrombus on the surface within hours.[9]

1.1.3 Improving Hemocompatibility of Biomedical Devices

In contrast to many polymers used in blood-contacting devices, the endothelium layer lining the human vasculature remains thrombus-free through several control mechanisms: a non-fouling phospholipid coating, membrane bound/released inhibitors of platelet and coagulation factors, as well as an efficient fibrinolytic system that removes fibrin deposits. Many of the major approaches for developing polymeric materials that are more hemocompatible are aimed at decreasing activation of key components of the coagulation cascade. Surface pacification is one approach, where the polymer surfaces aim to minimize protein adsorption (e.g., fibrinogen) and platelet adhesion/activation. Another approach is utilizing active polymer surfaces (e.g., immobilized heparin or nitric oxide (NO) release) that can interact with proteins, cells, and platelets to inhibit parts of the coagulation cascade. Research groups have worked to develop materials with suppressed blood-material interactions (e.g., polymeric materials which exhibit reduce protein and cell adhesion) and materials that mimic the non-thrombogenic endothelium. Polymers for blood-contacting devices are evaluated using various *in vitro* and *in vivo* testing methods, where protein and platelet adhesion are common markers to demonstrate the enhanced hemocompatibility properties of the material.

1.2 Overview of Current Technology/Strategies

1.2.1 Hydrophilic and Hydrophobic Materials

Protein adsorption on polymer surfaces is a well-recognized initiator of thrombus formation. Protein adsorption is dependent on a variety of material properties including surface charge, surface free energy, surface roughness, and a balance between hydrophobic and hydrophilic groups.[10] Ikada et al. suggested that protein adhesion can be minimized when surface free energy is minimized, which occurs on strongly hydrophilic and strongly hydrophobic surfaces.[11] One widely used approach has been to utilize hydrophilic surfaces in order to reduce protein adsorption and surface thrombogenicity. It has been concluded that hydrophilic polymers exert a steric repulsion effect towards blood proteins and cells.[12, 13] Hydrogels for blood contacting devices have been prepared using poly(vinyl alcohol) (PVA), polyacrylamides (PAAm), poly(N-vinyl pyrrolidone) (PNVP), poly(hydroxyethyl methacrylate) (PHEMA), poly(ethylene oxide) (PEO), poly(ethylene glycol) (PEG), poly(ethylene glycol) monomethyl ether (PEGME), and cellulose.[14] These hydrophilic materials strongly adsorb water, increasing its similarity to biological tissue and producing minimal interface tension with blood.[15] This strongly bound water also prevents cells and proteins from coming into contact with the polymer, reducing their adsorption to the surface.[16]

Many hydrogels have poor mechanical properties, thus they have been grafted or coated onto other polymeric substrates and have improved hemocompatibility.[15, 17-31] Immobilization of PEG ($-CH_2CH_2O-$) is another popular means to make a polymer more protein and cell resistant.[32] Balakrishnan et al. demonstrated that PEGylated poly(viny chloride) had significantly less fibrinogen and platelet adsorption in comparison to a PVC control.[21] Li et al. reported that poly(poly(ethylene glycol) dimethacrylate) (P(PEGDMA)) grafted on silicone rubber reduced platelet adhesion by 90% and also reduced plasma protein adsorption.[26] However, platelets still adsorbed on some PEG surfaces during *in vivo* experiments, despite the low protein adsorption observed during *in vitro* studies.[33] Plasma oxidation of polyethylene caused increased wettability with increased protein adsorption, but still reduced platelet adhesion.[34] Some hydrogels (e.g., cellulose) typically used as dialysis membranes/fibers are known to be thrombogenic, and

therefore it can be concluded that low-protein adhesion does not necessarily result in hemocompatible surfaces.[35] Poly(2-methoxyethyl acrylate) (PMEA), which has been approved by the U.S. Food and Drug administration for medical use, not only exhibits lower protein adsorption and platelet adhesion than other hydrophilic surfaces, but it also reduces the amount of conformational changes that proteins undergo when adsorbed.[16, 36] This is of benefit since denaturation of adsorbed proteins can lead to platelet activation and subsequent thrombus formation, whereas, in contrast, when adsorbed proteins remain in their native confirmation, platelets cannot adhere (see discussion in Section 1.2.2).

Strongly hydrophobic polymers are also known to have good hemocompatibility properties. Some hydrophobic polymers that are commonly used for medical applications include polyurethanes, silicones, polytetrafluoroethylene (PTFE), poly(vinyl chloride) (PVC), and polyethylene.[37] Very smooth silicone rubber and polyurethanes are known to have good thromboresistant properties.[38, 39] Hydrophobic polymers are conducive to non-specific protein adsorption (e.g., fibrinogen, albumin), and the adsorbed albumin appears to prevent subsequent protein adsorption.[40] It has been shown that increasing surface hydrophobicity also increases the amount of protein adsorbed, which, in turn, decreases the amount of conformational changes, potentially having a role in pacifying the surface.[41] For example, Elast-eon polymers (polyurethane and polydimethylsiloxane copolymers) are reported to have low surface energy and stronger binding to albumin (over fibrinogen).[42] Alkyl chains have also been grafted on relatively hydrophilic polymers in order to increase the hydrophobicity of the surface.[43-45] Khorasani et al. reported that both superhydrophobic and superhydrophilic surfaces were able to reduce platelet adhesion in comparison to controls.[46] However, materials that are hydrophobic exhibit high protein adsorption and conformational changes of the adsorbed proteins.[47, 48] Polymeric materials with both hydrophilic and hydrophobic domains have also been reported to improve hemocompatibility (see Section 1.2.3). Ultimately, there is still no consensus as to which is better, hydrophilic or hydrophobic surfaces, for blood-contacting biomedical device applications.[49]

1.2.2 Albumin Coated Surfaces

It is a widely accepted fact that protein adsorption is the first event that occurs upon foreign surface-blood contact. Human albumin (Alb) is the most abundant protein in the body with a concentration of 35-53 mg/mL in blood plasma. Due to its high concentration and low molecular weight, it is the first protein that adsorbs on the surface of implanted materials. Unlike fibrinogen, albumin is not known to have a peptide sequence that can facilitate binding of the platelet receptors and hence has been used as a coating to block non-specific platelet-surface interactions.

Since the early finding that Alb coated surfaces prevent adhesion of proteins and platelets,[50] Alb has been extensively used as one of the strategies to develop hemocompatible surfaces. In one study, Alb was shown to significantly improve short-term thrombogenicity of Dacron arterial prostheses.[51] In another study, Guidoin et al. showed that Alb treatment does not affect the strength of polyester arterial prosthesis, but also found that within 1-2 weeks of implantation the Alb coating begins to disappear.[52] In a comparison of carbon dioxide gas plasma-treated polystyrene (PS-CO_2) coated Alb and PS-CO2 treated Alb-heparin conjugate, albumin treated surfaces were found to be more effective in reducing platelet adhesion.[53] Albumin-heparin conjugate surface was also found to be suitable for endothelial cell seeding, which can further improve the hemocompatibility of the surfaces. Mohammad et al. demonstrated that combining Alb with Immunoglobulin G (IgG) results in a significant reduction in platelet adhesion in a 7 d *in vitro* study.[54]

One of the limitations of Alb coating is that other proteins can displace Alb on the surface and reduce the long-term effectiveness of this approach. To prevent this displacement, covalent immobilization of Alb has been reported.[55] Another challenge with the Alb coating approach is that it adsorbs to hydrophobic surfaces more tightly than the hydrophilic surfaces, which necessitates increasing the hydrophobicity of the surface, a modification that is considered undesirable because platelets also adhere strongly to hydrophobic surfaces.[56, 57] Some other limitations of Alb coatings include conformational changes, physical degradation, and challenges with sterilization and shelf stability. In a recent study by the Latour group, it was shown that non-activated platelets can adhere to adsorbed Alb once a critical degree of adsorption-induced unfolding is

reached.[58, 59] The platelet response shows a strong correlation with the degree of adsorption induced unfolding, very similar to the platelet adhesion response to adsorbed fibrinogen. These studies demonstrate the potential challenges with Alb coated surfaces, in that, while they may pacify the surface initially, the adsorbed Alb will show a time-dependent conformational change potentially leading to increased platelet adhesion/activation.

1.2.3 Patterned Modifications of Surfaces

Surfaces with patterns at the micro- and nanoscale level have also been investigated for their hemocompatibility properties. Copolymers containing both hydrophilic and hydrophobic domains (ABA-type block copolymers) have exhibited good antithrombotic properties,[60-66] where the balance between the hydrophilicity and hydrobphobicity is important to enhance the biocompatibility.[67] Surfaces with hydrophilic/hydrophobic microdomains are reported to create an organized protein structure, albumin adsorbing on hydrophilic domains and fibrinogen adsorbing on hydrophobic domains, which suppresses platelet adhesion/activation.[64, 68] Okano et al. reported that copolymers composed of hydrophilic monomers, 2-hydroxyethyl methacrylate (HEMA) or poly(2-hydroxyethyl methacrylate) (PHEMA), and hydrophobic styrene had excellent thromboresistance properties, in terms of preventing platelet adhesion and deformation, during *in vitro* experiments.[61, 62] The PHEMA-styrene copolymer was coated on vascular grafts and had an occlusion time of 20 d (vs. 2 d for controls) when implanted in rabbits.[61] However, some of these ABA-type copolymers have the disadvantage that the hydrophilic segments have high surface free energy and bury themselves in the hydrophobic segments.[69] Oyane et al. has reported a new block copolymer (PS-PME3MA) where the hydrophilic blocks remain at the surface when in contact with water.[60] The PS-PME3MA polymer was found to be highly resistant to protein adsorption, cell adhesion, and platelet adhesion/activation.

Another type of surface modification that has been shown to exhibit improved hemocompatibility is attachment of hydrophilic polymer brushes, such as PEO[70, 71] or PEG.[72-75] These hydrophilic polymer brushes create an antifouling surface on the substrate due to steric repulsion. Long-chain polymer brushes have been attached to

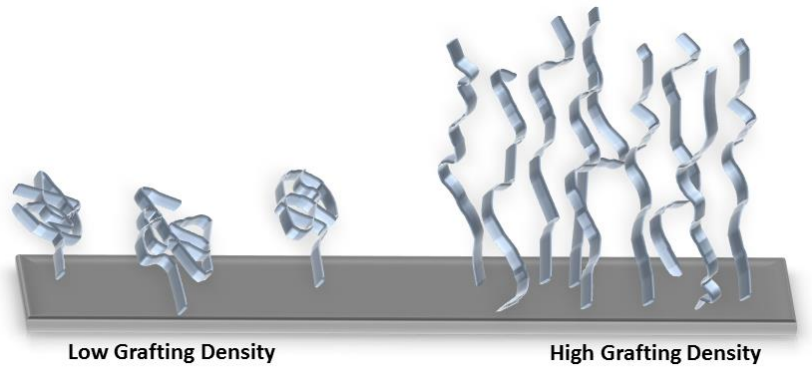

Figure 1.3. Illustration showing relationship between polymer brush grafting density and chain length.

surfaces using physical adsorption or covalent binding techniques.[76] Polymer brushes that are more densely packed (high graft density) and have longer chain lengths further reduce protein adhesion and platelet adhesion/activation on the surface (**Figure 1.3**).[77-79] Stents coated with a chitosan-PEO coating were tested in an *ex vivo* porcine model, and had low platelet adhesion (similar to the endothelium).[80] Dialysis membranes grafted with PEG brushes also had reduced platelet adhesion and improved hemocompatibility.[72, 81, 82] Tetraethylene glycol dimethyl ether grafted on polyethylene tubing was able to significantly reduce plasma protein (both fibrinogen and von Willebrand's factor) and platelet adsorption, in comparison to control tubing (PVC/Tygon, polyurethane, silicone, and polyethylene).[83] Rodreguez-Emmenegger et al. recently reported an ultra-low fouling surface using poly[*N*-(2-hydroxypropyl) methacrylamide] (poly(HPMA)) brushes which was able to maintain the antifouling properties for up to two years of storage.[84]

1.2.4 Attached Endothelial Cells

Another approach to making a surface more hemocompatible is to mimic the inner surface of blood vessels by attaching endothelial cells on the artificial surface, which provides an advantage in that the blood will come in contact with a surface that functions just like the endothelium. Endothelial cells (EC) line the inner walls of blood vessels and help in preventing thrombus formation by releasing anti-platelet agents such as nitric oxide (NO) and prostacyclin. Several research groups have used EC seeding on artificial surfaces for various biomedical applications including vascular grafts,[85-87] stents,[88] resorbable meshes,[89] etc.

Williams and co-workers used a pressure sodding method to introduce EC cells into the luminal surface of PTFE grafts before implantation.[86] These grafts were tested for 12 weeks in carotid arteries of dogs. All of the control grafts clotted, whereas 86% of the EC sodded grafts were found to be patent after the 12 week implantation period. To improve the hemocompatibility of vascular grafts, Taite et al. used NO releasing PU-PEG copolymer containing cell adhesive pentapeptide sequence to promote EC cell adhesion and migration.[90] In another study, Kutryk et al. used xenotransplantation to seed endothelial cells on the surface of the stents to reduce blood contact with the stent surface.[88] Zünd and co-workers seeded fibroblasts and ECs on polyglycolic acid (PGA) resorbable mesh as a precursor to vessels or cardiac valves.[89]

Despite these encouraging results, EC proliferation and seeding on artificial surfaces is complex and still has challenges to overcome. One of the challenges of using the EC seeding approach is the difficulty in growing and maintaining the cells on artificial surfaces.[91] Various studies have been conducted to modify the surfaces in such a way that they can improve and promote endothelial cell adhesion. Kawamoto et al. showed that by plasma treatment of a PU surface, EC adhesion and proliferation can be dramatically improved.[92] In another study, Li and co-workers showed that increased proliferation and cell spreading can be achieved with arg-gly-asp (RGD) peptide grafted surfaces.[93] In yet another study, Yin et al. reported that mussel adhesive polypeptide mimic, containing dihydroxyphenylalanine and L-lysine (MAPDL) with PEG spacer, improved the cell attachment and growth and also reduced platelet adhesion in comparison to the controls.[94] Other challenges associated with the EC seeding approach include complex and expensive experimental procedures and long-term stability issues which still need to be addressed.

1.2.5 Zwitterionic Surfaces

Another effective approach to obtain a hemocompatible surface includes introducing a zwitterionic group, such as phosphobetaine, sulfobetaine or carboxylbetaine, to the substrate material (**Figure 1.4**). These zwitterionic materials have been considered as biomimetic, antifouling, and hemocompatible materials because they contain phosphorylcholine-like groups which are present on the lipid bilayers of the cell

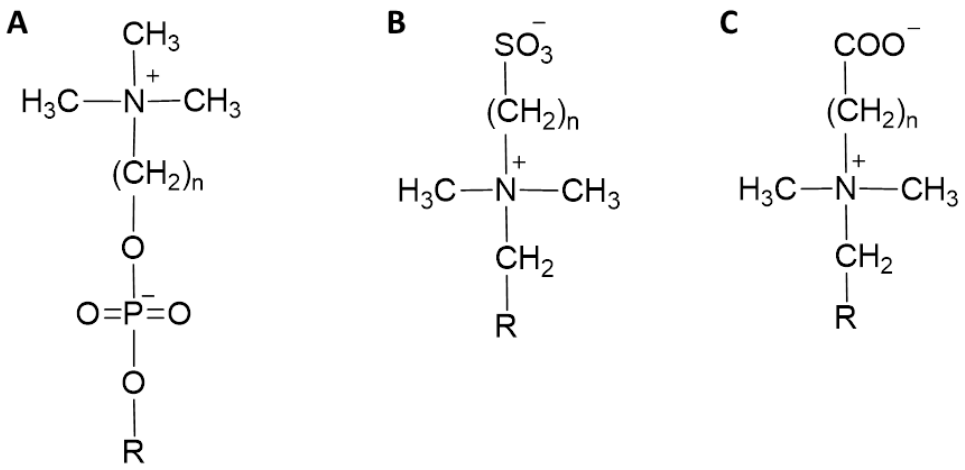

Figure 1.4. Generic structures of phosphobetaines (A), sulfobetaines (B), and carboxylbetaines (C).

membranes.[95, 96] Zwitterionic betaines have both anionic and cationic charged moieties in the same side chain which maintains an overall neutral charge. As discussed earlier, PEG and other hydrophilic materials, such as PEO and PHEMA, become hydrated via hydrogen bonding with water to prevent fouling. Zwitterionic materials can bind water molecules even more strongly (induced by electrostatic interactions) and hence can prevent significant change in protein conformation.[97, 98]

There have been numerous publications showing the potential of zwitterion-based surfaces in resisting protein adsorption,[95, 99] platelet adhesion,[100-103] and consequently reduced thrombus formation compared to the control materials. Atom transfer radical polymerization (ATRP) is one of the commonly used methods to graft polymer surfaces with zwitterionic groups.[97, 104-106] Recently, various research teams have modified polymers using zwitterionic groups (carboxybetaine and sulfobetaine monomers) to mimic cell membrane surfaces.[100, 102, 107, 108] These surfaces have shown significantly lower fouling and platelet adhesion properties. In an another study, a zwitterionic silane coupling agent, N,N-dimethyl, N-(2-ethyl phosphate ethyl)-aminopropyltrimethyoxysilane (DMPAMS) was synthesized and studied for *in vitro* hemocompatibility.[96] Surfaces grafted with DMPAMS showed a steep drop in the water contact angle from 48º to 21.5º, indicating a more hydrophilic surface. At 200 mM surface concentration of DMPAMS, activated partial thromboplastin time (APTT) was prolonged from 28.8 sec for the control to 37.8 sec for the modified surface. Almost no platelet attachment was seen on the DMPAMS modified surface even after 3 h of blood

contact. Lee et al. combined PEG with zwitterions for stent coating applications.[109] Significant reduction in protein adsorption and platelet adhesion was observed in addition to a substantial increase (compared to controls) in blood coagulation time for the zwitterionic-PEG grafted stents.[109] Polyurethane catheters grafted with a zwitterionic sulfobetain monomer (*N*,*N*-dimethyl-*N*-methacryloxyethyl-*N*-(3-sulfopropyl) ammonium, DMMSA) were also able to prevent platelet adhesion when soaked in platelet rich plasma (PRP) for 120 min.[110] Stents coated with phosphorylcholine, such as the commercial Bio*div Ysio* ™, have also been shown to exhibit enhanced hemocompatibility and increased endothelialization.[111, 112]

1.2.6 Heparin Immobilization

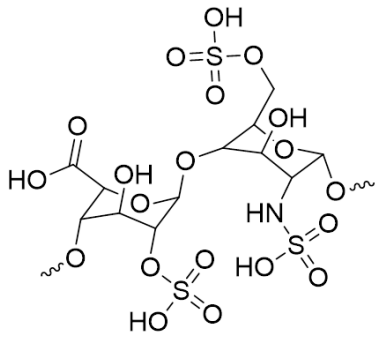

Figure 1.5. Structure of a disaccharide sequence of heparin.

Heparin (**Figure 1.5)** is a highly sulfonated, anionic blood polysaccharide that binds to antithrombin III through ionic interactions, which inactivates thrombin and factor Xa and thereby inhibits blood coagulation. Heparin has been clinically used since 1935 and is one of the most common anticoagulants employed during surgery and treatment of post-operative thrombosis and embolism.[113] However, systemic administration of anticoagulants, such as heparin, increases the risks of hemorrhage, thrombocytopenia, and thrombosis.[7] It is well known that some heparinized and sulfonated materials have anticoagulant activity, resulting in prolongation of the blood clotting time.[114] Heparin immobilized on surfaces also suppresses platelet adhesion and protein adsorption.[115] Heparinization of surfaces is one of the most popular techniques to improve hemocompatibility and has been commercialized and used in the preparation of

different medical devices (e.g., catheters, extracorporeal circuits, stents, grafts, etc.).[116, 117]

Heparin has been physically adsorbed, as well as ionically and covalently immobilized, on various polymer surfaces.[117-122] Ionic immobilization techniques require cationic residual groups in the polymer which interact with the ionic groups on heparin (e.g., COO^-, SO_4^{2-}, $NHSO_3^-$), while covalent binding of heparin utilizes the hydroxyl, carboxyl, or amino groups of heparin.[120] Heparin that is ionically bound to a surface will slowly be released due to ion-exchange with blood components, and this ultimately shortens the usage lifetime of the material.[123] The success of heparinized materials depends on the covalently bound heparin remaining in its native confirmation and its ability to complex with antithrombin III, which is most efficient when heparin is coupled by endpoint (vs. multipoint) attachment.[124] Michanetzis et al. compared common heparin immobilization techniques, direct[125] and indirect[126] covalent binding, applied to the surfaces of commercially available polymers (silicone rubber, polyethylene, polypropylene, and poly(viny chloride).[120] While both techniques suffered from a low yield of immobilized heparin in comparison to the initial amount of heparin, the direct method produced a better heparinization yield (10.5%) and both methods were able to improve the hemocompatibility in terms of reduced platelet activation and, therefore, an increased platelet retention rate. The anticoagulation properties of immobilized heparin have also been improved by using hydrophilic spacers (e.g., PEG), in comparison to heparin immobilized directly to the polymer. This reduces protein adsorption.[127, 128] Polyethylene tubing was modified with immobilized heparin via the method developed by Larm et al.[119] (commercialized as Carmeda ® BioActive Surface) and was able to maintain efficacy for up to 4 months when implanted in pigs.[129] The advantage of heparinized surfaces, in addition to the binding of antithrombin III, is the reduced/selective adhesion of certain plasma proteins, which alters the composition of the surface-adsorbed layer of proteins.[130-133] Heparin-coated devices, however, also suffer challenges, especially for long-term applications, due to heparin's short half-life and that surface-bound heparin only has ~1% of the activity of free heparin.[134] Other immobilized direct thrombin inhibitors, such as hirudin, have demonstrated thromboresistant properties as well.[116, 135]

1.2.7 Nitric Oxide (NO) Releasing/Generating Polymers

Nitric oxide (NO) is known to be a potent inhibitor of platelet activation and adhesion. Healthy endothelial cells exhibit an NO flux of 0.5-4.0 x 10^{-10} mol cm^{-2} min^{-1}.[136] Polymeric materials with an NO flux that is equivalent to this level are expected to have similar anti-thrombotic properties. Nitric oxide is highly reactive under physiological conditions, thus a wide range of NO donor molecules, with functional groups that can store and release NO, have been studied for potential biomedical applications. Various reviews have been published that are devoted to a comprehensive discussion of different NO releasing/generating materials and their many potential biomedical applications.[137-144] The two major approaches to achieving localized NO release from polymeric surfaces are to (1) incorporate NO donor molecules or functional groups (e.g., diazeniumdiolates or *S*-nitrosothiols) into the polymer that will release the bound NO under physiological conditions (NO-releasing polymers), or (2) incorporate catalysts into the polymers which can react with endogenous *S*-nitrosothiol (RSNO) species (present in blood) to locally generate NO (NO-generating polymers) (**Figure 1.6)**.

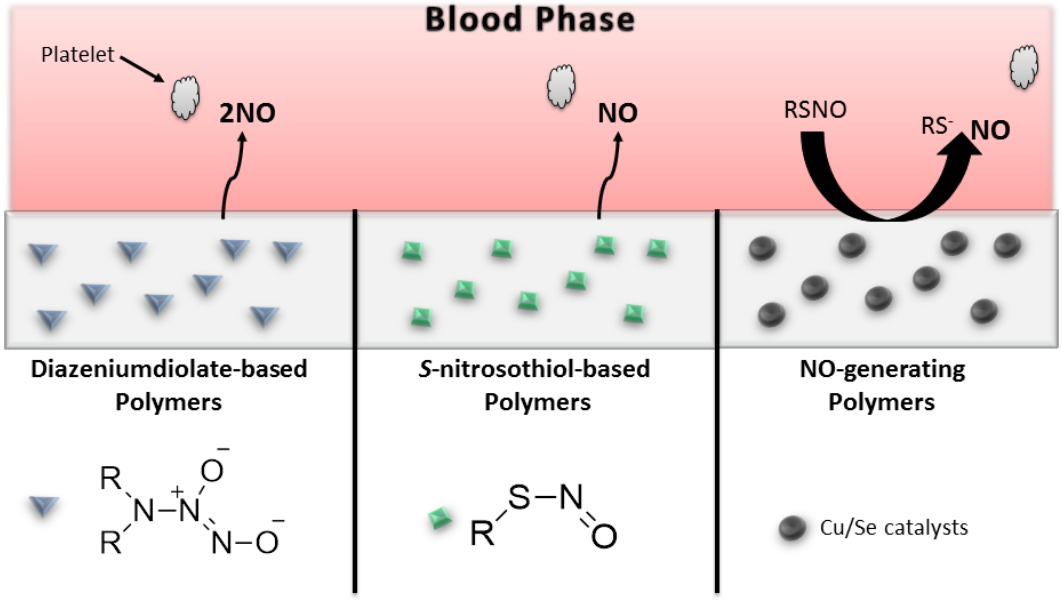

Figure 1.6. Types of NO-releasing/generating polymers, where the NO that is released/generated can prevent activation of platelets that approach the polymer surface. Diazeniumdiolate-based materials undergo proton and thermal driven mechanisms to release NO. *S*-nitrosothiol (RSNO)-based polymers can release NO in the presence of heat, light, or metal ions (e.g., Cu^{+}). NO-generating materials consist of immobilized catalysts (e.g., Cu or Se compounds) that generate NO from endogenous RSNOs.

Nitric oxide has many other biological roles, including its antimicrobial action, which could potentially be utilized to also reduce the infection and biofilm formation that plagues many implantable biomedical devices. Thus, NO releasing/generating chemistries have the potential to create a dual-functioning material that is both antithrombotic and antimicrobial. Duration of the NO release can be tailored to fit the specific biomedical application of the device, and NO-generating materials can continuously generate NO in the presence of endogenous RSNO species (e.g., *S*-nitrosoglutathione (GSNO), *S*-nitrosocysteine (CysNO), etc.).

A wide variety of NO donor molecules have been investigated. The two most widely studied and used in combination with biomaterials are diazeniumdiolates and *S*-nitrosothiols. Diazeniumdiolates, also called NONOates, are relatively stable species that undergo proton or thermally driven mechanism to release two molecules of NO per diazeniumdiolate molecule. Diazeniumdiolates have been a popular NO donor that can easily be dispersed within polymers to facilitate localized NO release.[145-149] Mowery et al. reported that water-soluble diamine-based diazeniumdiolates (e.g., diazeniumdiolated *N,N'*-dimethyl-1,6-hexanediamine (DMHD/N_2O_2), diazeniumdiolated linear polyethylenimine (LPEI/N_2O_2)) leached from polymer matrices.[145] Significant leaching of the NO donor species can result in non-localized NO release where the therapeutic action of NO occurs downstream from the biomedical device. Another concern with diazeniumdiolated-based polymers is the formation and leaching of some potentially carcinogenic decomposition products (e.g., *N*-nitrosamines) that are not intended for release into the bloodstream.[145, 150] To overcome the leaching concerns, strategies to covalently bind diazeniumdiolated functional groups to polydimethylsiloxane,[151] xerogels,[152-154] medical-grade polyurethanes,[137, 155, 156] silica nanoparticles,[157, 158] dendrimers,[159-161] and other nanomaterials[138] have also been reported. Zhang et al. covalently linked diaminoalkyltrimethoxysilane (DACA) to polydimethylsiloxane and then loaded this materials with NO under high pressure to form the diazeniumdiolated coating, DACA/N_2O_2-SR, which released NO for up to 20 d.[151] The DACA/N_2O_2–SR was coated on extracorporeal circuits (ECC) and was able to reduce platelet consumption and thrombus formation during the 4 h blood flow in a rabbit model.

Attempts have also been made to add polymer top coats and/or create more lipophilic diazeniumdiolated species to minimize leaching into the aqueous phase and therefore maintain the localized NO release at the blood-polymer interface.[147, 150, 162, 163] Poly(vinyl chloride) and polyurethane have been doped with the lipophilic diazeniumdiolated dibutylhexanediamine (DBHD/N_2O_2).[147, 148, 164, 165] Vascular grafts coated with DBHD/N_2O_2–doped polyurethane had significantly less thrombus formation than controls after 21 d implantation in sheep.[148] However, the loss of NO from DBHD/N_2O_2 creates free lipophilic amine species within the polymer that react with water, thereby increasing the pH within the polymer phase and effectively turning off the NO release. A recent report demonstrated that NO release can be prolonged, by using poly(lactic-co-glycolic acid) additives, for up to 14 d from poly(vinyl chloride) (PVC) doped with diazeniumdiolated dibutylhexanediamine (DBHD/N_2O_2) (**Figure 1.7**) (see also Chapter 4 of this thesis).[165] The ester linkages of the PLGA hydrolyze in the

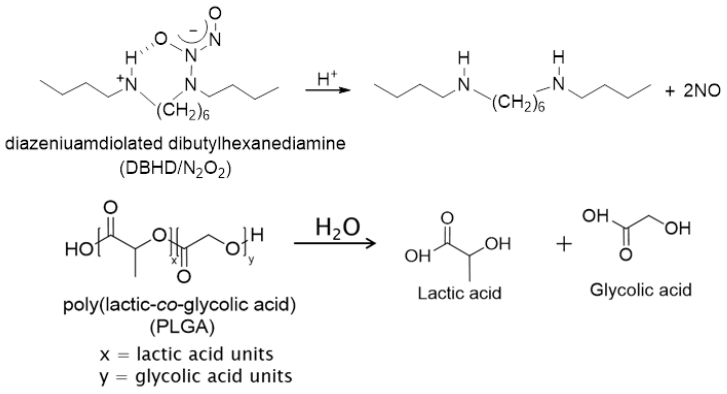

Figure 1.7. Key reactions involved in NO release from diazeniumdiolated dibutylhexanediamine (DBHD/N_2O_2) in the presence of poly(lactic-*co*-glycolic acid additive, that provides additional protons to drive the NO release reaction.

presence of water, producing lactic and glycolic acids that can act as proton sources to control the NO release from DBHD/N_2O_2-doped polymers. PLGAs can have varying hydrolysis rates, which is primarily determined by the copolymer ratio, the end group chemistry (either a free carboxylic acid or ester end group), and molecular weight. Handa et al. also demonstrated the importance of the inherent hemocompatibility of the base polymer (in which the NO chemistry is incorporated) (see Chapter 4).[166] By incorporating the same DBHD/N_2O_2 and PLGA chemistry into the Elast-eon E2As

polymer (a copolymer with a mixed soft segment of poly(dimethylsiloxane) and poly(hexamethylene oxide) with a methylene diphenyl isocyante (MDI) hard segment), which inherently is more hemocompatible than PVC, the platelet count after 4 h of ECC (97±10% of baseline) was significantly improved over the PVC/DOS-based coating (79±11% of baseline).[165, 166]

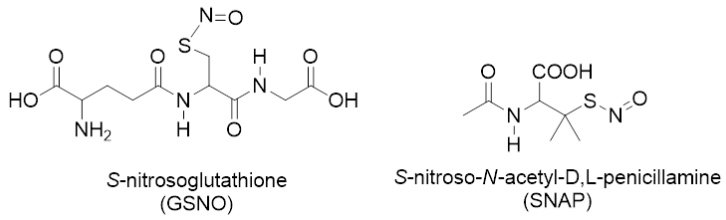

Figure 1.8. Structures of example *S*-nitrosothiols species, *S*-nitrosoglutathione (GSNO) and *S*-nitroso-*N*-acetyl-D,L-penicillamine (SNAP).

Another widely studied class of NO donor molecules is *S*-nitrosothiol (RSNO) species (examples shown in **Figure 1.8**). Physiological RSNOs, including *S*-nitrosoalbumin, *S*-nitrosocysteine (CysNO), and *S*-nitrosoglutathione (GSNO), are considered an endogenous reservoir of NO *in vivo*.[167-169] Other synthetic RSNOs, such as *S*-nitroso-*N*-acetylpenicillamine (SNAP) and *S*-nitroso-*N*-acetylcysteine (SNAC), have been shown to exhibit significant antimicrobial and antithrombotic effects.[170-173] It has also been demonstrated that RSNOs are both vasodilators and potent inhibitors of platelet aggregation.[174-176] RSNOs undergo thermal decomposition to release NO and produce a corresponding disulfide species (RSSR). The NO release from RSNOs can also be catalyzed by metal ions (e.g., Cu^{+})[177] and by light, through irradiation at energies that correspond to the *S*-nitroso absorption bands at 340 and/or 590 nm.[178-180] Incorporation of RSNOs into polymers can extend the utility of these NO donors to be applicable in biomedical devices.

Low molecular weight RSNOs have been non-covalently dispersed within various polymer matrices.[181-187] Seabra et al. prepared GSNO-doped poly(vinyl alcohol) and poly(vinyl pyrrolidone) blended films.[182] This polymer matrix provided a stabilization effect on GSNO decomposition, in comparison to aqueous solutions of GSNO. However, due to leaching, 90% of the NO was released during the first 24 h under physiological

conditions. SNAP-doped polyurethanes (Tecoflex SG-80A and Tecophillic SP-60D-60) also exhibit rapid leaching of SNAP when soaked in buffer (see Chapter 2).[186] The rapid leaching of the RSNOs significantly shortened the duration of the NO release from these materials. Therefore, strategies to synthetically bind RSNO functionalities to the polymer backbone have also been explored. *S*-Nitrosothiol functionalities have been covalently bound to polymers such as xerogels,[188, 189] polyurethanes,[137, 190, 191] degradable polyesters,[192-196] polyester/poly(methyl methacrylate) blends,[197] poly(vinyl methyl ether-*co*-malic anhydride) (PVMMA) and poly(vinyl pyrrolidone) (PVP),[198] and poly(dimethylsiloxane).[199] Dendrimers,[200] fumed silica particles,[180, 191] and silica nanoparticles[155, 156, 201] have also been synthetically modified with covalently bound RSNO functionalities and these materials can be doped into various polymer matrices to create coatings for biomedical devices.

Many of the RSNO-modified materials reported to date have not proven clinically useful due to their limited NO release lifetimes, low conversion to RSNO during synthesis, or lack of RSNO stability during storage. Recently, the RSNO-doping method has been revisited, utilizing more hydrophobic polymers. GSNO-doped Tygon, a proprietary plasticized poly(vinyl chloride) polymer, exhibited minimal leaching of GSNO during soaking under physiological conditions.[187] Incorporating SNAP into Elasteon E2As can create an NO-releasing polymer that is stable during storage (even at elevated temperatures), locally delivers NO under physiological conditions, significantly reduces the leaching of SNAP, and preserves platelets during a 4 h ECC study (see Chapter 2).[186]

Due to the limited NO reservoir from NO donors that can be incorporated into polymers (either covalently bound or non-covalently dispersed), these NO releasing materials typically have a finite duration of NO release. Another approach to achieving localized NO delivery at a polymer/blood interface for a longer period of time is to use NO generating (NOgen) materials that utilize endogenous RSNOs and/or nitrite to locally generate NO at the blood-polymer interface. Various thiol-containing species (L-cysteine, 2-iminothiolane, and cysteine polypeptide) have been immobilized on polyethylene terephthalate and polyurethane, where the free thiol undergoes a transnitrosation reaction with circulating RSNOs (e.g., *S*-nitroso-albumin).[202, 203] The

resulting CysNO on the PET and PU surface decomposes to elevate the NO levels locally at the polymer/blood interface, which reduces platelet adhesion on the surface by more than 50%. Other NOgen materials consist of catalysts (e.g., Cu (I/II) complexes or organoselenium species) that are immobilized within the polymer and are capable of locally generating NO from endogenous RSNOs and/or nitrite. Copper (II) sites within a polymer can be reduced to Cu(I) by endogenous reducing agents that are present in the blood (e.g., thiols, ascorbate). The Cu(I) sites then can reduce endogenous RSNOs in the blood (e.g., GSNO, CysNO, etc.) to NO and free thiolate anions in a catalytic manner.[177] Lipophilic copper complexes that were incorporated into polymers were able to reduce physiological levels of RSNOs and nitrite to locally generate NO.[204-207] Another reported NOgen polymer consists of copper nanoparticles (Cu^0) dispersed within a hydrophilic polymer (Tecophillic SP-60D-60), which was evaluated using a rabbit model for extracorporeal circulation (ECC).[208] However, continuous infusion of SNAP was needed to supplement the endogenous RSNO levels in order to achieve good efficacy in reducing thrombus formation.

Organoselenium species have been studied as mimics of glutathione peroxidase (GPx), a selenoenzyme that protects cells from oxidative stress by reducing hydroperoxides using glutathione (GSH),[209] and investigated for their ability to generate NO from RSNOs.[210] Selenium catalysts are highly selective for reduction of RSNOs and exhibit no catalytic activity for nitrite or nitrate reduction.[211] Low molecular weight organoselenum species, selenocystamine (SeCA) and 3,3'-diselenidedipropionic acid (SeDPA), were immobilized on cellulose filter paper and polyethylenimine (PEI), demonstrating potential dialysis membrane applications.[212] In the presence of reducing agents at physiological pH, the diselenides can be converted into selenolates, which are the key intermediates that can reduce RSNOs into NO and thiolates.[212] Selenium species were also incorporated into layer-by-layer coatings containing alternating layers of sodium alginate (Alg) and selenium-modified PEI. Alg-PEI layer-by-layer films modified with SeDPA were able to generate physiological levels of NO from GSNO and also exhibited minimal leaching of catalytic sites after soaking in blood.[211] The Alg-PEI layer-by-layer coating was also modified to immobilize ebselen (2-phenyl-1,2-benzisoselenazol-3-(2H)-one), an aromatic selenium species with good GPx activity, and

coated on catheters.[213] These selenium-based materials were able to generate physiological levels of NO from RSNOs; however, some reduction of NO flux was observed after soaking in blood, potentially from catalytic sites being blocked by adsorbed plasma proteins or low levels leaching into the solution. These NOgen polymers have an advantage in that they could potential generate NO at the blood-polymer interface indefinitely, provided that the blood contacting the polymer has adequate levels of RSNOs present at all times.[214]

1.3 Methods to Assess Hemocompatibility

Extensive reviews on the various methods to evaluate the hemocompatibility of polymers and medical devices have been published (summarized in **Table 1.1**).[1, 215-223]

Table 1.1. Common surface characterization and blood compatibility tests used to evaluate the hemocompatibility of blood-contacting polymers.

<table>
<tr><th colspan="2">Surface Characterization</th></tr>
<tr><td>Elemental and chemical composition

Physical properties</td><td>Porosity
Roughness
Charge and charge density
Elasticity
Surface energy (wettability)</td></tr>
<tr><th colspan="2">Blood Compatibility Testing</th></tr>
<tr><td><u>In vitro</u> Testing
Static (soaking in blood or plasma)
Dynamic (agitators, centrifugation systems, flow chambers, Chandler loops, closed loops)</td><td rowspan="2">Platelet adhesion (LDH assay)
Protein adsorption (fluorescent assay)
Platelet, plasma fibrinogen, white blood cell counts
Prothrombin time (PT)
Activated partial thromboplastin time (aPTT)
Thrombin clotting time (TCT)
Platelet function via aggregation
Flow cytometry (FACS) analysis of activation
Thrombus area on the device
Embolism (e.g., visual, Doppler ultrasound)
Patency and occlusion time</td></tr>
<tr><td><u>In Vivo</u> Models
Coated or fabricated medical devices:
Catheters
Stents
Vascular grafts
Extracorporeal circuits
Dialysis membranes
Biomedical sensors</td></tr>
</table>

Clinical devices still suffer challenges due to thrombosis, even after standard testing as developed by the International Organization for Standardization (ISO 10993-4, "Selection of Tests for Interactions with Blood").[219, 224] The ISO hemocompatibility testing requires evaluation of thrombosis, coagulation, hematology, platelet count and function, and immunology. Initial surface and physical-chemical characterization studies can provide useful information in order to correlate surface characteristics with hemocompatibility. Surface roughness, surface chemistry, surface charge distribution, and interfacial free energy are well known factors that can influence protein adsorption and cell-material surface interaction.[225] Many of the common hemocompatibility testing methods involve flowing blood through tubing (both *in vitro* and *in vivo*), and then conducting hemocompatibility evaluations of the blood exiting the test system. However, while they have potential to still be used as preliminary screening methods, *in vitro* static assays, such as fluorescent-based fibrinogen adsorption or platelet adhesion,[164, 226] and dynamic systems (e.g., Chandler loops [227]) are limited due to the blood death over time. Various medical devices (e.g., catheters, stents, vascular grafts, dialysis membranes, etc.) have been fabricated or coated with polymers for evaluation in animal models in order to mimic clinical application. Arterio-venous (A-V) and areterio-arterial (A-A) shunts models have been used to test hemocompatibility, and they allow for evaluation of both local and systemic effects of the test polymer. For example, the rabbit model of thrombogenicity is a useful model of extracorporeal circulation, where the polymer is coated on the inner walls of Tygon tubing that form the ECC circuit.[164, 208] The ECC circuit is placed on the rabbit using an A-V shunt, and blood flows through the circuit for 4 h. This model allows a comprehensive evaluation of hemocompatibility (platelet preservation/consumption, plasma fibrinogen levels, and occlusion time) as well as the thrombus area in the ECC circuit after 4 h of blood flow.

Despite the encouraging results published for many of the polymer strategies discussed above, there are still some challenges with hemocompatibility testing and clinical application. For example, counting adhered platelets on the surface is a common method to evaluate hemocompatibility, and has been used as a functional test for many of the polymers discussed above. This may be a good initial test; however, it does not provide the complete picture because platelets could be activated by the foreign surface

and aggregate downstream from the device.[223] Similarly, during *in vivo* testing of a new material, any thrombus that forms on the surface may also be carried downstream. In addition, results from short-term *in vitro* testing cannot necessarily be used to predict long-term *in vivo* results.[220] Another challenge is the fact that research groups use a wide variety of testing methods and controls, so it remains unclear as to how significant the improvement is of these new materials over other materials (either published or clinically used).[220] Defining standardized testing methods and appropriate controls/reference materials used by researchers (commercial, clinical, and academic) will help improve the advancement of novel materials to clinical application.

1.4 Summary

Over the last 50 years, much has been learned about blood-material interactions, and a variety of strategies have been reported to improve the hemocompatibility of blood-contacting medical devices. Materials reported to date primarily target different parts of the coagulation cascade (e.g., protein adsorption, platelet adhesion and activation, fibrin formation, etc.). Although many of the approaches described above are promising individually, combining two or more of these approaches may prove most beneficial. When these materials are effective, they may reduce or eliminate the need for administration of systemic anti-coagulation therapeutics (e.g., heparin) which is currently clinically utilized to reduce the risk of thrombus formation and other complications during use of blood-contacting devices. However, challenges still exist (e.g., shelf life and sterilization stability) and need to be addressed for some of the polymer approaches discussed here in order to achieve widespread clinical application. Standard testing methods should be utilized to test and compare the hemocompatibility of commercially available and new polymeric materials for biomedical applications.

1.5 Statement of Dissertation Research

Various NO-releasing polymers have been reported in the literature with encouraging results for potential biomedical applications. However, none of the materials reported to date have been clinically applied, despite their potential benefits. This is primarily due to: 1) short durations of NO release (from a few hours to a few

days); 2) the need for toxic additives to prolong the NO release; 3) prohibitive costs of the NO donor molecules; and 4) instability of the NO donor during storage and/or sterilization. The primary purpose of this dissertation research is to use novel approaches to develop polymers with long-term NO release, addressing some of the challenges mentioned above, and to demonstrate their potential biomedical applications for reducing thrombosis and infection. This dissertation was prepared using the multiple manuscript type format, where the chapters are basically the text as it appears in the publications derived from this work, and hence the introduction sections in the chapters are somewhat repetitive. Chapter 1, a review of various approaches to improve hemocompatibility, is a section in the book *Advanced Polymers in Medicine*.[228]

In Chapters 2 and 3, new *S*-nitroso-*N*-acetypenicillamine (SNAP)-doped polymers are studied for potential hemocompatibility applications. The NO release and SNAP leaching from various SNAP-doped polymers is measured over 20 d. A shelf-life stability study is conducted with the SNAP-doped Elast-eon polymer, and it is shown that this formulation exhibits attractive shelf-live stability. Finally, the SNAP/E2As polymer is coated on the inner walls of extracorporeal circulation (ECC) circuits and tested in a rabbit model of thrombogenicity. This work has been published in *Biomaterials* in 2013.[186]

In Chapter 3, the SNAP/E2As polymer is used to fabricate intravascular catheters using a dip-coating method. The long-term NO release and stability during ethylene oxide sterilization is evaluated. The SNAP/E2As and E2As catheters are implanted in sheep veins for 7 d and evaluated for thrombus formation and bacterial adhesion.

Chapters 4 and 5 discuss the optimization and potential applications of polymers doped with diazeniumdiolated dibutylhexanediamine (DBHD/N_2O_2). In Chapter 4, various poly(lactic-*co*-glycolic acid) are used as additives to promote and control the NO release properties of these new biomaterials. A comparison between using acid-capped and ester-capped PLGA additives is conducted, where the pH changes corresponding to the NO release profiles from these films are visualized by doping films with pH indicator dyes. The efficiency of the NO release (in terms of platelet count and thrombus area) from DBHD/N_2O_2 and PLGA doped coatings prepared with 2 different base polymers, poly (vinyl chloride) and Elast-eon E2As, is compared by coating these materials on the

inner walls of ECC circuits and testing in the rabbit model of thrombogenicity. This chapter is a summary of two papers that have been published in *Journal of Materials Chemistry B*.[165, 166]

Chapter 5 focuses on optimizing the NO release from DBHD/N_2O_2 and PLGA doped within two polymers, Tecoflex SG-80A and Tecophilic SP-60D-20. The optimal SG-80A-based NO-releasing and control patches are applied to scald burn wounds on mice infected with *Acinetobacter baumannii* to observe the effects on infection after 24 h. The work presented in this chapter has been submitted as a manuscript.[229]

Chapter 6 summarizes the findings and conclusions of this dissertation work, and also provides some directions for future work. Potential methods to improve the rate of NO release from the SNAP/E2As polymer and methods to make clinical applications more feasible are discussed. Also, plans for future toxicity and long-term animal studies with the DBHD/N_2O_2 and PLGA based polymers will be presented.

1.6 References

1. B. D. Ratner, *Biomaterials*, **2007**, *28*, 5144-5147.

2. R. W. Colman, *Cardiovasc Pathol*, **1993**, *2*, 23-31.

3. M. B. Gorbet and M. V. Sefton, *Biomaterials*, **2004**, *25*, 5681-5703.

4. A. Dwyer, in *Seminars in dialysis*, Wiley Online Library, 2008, pp. 542-546.

5. B. D. Ratner, *J Biomater Sci Polym Ed*, **2000**, *11*, 1107-1119.

6. A. M. Gaffney, S. M. Wildhirt, M. J. Griffin, G. M. Annich and M. W. Radomski, *BMJ*, **2010**, *341*.

7. T. M. Robinson, T. S. Kickler, L. K. Walker, P. Ness and W. Bell, *Crit Care Med*, **1993**, *21*, 1029-1034.

8. T. A. Horbett, *Cardiovasc Pathol*, **1993**, *2*, 137-148.

9. S. Schopka, T. Schmid, C. Schmid and K. Lehle, *Materials*, **2010**, *3*, 638-655.

10. J. Brash and T. Horbett, in *ACS Symp Ser*, American Chemical Society Washington, DC, 1987, p. 1.

11. Y. Ikada, M. Suzuki and Y. Tamada, in *Polymers as biomaterials*, Springer, **1984**, pp. 135-147.

12. S. Nagaoka, Y. Mori, H. Takiuchi, K. Yokota, H. Tanzawa and S. Nishiumi, in *Polymers as biomaterials*, Springer, **1984**, pp. 361-374.

13. S. Jeon, J. Lee, J. Andrade and P. De Gennes, *J Colloid Interface Sci*, **1991**, *142*, 149-158.

14. N. A. Peppas, Y. Huang, M. Torres-Lugo, J. H. Ward and J. Zhang, *Annu Rev Biomed Eng*, **2000**, *2*, 9-29.

15. T. Okada and Y. Ikada, *Makromol Chem*, **1991**, *192*, 1705-1713.

16. M. Tanaka, T. Hayashi and S. Morita, *Polym J*, **2013**, *45*, 701-710.

17. H. Wang, T. Yu, C. Zhao and Q. Du, *Fibers and Polym*, **2009**, *10*, 1-5.

18. S. R. Hanson, L. A. Harker, B. D. Ratner and A. Hoffman, *J Lab Clin Med*, **1980**, *95*, 289-304.

19. M. Morra, E. Occhiello and F. Garbassi, *Clin Mater*, **1993**, *14*, 255-265.

20. O. H. Kwon, Y. C. Nho, K. D. Park and Y. H. Kim, *J Appl Polym Sci*, **1999**, *71*, 631-641.

21. B. Balakrishnan, D. Kumar, Y. Yoshida and A. Jayakrishnan, *Biomaterials*, **2005**, *26*, 3495-3502.

22. M. M. Amiji, *Carbohydr Polym*, **1997**, *32*, 193-199.

23. J. Wang, C. J. Pan, N. Huang, H. Sun, P. Yang, Y. X. Leng, J. Y. Chen, G. J. Wan and P. K. Chu, *Surf Coat Technol*, **2005**, *196*, 307-311.

24. R. Okner, A. J. Domb and D. Mandler, *New J Chem*, **2009**, *33*, 1596-1604.

25. Y. C. Nho and O. H. Kwon, *Radiat Phys Chem*, **2003**, *66*, 299-307.

26. M. Li, K. G. Neoh, L. Q. Xu, R. Wang, E. T. Kang, T. Lau, D. P. Olszyna and E. Chiong, *Langmuir*, **2012**, *28*, 16408-16422.

27. J. Jin, W. Jiang, J. H. Yin, X. L. Ji and P. Stagnaro, *Langmuir*, **2013**, *29*, 6624-6633.

28. C. W. Chung, H. W. Kim, Y. B. Kim and Y. H. Rhee, *Int J Biol Macromol*, **2003**, *32*, 17-22.

29. Y. C. Chiag, Y. Chang, W. Y. Chen and R. C. Ruaan, *Langmuir*, **2012**, *28*, 1399-1407.

30. A. K. Bajpai, *Polym Int*, **2005**, *54*, 304-315.

31. S. Alibeik, S. Zhu and J. L. Brash, *Colloids Surf, B*, **2010**, *81*, 389-396.

32. J. M. Harris, *Poly(ethylene glycol) Chemistry: Biotechnical and Biomedical Applications*, Springer, **1992**.

33. G. R. Llanos and M. V. Sefton, *J Biomed Mater Res*, **1993**, *27*, 1383-1391.

34. J. H. Lee and H. B. Lee, *J Biomed Mater Res*, **1998**, *41*, 304-311.

35. M. Sefton, C. Gemmell and M. Gorbet, *Biomaterials Science: An Introduction to Materials in Medicine New York: Elsevier*, **2004**, 456-470.

36. M. Tanaka, T. Motomura, M. Kawada, T. Anzai, K. Yuu, T. Shiroya, K. Shimura, M. Onishi and M. Akira, *Biomaterials*, **2000**, *21*, 1471-1481.

37. U. Nydegger, R. Rieben and B. Lämmle, *Transfus Sci*, **1996**, *17*, 481-488.

38. T. Kolobow, E. Stool, P. Weathersby, J. Pierce, F. Hayano and J. Suaudeau, *ASAIO Trans*, **1974**, *20*, 269.

39. M. Szycher, *J Biomater Appl*, **1988**, *3*, 297-402.

40. B. Lassen and M. Malmsten, *J Colloid Interface Sci*, **1996**, *180*, 339-349.

41. B. Sivaraman, K. P. Fears and R. A. Latour, *Langmuir*, **2009**, *25*, 3050-3056.

42. D. Cozzens, A. Luk, U. Ojha, M. Ruths and R. Faust, *Langmuir*, **2011**, *27*, 14160-14168.

43. R. Bahulekar, N. Tamura, S. Ito and M. Kodama, *Biomaterials*, **1999**, *20*, 357-362.

44. T. Matsuda and S. Ito, *Biomaterials*, **1994**, *15*, 417-422.

45. A. S. Hoffman, D. Cohn, S. R. Hanson, L. A. Harker, T. A. Horbett, B. D. Ratner and L. O. Reynolds, *Radiat Phys Chem*, **1983**, *22*, 267-283.

46. M. Khorasani and H. Mirzadeh, *J Appl Polym Sci*, **2004**, *91*, 2042-2047.

47. M. Okubo and H. Hattori, *Colloid Polym Sci*, **1993**, *271*, 1157-1164.

48. T. Klose, P. B. Welzel and C. Werner, *Colloids Surf, B*, **2006**, *51*, 1-9.

49. M. V. Sefton, C. H. Gemmell and M. B. Gorbet, *J Biomater Sci Polym Ed*, **2000**, *11*, 1165-1182.

50. J. Andrade and V. Hlady, in *Biopolymers/Non-Exclusion HPLC*, Springer, **1986**, pp. 1-63.

51. K. Kottke-Marchant, J. M. Anderson, Y. Umemura and R. E. Marchant, *Biomaterials*, **1989**, *10*, 147-155.

52. R. Guidoin, R. Snyder, L. Martin, K. Botzko, M. Marois, J. Awad, M. King, D. Domurado, M. Bedros and C. Gosselin, *Ann Thorac Surg*, **1984**, *37*, 457-465.

53. G. W. Bos, N. M. Scharenborg, A. A. Poot, G. H. Engbers, T. Beugeling, W. G. van Aken and J. Feijen, *J Biomed Mater Res*, **1999**, *47*, 279-291.

54. S. Mohammad and D. Olsen, *ASAIO J*, **1989**, *35*, 384-387.

55. A. Hoffman, G. Schmer, C. Harris and W. Kraft, *ASAIO J*, **1972**, *18*, 10-16.

56. L. I. Mikhalovska, M. Santin, S. P. Denyer, A. W. Lloyd, D. G. Teer, S. Field and S. V. Mikhalovsky, *Thromb Haemost*, **2004**, *92*, 1032-1039.

57. I. Dion, X. Roques, H. Baquey, E. Baudet, B. Basse Cathalinat and N. More, *Bio-Med Mater Eng*, **1993**, *3*, 51-55.

58. B. Sivaraman and R. A. Latour, *Biomaterials*, **2010**, *31*, 1036-1044.

59. B. Sivaraman and R. A. Latour, *Biomaterials*, **2011**, *32*, 5365-5370.

60. A. Oyane, T. Ishizone, M. Uchida, K. Furukawa, T. Ushida and H. Yokoyama, *Adv Mater*, **2005**, *17*, 2329-+.

61. T. Okano, T. Aoyagi, K. Kataoka, K. Abe, Y. Sakurai, M. Shimada and I. Shinohara, *J Biomed Mater Res*, **1986**, *20*, 919-927.

62. T. Okano, S. Nishiyama, I. Shinohara, T. Akaike, Y. Sakurai, K. Kataoka and T. Tsuruta, *J Biomed Mater Res*, **1981**, *15*, 393-402.

63. H. Sato, A. Nakajima, T. Hayashi, G. W. Chen and Y. Noishiki, *J Biomed Mater Res*, **1985**, *19*, 1135-1155.

64. C. Nojiri, T. Okano, H. A. Jacobs, K. D. Park, S. F. Mohammad, D. B. Olsen and S. W. Kim, *J Biomed Mater Res*, **1990**, *24*, 1151-1171.

65. A. Takahara, J.-i. Tashita, T. Kajiyama, M. Takayanagi and W. J. MacKnight, *Polymer*, **1985**, *26*, 978-986.

66. A. Takahara, J.-i. Tashita, T. Kajiyama, M. Takayanagi and W. J. MacKnight, *Polymer*, **1985**, *26*, 987-996.

67. T. Sasaki, B. D. Ratner and A. S. Hoffman, in *Abstracts of papers of ACS*, ACS, Washington, DC 1975.

68. T. Okano, M. Uruno, N. Sugiyama, M. Shimada, I. Shinohara, K. Kataoka and Y. Sakurai, *J Biomed Mater Res*, **1986**, *20*, 1035-1047.

69. K. B. Lewis and B. D. Ratner, *J Colloid Interface Sci*, **1993**, *159*, 77-85.

70. H. Chen, Z. Zhang, Y. Chen, M. A. Brook and H. Sheardown, *Biomaterials*, **2005**, *26*, 2391-2399.

71. M. Shen, L. Martinson, M. S. Wagner, D. G. Castner, B. D. Ratner and T. A. Horbett, *J Biomater Sci Polym Ed*, **2002**, *13*, 367-390.

72. F. Fushimi, M. Nakayama, K. Nishimura and T. Hiyoshi, *Artif Organs*, **1998**, *22*, 821-826.

73. M. B. Gorbet and M. V. Sefton, *J Lab Clin Med*, **2001**, *137*, 345-355.

74. K. M. Hansson, S. Tosatti, J. Isaksson, J. Wetterö, M. Textor, T. L. Lindahl and P. Tengvall, *Biomaterials*, **2005**, *26*, 861-872.

75. L. J. Suggs, M. S. Shive, C. A. Garcia, J. M. Anderson and A. G. Mikos, *J Biomed Mater Res*, **1999**, *46*, 22-32.

76. W. R. Gombotz, W. Guanghui, T. A. Horbett and A. S. Hoffman, *J Biomed Mater Res*, **1991**, *25*, 1547-1562.

77. W. Norde and D. Gage, *Langmuir*, **2004**, *20*, 4162-4167.

78. J. N. Kizhakkedathu, J. Janzen, Y. Le, R. K. Kainthan and D. E. Brooks, *Langmuir*, **2009**, *25*, 3794-3801.

79. B. F. Lai, A. L. Creagh, J. Janzen, C. A. Haynes, D. E. Brooks and J. N. Kizhakkedathu, *Biomaterials*, **2010**, *31*, 6710-6718.

80. B. Thierry, Y. Merhi, J. Silver and M. Tabrizian, *J Biomed Mater Res A*, **2005**, *75*, 556-566.

81. M. J. Wright, G. Woodrow, S. Umpleby, S. Hull, A. M. Brownjohn and J. H. Turney, *Am J Kidney Dis*, **1999**, *34*, 36-42.

82. V. Sirolli, S. Di Stante, S. Stuard, L. Di Liberato, L. Amoroso, P. Cappelli and M. Bonomini, *Int J Artif Organs*, **2000**, *23*, 356-364.

83. L. Cao, S. Sukavaneshvar, B. D. Ratner and T. A. Horbett, *J Biomed Mater Res A*, **2006**, *79*, 788-803.

84. C. Rodriguez-Emmenegger, E. Brynda, T. Riedel, M. Houska, V. Šubr, A. B. Alles, E. Hasan, J. E. Gautrot and W. T. Huck, *Macromol Rapid Commun*, **2011**, *32*, 952-957.

85. M. B. Herring, R. Compton, D. R. Legrand and A. L. Gardner, in *Semin Thromb Hemost*, 1989, p. 200.

86. S. K. Williams, D. G. Rose and B. E. Jarrell, *J Biomed Mater Res*, **1994**, *28*, 203-212.

87. P. Zilla, M. Deutsch, J. Meinhart, R. Puschmann, T. Eberl, E. Minar, R. Dudczak, H. Lugmaier, P. Schmidt and I. Noszian, *J Vasc Surg*, **1994**, *19*, 540-548.

88. M. Kutryk, L. Van Dortmont, R. De Crom, A. Van der Kamp, P. Verdouw and W. Van der Giessen, in *Seminars in interventional cardiology: SIIC*, 1997, pp. 217-220.

89. G. Zünd, S. P. Hoerstrup, A. Schoeberlein, M. Lachat, G. Uhlschmid, P. R. Vogt and M. Turina, *Eur J Cardiothorac Surg*, **1998**, *13*, 160-164.

90. L. J. Taite, P. Yang, H.-W. Jun and J. L. West, *J Biomed Mater Res B Appl Biomater*, **2008**, *84*, 108-116.

91. N. L'heureux, S. Pâquet, R. Labbé, L. Germain and F. A. Auger, *FASEB J*, **1998**, *12*, 47-56.

92. Y. Kawamoto, A. Nakao, Y. Ito, N. Wada and M. Kaibara, *J Mater Sci Mater Med*, **1997**, *8*, 551-557.

93. J. Li, M. Ding, Q. Fu, H. Tan, X. Xie and Y. Zhong, *J Mater Sci Mater Med*, **2008**, *19*, 2595-2603.

94. M. Yin, Y. Yuan, C. Liu and J. Wang, *Biomaterials*, **2009**, *30*, 2764-2773.

95. S. Jiang and Z. Cao, *Adv Mater*, **2010**, *22*, 920-932.

96. L. Wu, Z. Guo, S. Meng, W. Zhong, Q. Du and L. L. Chou, *ACS Appl Mater Interfaces*, **2010**, *2*, 2781-2788.

97. Z. Zhang, S. Chen, Y. Chang and S. Jiang, *J Phys Chem B*, **2006**, *110*, 10799-10804.

98. K. Ishihara, H. Nomura, T. Mihara, K. Kurita, Y. Iwasaki and N. Nakabayashi, *J Biomed Mater Res*, **1998**, *39*, 323-330.

99. R. E. Holmlin, X. Chen, R. G. Chapman, S. Takayama and G. M. Whitesides, *Langmuir*, **2001**, *17*, 2841-2850.

100. Y. Jiang, B. Rongbing, T. Ling, S. Jian and L. Sicong, *Colloids Surf, B*, **2004**, *36*, 27-33.

101. D. Y. Min, Z. Z. Li, J. Shen and S. C. Lin, *Colloids Surf, B*, **2010**, *79*, 415-420.

102. J. Yuan, S. Lin and J. Shen, *Colloids Surf B Biointerfaces*, **2008**, *66*, 90-95.

103. S. L. West, J. P. Salvage, E. J. Lobb, S. P. Armes, N. C. Billingham, A. L. Lewis, G. W. Hanlon and A. W. Lloyd, *Biomaterials*, **2004**, *25*, 1195-1204.

104. E. J. Lobb, I. Ma, N. C. Billingham, S. P. Armes and A. L. Lewis, *J Am Chem Soc*, **2001**, *123*, 7913-7914.

105. H. Ma, J. Hyun, P. Stiller and A. Chilkoti, *Adv Mater*, **2004**, *16*, 338-341.

106. Z. Zhang, M. Zhang, S. Chen, T. A. Horbett, B. D. Ratner and S. Jiang, *Biomaterials*, **2008**, *29*, 4285-4291.

107. J. Yuan, J. Zhang, J. Zhou, Y. Yuan, J. Shen and S. Lin, *J Biomater Sci Polym Ed*, **2003**, *14*, 1339-1349.

108. H. Kitano, S. Tada, T. Mori, K. Takaha, M. Gemmei-Ide, M. Tanaka, M. Fukuda and Y. Yokoyama, *Langmuir*, **2005**, *21*, 11932-11940.

109. B. Lee, H.-S. Shin, K. Park and D. Han, *J Mater Sci Mater Med*, **2011**, *22*, 507-514.

110. Y. Yuan, F. Ai, X. Zang, W. Zhuang, J. Shen and S. Lin, *Colloids Surf, B*, **2004**, *35*, 1-5.

111. M. Galli, L. Sommariva, F. Prati, S. Zerboni, A. Politi, R. Bonatti, S. Mameli, E. Butti, A. Pagano and G. Ferrari, *Catheter Cardiovasc Interv*, **2001**, *53*, 182-187.

112. A. Lewis, L. Tolhurst and P. Stratford, *Biomaterials*, **2002**, *23*, 1697-1706.

113. D. L. Rabenstein, *Nat Prod Rep*, **2002**, *19*, 312-331.

114. D. M. Hylton, S. W. Shalaby and R. A. Latour, *J Biomed Mater Res A*, **2005**, *73A*, 349-358.

115. N. Ayres, D. Holt, C. Jones, L. Corum and D. Grainger, *J Polym Sci, Part A: Polym Chem*, **2008**, *46*, 7713-7724.

116. A. G. Kidane, H. Salacinski, A. Tiwari, K. R. Bruckdorfer and A. M. Seifalian, *Biomacromolecules*, **2004**, *5*, 798-813.

117. S. E. Sakiyama-Elbert, *Acta Biomater*, **2013**, *10*, 1581-1587.

118. S. Wan Kim and H. Jacobs, *Blood Purif*, **1996**, *14*, 357-372.

119. O. Larm, R. Larsson and P. Olsson, *Biomater Med Devices Artif Organs*, **1983**, *11*, 161-173.

120. G. Michanetzis, N. Katsala and Y. Missirlis, *Biomaterials*, **2003**, *24*, 677-688.

121. H. Miyara, N. Harumiya, Y. Mori and H. Tanzawa, *J Biomed Mater Res*, **1977**, *11*, 251-265.

122. J. M. Goddard and J. H. Hotchkiss, *Prog Polym Sci*, **2007**, *32*, 698-725.

123. G. H. Engbers and J. Feijen, *Int J Artif Organs*, **1991**, *14*, 199-215.

124. C. Gölander, H. Arwin, J. Eriksson, I. Lundstrom and R. Larsson, *Colloids Surf*, **1982**, *5*, 1-16.

125. B. Seifert, P. Romaniuk and T. Groth, *J Mater Sci Mater Med*, **1996**, *7*, 465-469.

126. C. Bamford and K. Al-Lamee, *Polymer*, **1996**, *37*, 4885-4889.

127. Y. Byun, H. A. Jacobs and S. W. Kim, *J Biomater Sci, Polym Ed*, **1994**, *6*, 1-13.

128. K. D. Park, T. Okano, C. Nojiri and S. W. Kim, *J Biomed Mater Res*, **1988**, *22*, 977-992.

129. C. Arnander, D. Bagger-Sjoebaeck, S. Frebelius, R. Larsson and J. Swedenborg, *Biomaterials*, **1987**, *8*, 496-499.

130. L. Vroman, *Bull N Y Acad Med*, **1988**, *64*, 352.

131. H. P. Wendel and G. Ziemer, *Eur J Cardiothorac Surg*, **1999**, *16*, 342-350.

132. J. F. Keuren, S. J. Wielders, G. M. Willems, M. Morra and T. Lindhout, *Thromb Haemost*, **2002**, *87*, 742-747.

133. N. Weber, H. P. Wendel and G. Ziemer, *Biomaterials*, **2002**, *23*, 429-439.

134. C. Sperling, M. Houska, E. Brynda, U. Streller and C. Werner, *J Biomed Mater Res A*, **2006**, *76*, 681-689.

135. C. Werner, M. F. Maitz and C. Sperling, *J Mater Chem*, **2007**, *17*, 3376-3384.

136. M. W. Vaughn, *Am J Physiol Heart Circ Physiol*, **1998**, *274*, H2163-H2176.

137. M. C. Frost, M. M. Reynolds and M. E. Meyerhoff, *Biomaterials*, **2005**, *26*, 1685-1693.

138. A. B. Seabra, P. D. Marcato, L. B. de Paula and N. Durán, *J Nano Res*, **2012**, *20*, 61-67.

139. D. A. Riccio and M. H. Schoenfisch, *Chem Soc Rev*, **2012**, *41*, 3731-3741.

140. J. Kim, G. Saravanakumar, H. W. Choi, D. Park and W. J. Kim, *J Mater Chem B Mater Biol Med*, **2014**, *2*, 341-356.

141. M. C. Jen, M. C. Serrano, R. van Lith and G. A. Ameer, *Adv Funct Mater*, **2012**, *22*, 239-260.

142. G. M. Halpenny and P. K. Mascharak, *Anti-Infect Agents Med Chem* **2010**, *9*, 187-197.

143. A. A. Eroy-Reveles and P. K. Mascharak, *Future Med Chem*, **2009**, *1*, 1497-1507.

144. A. W. Carpenter and M. H. Schoenfisch, *Chem Soc Rev*, **2012**, *41*, 3742-3752.

145. K. A. Mowery, M. H. Schoenfisch, J. E. Saavedra, L. K. Keefer and M. E. Meyerhoff, *Biomaterials*, **2000**, *21*, 9-21.

146. A. M. Skrzypchak, N. G. Lafayette, R. H. Bartlett, Z. Zhou, M. C. Frost, M. E. Meyerhoff, M. M. Reynolds and G. M. Annich, *Perfusion*, **2007**, *22*, 193-200.

147. M. M. Batchelor, S. L. Reoma, P. S. Fleser, V. K. Nuthakki, R. E. Callahan, C. J. Shanley, J. K. Politis, J. Elmore, S. I. Merz and M. E. Meyerhoff, *J Med Chem*, **2003**, *46*, 5153-5161.

148. P. S. Fleser, V. K. Nuthakki, L. E. Malinzak, R. E. Callahan, M. L. Seymour, M. M. Reynolds, S. I. Merz, M. E. Meyerhoff, P. J. Bendick, G. B. Zelenock and C. J. Shanley, *J Vasc Surg*, **2004**, *40*, 803-811.

149. D. J. Smith, D. Chakravarthy, S. Pulfer, M. L. Simmons, J. A. Hrabie, M. L. Citro, J. E. Saavedra, K. M. Davies, T. C. Hutsell, D. L. Mooradian, S. R. Hanson and L. K. Keefer, *J Med Chem*, **1996**, *39*, 1148-1156.

150. G. M. Annich, J. P. Meinhardt, K. A. Mowery, B. A. Ashton, S. I. Merz, R. B. Hirschl, M. E. Meyerhoff and R. H. Bartlett, *Crit Care Med*, **2000**, *28*, 915-920.

151. H. Zhang, G. M. Annich, J. Miskulin, K. Osterholzer, S. I. Merz, R. H. Bartlett and M. E. Meyerhoff, *Biomaterials*, **2002**, *23*, 1485-1494.

152. S. M. Marxer, A. R. Rothrock, B. J. Nablo, M. E. Robbins and M. H. Schoenfisch, *Chem Mater*, **2003**, *15*, 4193-4199.

153. B. J. Nablo and M. H. Schoenfisch, *Biomaterials*, **2005**, *26*, 4405-4415.

154. E. M. Hetrick and M. H. Schoenfisch, *Biomaterials*, **2007**, *28*, 1948-1956.

155. A. Koh, A. W. Carpenter, D. L. Slomberg and M. H. Schoenfisch, *ACS Appl Mater Interfaces*, **2013**, *5*, 7956-7964.

156. A. Koh, D. A. Riccio, B. Sun, A. W. Carpenter, S. P. Nichols and M. H. Schoenfisch, *Biosens Bioelectron*, **2011**, *28*, 17-24.

157. J. H. Shin, S. K. Metzger and M. H. Schoenfisch, *J Am Chem Soc*, **2007**, *129*, 4612-4619.

158. J. H. Shin and M. H. Schoenfisch, *Chem Mater*, **2008**, *20*, 239-249.

159. Y. Lu, B. Sun, C. H. Li and M. H. Schoenfisch, *Chem Mater*, **2011**, *23*, 4227-4233.

160. N. A. Stasko and M. H. Schoenfisch, *J Am Chem Soc*, **2006**, *128*, 8265-8271.

161. B. Sun, D. L. Slomberg, S. L. Chudasama, Y. Lu and M. H. Schoenfisch, *Biomacromolecules*, **2012**, *13*, 3343-3354.

162. S. M. Lantvit, B. J. Barrett and M. M. Reynolds, *J Biomed Mater Res A*, **2013**, *101*, 3201-3210.

163. Y. Wu, Z. Zhou and M. E. Meyerhoff, *J Biomed Mater Res A*, **2007**, *81*, 956-963.

164. T. C. Major, D. O. Brant, M. M. Reynolds, R. H. Bartlett, M. E. Meyerhoff, H. Handa and G. M. Annich, *Biomaterials*, **2010**, *31*, 2736-2745.

165. H. Handa, E. J. Brisbois, T. C. Major, L. Refahiyat, K. A. Amoako, G. M. Annich, R. H. Bartlett and M. E. Meyerhoff, *J Mater Chem B Mater Biol Med*, **2013**, *1*, 3578-3587.

166. H. Handa, T. C. Major, E. J. Brisbois, K. A. Amoako, M. E. Meyerhoff and R. H. Bartlett, *J Mater Chem B Mater Biol Med*, **2014**, *2*, 1059-1067.

167. H. Al-Sa'doni and A. Ferro, *Clin Sci*, **2000**, *98*, 507-520.

168. N. Hogg, *Free Radical Biol Med*, **2000**, *28*, 1478-1486.

169. N. Hogg, R. J. Singh and B. Kalyanaraman, *FEBS Lett*, **1996**, *382*, 223-228.

170. E. J. Langford, A. S. Brown, R. J. Wainwright, A. J. Debelder, M. R. Thomas, R. E. A. Smith, M. W. Radomski, J. F. Martin and S. Moncada, *Lancet*, **1994**, *344*, 1458-1460.

171. M. W. Radomski, D. D. Rees, A. Dutra and S. Moncada, *Br J Pharmacol*, **1992**, *107*, 745-749.

172. E. Salas, M. A. Moro, S. Askew, H. F. Hodson, A. R. Butler, M. W. Radomski and S. Moncada, *Br J Pharmacol*, **1994**, *112*, 1071-1076.

173. G. F. P. de Souza, J. K. U. Yokoyama-Yasunaka, A. B. Seabra, D. C. Miguel, M. G. de Oliveira and S. R. B. Uliana, *Nitric Oxide*, **2006**, *15*, 209-216.

174. E. Salas, E. J. Langford, M. T. Marrinan, J. F. Martin, S. Moncada and A. J. de Belder, *Heart*, **1998**, *80*, 146-150.

175. J. Albert, M. Daleskog and N. H. Wallen, *Thromb Res*, **2001**, *102*, 161-165.

176. K. F. S. Ricardo, S. M. Shishido, M. G. de Oliveira and M. H. Krieger, *NITRIC OXIDE-BIOL CH*, **2002**, *7*, 57-66.

177. A. P. Dicks, H. R. Swift, D. L. H. Williams, A. R. Butler, H. H. Al-Sa'doni and B. G. Cox, *J Chem Soc, Perkin Trans 2*, **1996**, 481-487.

178. D. J. Sexton, A. Muruganandam, D. J. McKenney and B. Mutus, *Photochem Photobiol*, **1994**, *59*, 463-467.

179. P. D. Wood, B. Mutus and R. W. Redmond, *Photochem Photobiol*, **1996**, *64*, 518-524.

180. M. C. Frost and M. E. Meyerhoff, *J Am Chem Soc*, **2004**, *126*, 1348-1349.

181. S. l. M. Shishido, A. B. Seabra, W. Loh and M. Ganzarolli de Oliveira, *Biomaterials*, **2003**, *24*, 3543-3553.

182. A. B. Seabra and M. G. de Oliveira, *Biomaterials*, **2004**, *25*, 3773-3782.

183. A. B. Seabra, G. F. P. de Souza, L. L. da Rocha, M. N. Eberlin and M. G. de Oliveira, *NITRIC OXIDE-BIOL CH*, **2004**, *11*, 263-272.

184. A. B. Seabra, L. L. Da Rocha, M. N. Eberlin and M. G. De Oliveira, *J Pharm Sci*, **2005**, *94*, 994-1003.

185. M. Simoes and M. G. de Oliveira, *J Biomed Mater Res B Appl Biomater*, **2010**, *93B*, 416-424.

186. E. J. Brisbois, H. Handa, T. C. Major, R. H. Bartlett and M. E. Meyerhoff, *Biomaterials*, **2013**, *34*, 6957-6966.

187. J. M. Joslin, S. M. Lantvit and M. M. Reynolds, *ACS Appl Mater Interfaces*, **2013**, *5*, 9285-9294.

188. D. A. Riccio, K. P. Dobmeier, E. M. Hetrick, B. J. Privett, H. S. Paul and M. H. Schoenfisch, *Biomaterials*, **2009**, *30*, 4494-4502.

189. D. A. Riccio, P. N. Coneski, S. P. Nichols, A. D. Broadnax and M. H. Schoenfisch, *ACS Appl Mater Interfaces*, **2012**, *4*, 796-804.

190. P. N. Coneski and M. H. Schoenfisch, *Polym Chem*, **2011**, *2*, 906-913.

191. M. C. Frost and M. E. Meyerhoff, *J Biomed Mater Res A*, **2005**, *72A*, 409-419.

192. P. N. Coneski, K. S. Rao and M. H. Schoenfisch, *Biomacromolecules*, **2010**, *11*, 3208-3215.

193. V. B. Damodaran, L. W. Place, M. J. Kipper and M. M. Reynolds, *J Mater Chem*, **2012**, *22*, 23038-23048.

194. V. B. Damodaran and M. M. Reynolds, *J Mater Chem*, **2011**, *21*, 5870-5872.

195. V. B. Damodaran, J. M. Joslin, K. A. Wold, S. M. Lantvit and M. M. Reynolds, *J Mater Chem*, **2012**, *22*, 5990-6001.

196. A. B. Seabra, D. Martins, M. Simoes, R. da Silva, M. Brocchi and M. G. de Oliveira, *Artif Organs*, **2010**, *34*, E204-E214.

197. A. B. Seabra, R. Da Silva, G. F. P. De Souza and M. G. De Oliveira, *Artif Organs*, **2008**, *32*, 262-267.

198. Y. Li and P. I. Lee, *Mol Pharm*, **2009**, *7*, 254-266.

199. G. E. Gierke, M. Nielsen and M. C. Frost, *Sci Technol Adv Mat*, **2011**, *12*, 055007.

200. N. A. Stasko, T. H. Fischer and M. H. Schoenfisch, *Biomacromolecules*, **2008**, *9*, 834-841.

201. D. A. Riccio, J. L. Nugent and M. H. Schoenfisch, *Chem Mater*, **2011**, *23*, 1727-1735.

202. X. Duan and R. S. Lewis, *Biomaterials*, **2002**, *23*, 1197-1203.

203. H. Gappa-Fahlenkamp and R. S. Lewis, *Biomaterials*, **2005**, *26*, 3479-3485.

204. B. K. Oh and M. E. Meyerhoff, *J Am Chem Soc*, **2003**, *125*, 9552-9553.

205. B. K. Oh and M. E. Meyerhoff, *Biomaterials*, **2004**, *25*, 283-293.

206. S. Hwang and M. E. Meyerhoff, *Biomaterials*, **2008**, *29*, 2443-2452.

207. S. C. Puiu, Z. Zhou, C. C. White, L. J. Neubauer, Z. Zhang, L. E. Lange, J. A. Mansfield, M. E. Meyerhoff and M. M. Reynolds, *J Biomed Mater Res Part B Appl Biomater*, **2009**, *91B*, 203-212.

208. T. C. Major, D. O. Brant, C. P. Burney, K. A. Amoako, G. M. Annich, M. E. Meyerhoff, H. Handa and R. H. Bartlett, *Biomaterials*, **2011**, *32*, 5957-5969.

209. G. Mugesh and H. B. Singh, *Chem Soc Rev*, **2000**, *29*, 347-357.

210. Y. Hou, Z. Guo, J. Li and P. G. Wang, *Biochem Biophys Res Commun*, **1996**, *228*, 88-93.

211. J. Yang, J. L. Welby and M. E. Meyerhoff, *Langmuir*, **2008**, *24*, 10265-10272.

212. W. Cha and M. E. Meyerhoff, *Biomaterials*, **2007**, *28*, 19-27.

213. W. Cai, J. Wu, C. Xi, A. J. Ashe Iii and M. E. Meyerhoff, *Biomaterials*, **2011**, *32*, 7774-7784.

214. M. M. Reynolds, M. C. Frost and M. E. Meyerhoff, *Free Radical Biol Med*, **2004**, *37*, 926-936.

215. M. V. Sefton, C. H. Gemmell and M. B. Gorbet, *J Biomat Sci-Polym E*, **2000**, *11*, 1165-1182.

216. W. Lemm, V. Unger and E. S. Bucherl, *Med Biol Eng Comput*, **1980**, *18*, 521-526.

217. C. Kirkpatrick and C. Mittermayer, *J Mater Sci Mater Med*, **1990**, *1*, 9-13.

218. M. V. Sefton, *J Biomed Mater Res*, **2001**, *55*, 445-446.

219. U. T. Seyfert, V. Biehl and J. Schenk, *Biomol Eng*, **2002**, *19*, 91-96.

220. S. Braune, M. Grunze, A. Straub and F. Jung, *Biointerphases*, **2013**, *8*, 1-9.

221. B. D. Ratner, in *Contemporary Biomaterials: Material and Host Response, Clinical Applications, New Technology and Legal Aspects Noyes Publications*, **1984**, pp. 193-204.

222. S. R. Hanson and B. Ratner, in *Biomaterials science: an introduction to materials in medicine San Diego*, **2004**, pp. 367-378.

223. B. D. Ratner and T. A. Horbett, in *Biomaterials Science (Third Edition)*, eds. B. D. Ratner, A. S. Hoffman, F. J. Schoen and J. E. Lemons, Academic Press, **2013**, pp. 617-634.

224. M. V. Sefton, A. Sawyer, M. Gorbet, J. P. Black, E. Cheng, C. Gemmell and E. Pottinger-Cooper, *J Biomed Mater Res*, **2001**, *55*, 447-459.

225. A. G. Gristina, *Science*, **1987**, *237*, 1588-1595.

226. R. Tzoneva, M. Heuchel, T. Groth, G. Altankov, W. Albrecht and D. Paul, *J Biomater Sci Polym Ed*, **2002**, *13*, 1033-1050.

227. C. L. Haycox and B. D. Ratner, *J Biomed Mater Res*, **1993**, *27*, 1181-1193.

228. E. J. Brisbois, H. Handa and M. E. Meyerhoff, in *Advanced Polymers in Medicine*, ed. F. Puoci, Springer-Verlag Ltd., **2014 (in press)**.

229. E. J. Brisbois, J. Bayliss, J. Wu, T. C. Major, C. Xi, S. C. Wang, R. H. Bartlett, H. Handa and M. E. Meyerhoff, **2014 (submitted to Acta Biomater)**.

CHAPTER 2

Long-Term Nitric Oxide Release and Elevated Temperature Stability with *S*-Nitroso-*N*-acetylpenicillamine (SNAP)-Doped Elast-eon E2As Polymer

2.1 Introduction

Nitric oxide (NO) is an endogenous gas molecule that plays several key physiological roles, including prevention of platelet adhesion and activation, inhibiting bacterial adhesion and proliferation, enhancing vasodilation, promoting angiogenesis, and aiding in wound healing.[1-10] The effects of NO are highly dependent on the location and its concentration in the physiological system.[11] For example, endothelial cells that line the inner walls of healthy blood vessels produce an estimated NO surface flux of 0.5-4.0x10^{-10} mol cm^{-2} min^{-1}.[12] The function of many blood-contacting devices, including vascular grafts, stents, intravascular sensors, intravascular catheters, and extracorporeal life support circuits, can be impaired due to platelet activation and thrombus formation.[13, 14] One approach to improve the hemocompatibility of such devices is the use of coating materials that mimic the endothelial cells with respect to NO release. Indeed, in recent years there has been considerable interest in developing NO-releasing/generating materials that can be used to improve the biocompatibility of such devices.[15-23]

Nitric oxide is highly reactive under physiological conditions and thus a wide range of NO donor molecules, with functional groups that can store and release NO, have been studied for potential biomedical applications. Such molecules include organic nitrates, metal-NO complexes, *N*-diazeniumdiolates, and *S*-nitrosothiols (RSNOs).[4, 24] Physiological RSNOs, such as *S*-nitrosohemoglobin and *S*-nitrosoglutathione (GSNO), are considered an endogenous reservoir of NO *in vivo*.[4, 25-27] Other synthetic RSNOs,

such as *S*-nitroso-*N*-acetyl-*L*-cysteine (SNAC) and *S*-nitroso-*N*-acetylpenicillamine (SNAP, **Figure 2.1A**) have been shown to exhibit significant antimicrobial and antithrombotic effects.[28-31] It has also been demonstrated that RSNOs are both vasodilators and potent inhibitors of platelet aggregation.[32, 33] RSNOs undergo thermal decomposition releasing NO and producing a corresponding disulfide species (RSSR), as shown in **Figure 2.1B**. The NO release from RSNOs can be catalyzed by metal ions (e.g., Cu^{+})[34] and by light, through the irradiation at energies that correspond to the *S*-nitroso absorption bands at 340 and/or 590 nm.[35-37] It has been suggested that the more potent activity of RSNOs vs. NO as antiplatelet agents arises from the enhanced stability of RSNOs vs. NO, and generation of NO from RSNOs locally at the surface of platelets by membrane proteins that contain catalytic sites to convert RSNOs to NO.[38]

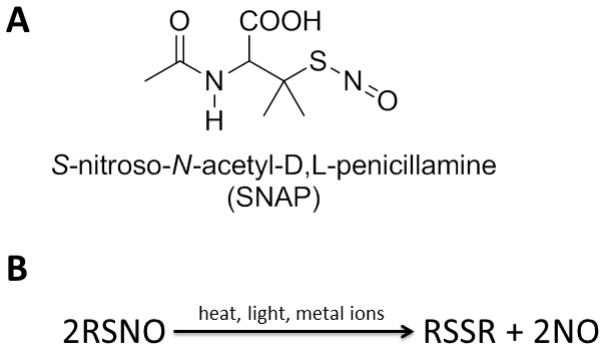

Figure 2.1. Structure of (A) *S*-nitroso-*N*-acetylpenicillamine (SNAP) and (B) scheme of *S*-nitrosothiol (RSNO) decomposition, which can be catalyzed by metal ions (e.g. Cu^{+}), light, and heat, yielding the disulfide (RSSR) product and nitric oxide (NO).

Incorporation of RSNOs into polymers can extend the utility of these NO donors to be applicable as coatings in biomedical devices, providing localized NO release at the blood/device interface. Several NO-release polymers consisting of small-molecule RSNOs dispersed in various polymer matrices, including polyethylene glycol (PEG), poly(vinyl alcohol), poly(vinyl pyrrolidone), and Pluronic F127 hydrogel, have been reported.[22, 23, 39-42] These materials have potential applications for topical NO delivery on wounds via the diffusion of the hydrophilic RSNOs from the polymer to the tissue. In fact, daily application of a GSNO-containing hydrogel has been shown to accelerate the wound healing process.[42] However, the rapid leaching of the RSNOs from such polymers can significantly shorten the NO/RSNO release lifetime, lasting only several

hours.[22, 39, 40] An alternate approach has been to synthesize RSNO-modified materials, where the RSNO functionality is covalently bound to the matrix. Fumed silica particles,[18] dendrimers,[43] polyurethanes,[16] polyesters,[15, 44-46] poly(dimethylsiloxane) (PDMS),[19] xerogels,[47, 48] self-assembled monolayers,[49] and poly(vinyl methyl ether-*co*-maleic anhydride) (PVMMA)[50] have all been modified with RSNO functionalities. Ricco et al. reported RSNO-modified xerogels that release NO for up to 14 d and exhibit reduced platelet and bacterial adhesion.[47, 48] However, such RSNO-modified xerogels suffer from synthesis complications leading to cracking and non-uniform films, low RSNO conversion efficiency (maximum of 40% for the tertiary RSNO-modified xerogels), and thermal instability at room temperature that would limit their shelf-life. Many of the other RSNO modified materials reported to date exhibit both thermal and photoinitiated NO release, but these materials have not proven clinically useful due to their limited NO release lifetimes, low conversion to RSNO during synthesis, or lack of RSNO stability during storage This lack of stability of most NO release materials reported to date could pose a significant hurdle with regard to commercializing medical devices that employ such materials, owing to the increased shipping costs to protect products from thermal degradation, etc. This could prevent the application of NO release materials in the biomedical market regardless of their potential benefits.

Another reported approach to achieve localized NO delivery at a polymer/blood interface is to use NO-generating coatings, in which immobilized catalysts (Cu(I/II) or organoselenium species) can generate NO from endogenous RSNOs.[20, 51-53] Recently, a NO generating coating containing Cu^0 nanoparticles was evaluated using a rabbit model for extracorporeal circulation (ECC).[20] However, to achieve good efficacy in reducing thrombus formation, continuous infusion of SNAP was required to supplement the endogenous RSNO levels.

As an alternative to the continuous infusion of RSNO species, in this study we investigate several biomedical polymers that are capable of storing RSNO species. Such RSNO-doped coatings can release NO as well as potentially supplement the endogenous RSNO levels, if NO generating catalysts are also employed. Five biomedical polymers are examined for their potential to act as a storage reservoir for SNAP (**Figure 2.2**).

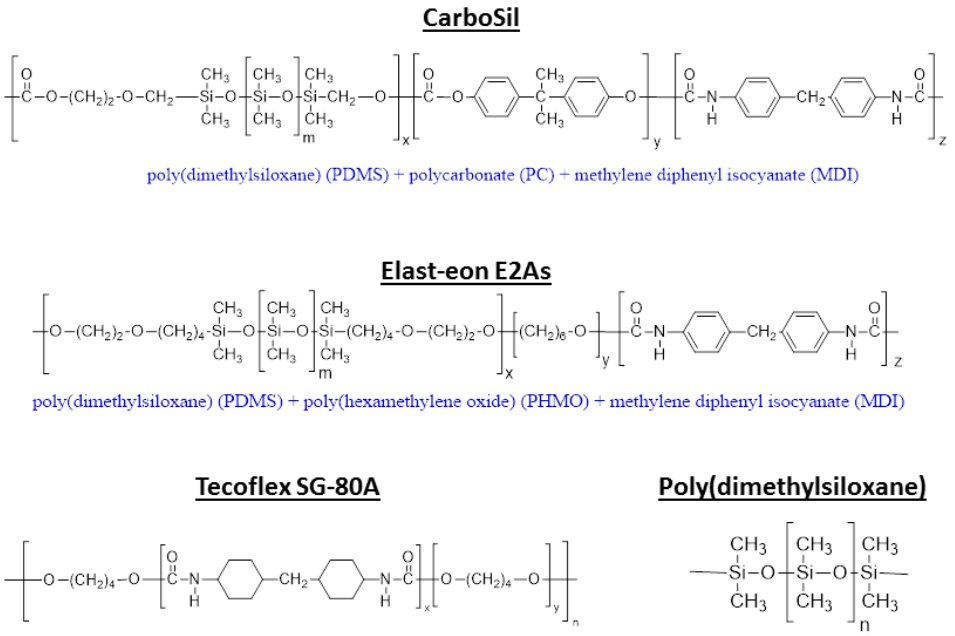

Figure 2.2. Structures of biomedical grade polymers.

These include: silicone rubber (poly(dimethylsiloxane)); Elast-eon E2As (a copolymer with a mixed soft segment of poly(dimethylsiloxane) and poly(hexamethylene oxide) with a methylene diphenyl isocyanate (MDI) hard segment); CarboSil (a thermoplastic urethane copolymer with a mixed soft segment of poly(dimethylsiloxane) and hydroxyl-terminated polycarbonate with a hard segment of an aromatic diisocyanate, MDI); Tecoflex SG-80A (a poly(tetramethylene glycol) polyurethane capped with diisocyanatodicyclohexylmethane); and Tecophillic SP-60D-60 (an aliphatic, hydrophilic polyether-based polyurethane). Each of the SNAP-doped polymers are examined as films or coatings that can release NO thermally (at physiological temperature) and/or can serve as a reservoir to supplement endogenous RSNO levels (by SNAP diffusion into blood from the polymer). The SNAP-doped polymers are characterized for their *in vitro* NO/SNAP release, where the more hydrophobic polymers are expected to have slower SNAP/NO release under physiological conditions. The Elast-eon polymer has been reported to have excellent intrinsic biocompatibility and biostability properties, and exhibits low levels of blood protein adhesion.[54, 55] Therefore, the SNAP/E2As polymer is further tested for the stability of SNAP during a 4-month storage period, in order to ascertain any self-life concerns. The new SNAP/E2As

polymer is also examined for potential biomedical applications via an ECC rabbit model of thrombogenicity to assess preservation of platelet count and function, and thrombus area after 4 h of ECC.

2.2 Materials and Methods

2.2.1 Materials

N-Acetyl-DL-penicillamine (NAP), sodium chloride, potassium chloride, sodium phosphate dibasic, potassium phosphate monobasic, ethylenediaminetetraacetic acid (EDTA), tetrahydrofuran (THF), sulfuric acid and *N*,*N*-dimethylacetamide (DMAc) were purchased from Sigma-Aldrich (St. Louis, MO). Methanol, hydrochloric acid and sulfuric acid were obtained from Fisher Scientific (Pittsburgh, PA). Tecophilic SP-60D-60 and Tecoflex SG-80A were products of Lubrizol Advanced Materials Inc. (Cleveland, OH). Dow Corning RTV 3140 Silicone Rubber (SR) was purchased from Ellsworth Adhesives (Germantown, WI). CarboSil 20 90A was from the Polymer Technology Group (Berkeley, CA). Elast-eon^{TM} E2As was obtained from AorTech International, plc (Scoresby, Victoria, Australia). Human plasma fibrinogen containing $\geq$ 90% clottable proteins was a product of Calbiochem (La Jolla, CA) and fluorescein-labeled goat IgG (polyclonal) against denatured human fibrinogen was purchased from MP Biomedicals, LLC (Solon, OH). Black, polypropylene 96-well microtiter plates used for fluorescence measurements were obtained from Nalge Nunc International (Rochester, NY). All aqueous solutions were prepared with 18.2 MΩ deionized water using a Milli-Q filter (Millipore Corp., Billerica, MA). Phosphate buffered saline (PBS), pH 7.4, containing 138 mM NaCl, 2.7 mM KCl, 10 mM sodium phosphate, 100μM EDTA was used for all *in vitro* experiments.

2.2.2 Synthesis of SNAP

SNAP was synthesized using a modified version of a previously reported method.[56] Briefly, an equimolar ratio of NAP and sodium nitrite was added to a 1:1 mixture of water and methanol containing 2 M HCl and 2 M H_2SO_4. After 30 min of stirring, the reaction vessel was cooled in an ice bath to precipitate the green SNAP

crystals. The crystals were collected by filtration, washed with water, and allowed to air dry. The reaction and crystals were protected from light at all times.

2.2.2 Preparation of SNAP-Doped Films

Polymer films containing 5 and 10 wt% SNAP were prepared by solvent evaporation. For the 10 wt% SNAP films, the casting solutions were prepared by dissolving 180 mg of the respective polymer in THF. The polyurethanes (SP-60D-60, SG-80A, CarboSil and Elast-eon E2As) were dissolved in 3 mL THF and SR was dissolved in 1 mL THF. SNAP (20 mg) was then added to the polymer solution and the mixture was stirred for 10 min. The 5 wt% SNAP films were prepared similarly with SNAP (10 mg) and polymer (190 mg). The film solution was cast in Teflon ring (d=2.5 cm) on a Teflon plate and dried overnight under ambient conditions. Small disks (d=0.7 cm) were cut from the parent films and were dip coated 2 times with a topcoat solution (200 mg polymer (no SNAP added) in 4 mL THF) and dried overnight under ambient conditions, followed by 48 h of drying under vacuum to remove any residual solvent. The weight of each small disk was recorded prior to top coating. All films and film solutions were protected from light. The thickness of the films before and after dip coating was measured using a Mitutoya digital micrometer. The final films had a SNAP-doped layer that was ~150 μm thick and a top coat layer that was ~50 μm thick.

2.2.3 Preparation of SNAP/E2As Coated ECC Loops

The ECC configuration employed in the *in vivo* rabbit study was previously described.[20, 21] Briefly, the ECC loops consisted of a 16-gauge and 14-gauge IV polyurethane angiocatheters (Kendall Monoject Tyco Healthcare Mansfield, MA), two 16 cm in length ¼ inch inner diameter (ID) Tygon™ tubing and an 8 cm length of 3/8 inch ID Tygon™ tubing that created a thrombogenicity chamber where thrombus could form more easily due to more turbulent blood flow.

Due to the short duration of the ECC experiments (4 h), the NO release ECC loops were coated with only 5 wt% SNAP in E2As. The SNAP/E2As solution was prepared by dissolving SNAP (125 mg) and E2As (2375 mg) in THF (15 mL). The E2As control solution consisted of E2As in THF (2500 mg in 15 mL). SNAP/E2As loops were

first coated with 2 layers of the SNAP/E2As solution, followed by 1 coat of the E2As control solution. E2As control loops were coated with 2 coats of the E2As control solution. ECC loops were allowed to air dry for 1 h in the dark between each coat. The completely coated ECC was welded together using THF, starting at the left carotid artery side, with the 16-gauge angiocatheter, one 15 cm length ¼ inch ID tubing, the 8 cm length thrombogenicity chamber, the second 15 cm length ¼ inch ID tubing and finally the 14-gauge angiocatheter. The angiocatheters were interfaced with tubing using two luer-lock PVC connectors. The assembled ECC loops were dried under vacuum while protected from light for at least 48 h. Prior to the ECC experiment, the loops were filled with saline solution for overnight soaking, and this solution was discarded immediately before the rabbit experiment.

2.2.4 Diffusion of SNAP from SNAP-Doped Polymer Films Immersed in PBS

All UV-Vis spectra were recorded in the wavelength range of 200-700 nm using a UV-Vis spectrophotometer (Lambda 35, Perkin-Elmer, MA) at room temperature. The presence of the S-NO group of SNAP provides characteristic absorbance maxima at 340 and 590 nm, corresponding to the $\pi \rightarrow \pi^*$ and $n_N \rightarrow \pi^*$ electronic transitions.[22, 37, 50]

Top coated films were placed in individual vials soaked in 10 mM PBS, pH 7.4, containing 100 μM EDTA to minimize any trace metal ion catalyzed decomposition of SNAP. Films were incubated in the dark at room temperature (22 ºC) or 37 ºC. At various time points the UV-Vis spectra of a 1 mL aliquot of the PBS was taken for rapid determination of the SNAP concentration. The aliquots were protected from light and were immediately returned to the sample vials for the duration of the experiment. The films were placed in fresh PBS buffer daily. The molar absorption coefficient for SNAP in PBS at 340 nm was determined to be: ε_{SNAP}=1024 M^{-1} cm^{-1}. PBS buffer was used as the blank. The % SNAP remaining in the film was determined by the difference between the amount of SNAP that had leached into the PBS and the initial amount of SNAP in the film.

2.2.5 Cumulative NO Release from SNAP/E2As Films

After the 10 wt% SNAP in E2As films were prepared, the UV-Vis spectra were recorded of individual films dissolved in DMAc to determine the initial concentration of SNAP within the films (nmol SNAP/mg film). Equivalent films were then placed in individual vials containing 3 mL PBS (pH 7.4) containing 100 μM EDTA. Films were incubated under various conditions: RT under ambient light, 37 ºC under ambient light, 37 ºC in dark, and 37 ºC under a 100W floodlight. These experiments were conducted in a basement lab without any windows, so the fluorescent lights in the laboratory are referred to as ambient light. Films were placed in fresh PBS daily. At various time points, the films were dissolved in DMAc for rapid determination of the SNAP present in the film. The amount of NO released was determined indirectly from the amount of SNAP decomposed at various time points. The cumulative NO released over time ($[NO]_t$) was calculated by the difference between the initial amount of SNAP in the film ($[SNAP]_0$) and the amount of SNAP at time *t* ($[SNAP]_t$): $[NO]_t = [SNAP]_0 - [SNAP]_t$ (where concentrations are in nmol/mg film). This calculation was based on the fact that the decay of the 340 nm absorption band of SNAP is directly associated with the homolytic cleavage of the S-NO bond and concomitant NO release. The molar absorption coefficient for SNAP in DMAc at 340 nm was determined to be: ε_{SNAP}=1025 M^{-1} cm^{-1}. DMAc was used as the blank.

2.2.6 NO Release Measurements

Nitric oxide released from the films was measured using a Sievers chemiluminescence Nitric Oxide Analyzer (NOA) 280 (Boulder, CO). Films were placed in the sample vessel immersed in PBS (pH 7.4) containing 100 μM EDTA. Nitric oxide was continuously purged from the buffer and swept from the headspace using an N_2 sweep gas and bubbler into the chemiluminescence detection chamber. Clear glass sample vessels were used for the ambient light and photoinitiated NO release experiments. A 100W halogen floodlight (GE model 17986) was used as a broad spectrum light source to initiate NO release and was placed ~60 cm from the sample cell for the photolysis experiments. Films were incubated in the PBS under the same

conditions as the NOA measurements (ambient light or 100W floodlight irradiation at 37 ºC).

2.2.7 SNAP/E2As Stability Study

SNAP/E2As films (consisting of 10 wt% SNAP) were placed under the following conditions in vials with desiccant: room temperature with ambient light, room temperature in dark, 37 ºC in dark, 50 ºC in dark, and in the freezer (-20 ºC) in dark. At various time points over a 4 month period, films were dissolved in DMAc and the UV-Vis spectra was recorded to determine the % SNAP remaining in the film, as compared to the initial 10 wt% SNAP.

2.2.8 In Vitro Fibrinogen Adsorption Assay

The *in vitro* fibrinogen adsorption immunofluorescence assay was performed in a 96-well format. The SNAP/E2As and E2As control polymer solutions used to prepare the ECC circuits were also employed to coat microwells of the 96-well microtiter plates and were dried under the same conditions as the ECC loops. Briefly, human fibrinogen was diluted to 3 mg/mL with Dulbecco's phosphate-buffered saline (dPBS) without $CaCl_2$ and $MgCl_2$ (Gibco Invitrogen, Grand Island, NY), equivalent to the human plasma concentration, and then used for adsorption experiments.[20] One hundred µL of this solution were added to each well and the coated wells were incubated with this solution for 1.5 h at 37 ºC. This was followed by eight washing steps using wash buffer (100 µL) for each wash, which consisted of a 10-fold dilution of the AbD Serotec Block ACE buffer (Raleigh, NC) containing 0.05% Tween 20 (Calbiochem La Jolla, CA). To block nonspecific antibody binding, coated wells were incubated with 100 µL of blocking buffer (4-fold dilution of Serotec Block ACE buffer) for 30 min at 37 ºC. After rinsing 3 times with wash buffer (100 µL per well), a background fluorescence measurement of the plates was performed at 485 nm (excitation) and 528 nm (emission) on a Synergy 2 fluorescence microplate reader (Biotek Winooski, VT). To detect the adsorbed fibrinogen, fluorescein-labeled goat anti-human fibrinogen antibody was diluted (1:10) in a 10-fold dilution of the Serotec Block ACE buffer and 100 µL of this final solution was added to each well. The antibody was allowed to bind to the surface-adsorbed fibrinogen

for 1.5 h at 37 ºC. Human fibrinogen adsorption to non-coated polypropylene was used as an internal control to normalize the fluorescence signals within different plates. All measurements were conducted in triplicate.

2.2.9 Rabbit ECC Thrombogenicity Experiments

Rabbit thrombogenicity protocol: All animal handling and surgical procedures employed were approved by the University Committee on the Use and Care of Animals in accordance with university and federal regulations. A total of 8 New Zealand white rabbits (Covance, Battle Creek, MI) were used in this study. All rabbits (2.5-3.5 kg) were initially anesthetized with intramuscular injections of 5 mg/kg xylazine injectable (AnaSed® Lloyd Laboratories Shenandoah, Iowa) and 30 mg/kg ketamine hydrochloride (Hospira, Inc. Lake Forest, IL).

Maintenance anesthesia was administered via isoflurane gas inhalation at a rate of 1.5-3% via mechanical ventilation which was done via a tracheotomy and using an A.D.S. 2000 Ventilator (Engler Engineering Corp. Hialeah, FL). Peek inspiratory pressure was set to 15 cm of H_2O and the ventilator flow rate set to 8 L/min. In order to aid in maintenance of blood pressure stability, IV fluids of Lactated Ringer's were given at a rate of 10 mL/kg/h. For monitoring blood pressure and collecting blood samples, the rabbits' right carotid artery were cannulated using a 16-gauge IV angiocatheter (Jelco®, Johnson & Johnson, Cincinnati, OH). Blood pressure and derived heart rate were monitored with a Series 7000 Monitor (Marquette Electronics Milwaukee, WI). Body temperature was monitored with a rectal probe and maintained at 37 ºC using a water-jacketed heating blanket. Prior to placement of the arteriovenous (A-V) custom-built extracorporeal circulation (ECC) circuit, the rabbit left carotid artery and right external jugular vein were isolated and baseline hemodynamics as well as arterial blood pH, PCO_2, PO_2, total hemoglobin and methemoglobin were measured using an ABL 825 blood-gas analyzer and an OSM3 Hemoximeter (Radiometer Copenhagen, DK). In addition, baseline blood samples were collected for platelet and total white blood cell (WBC) counts which were measured on a Coulter Counter Z1 (Coulter Electronics Hialeah, FL). Plasma fibrinogen levels were determined using a Dade Behring BCS Coagulation Analyzer (Siemens Deerfield, IL), activated clotting times (ACT) were

monitored using a Hemochron Blood Coagulation System Model 801 (International Technidyne Corp. Edison, NJ), and platelet function was assessed using a Chrono-Log optical aggregometer model 490 (Havertown, PA).

After baseline blood measurements, the A-V custom-built ECC was placed into position by cannulating the left carotid artery for ECC inflow and the right external jugular vein for ECC outflow. The flow through the ECC was initiated by unclamping the arterial and venous sides of ECC and blood flow in circuit was monitored with an ultrasonic flow probe and flow meter (Transonic HT207 Ithaca, NY). Animals were not systemically anticoagulated during the experiments.

After 4 h on ECC, the circuits were clamped, removed from animal, rinsed with 60 mL of saline and drained. Any residual thrombus in the larger tubing of ECC (i.e., thrombogenicity chamber) was photographed and the degree of thrombus was quantitated using Image J imaging software from National Institutes of Health (Bethesda, MD). Prior to euthanasia, all animals were given a dose of 400 U/kg sodium heparin to prevent necrotic thrombosis. The animals were euthanized using a dose of Fatal Plus (130 mg/kg sodium pentobarbital) (Vortech Pharmaceuticals, Dearborn, MI). All animals underwent gross necropsy after being euthanized, including examination of the lungs, heart, liver and spleen for any signs of thromboembolic events.

Blood Sampling: Rabbit whole blood samples were collected in non-anticoagulated 1 cc syringes for ACT, and in 3.2% sodium citrate vacutainers (Becton, Dickinson. Franklin Lakes, NJ) with 3 cc volumes for cell counts and aggregometry, and 1 cc syringes containing 40 U/mL of sodium heparin (APP Pharmaceuticals, LLC Schaumburg, IL) for blood-gas analysis. Following the initiation of ECC blood flow, blood samples were collected every hour for 4 h for these *in vitro* measurements. Samples were used within 2 h of collection to avoid any activation of platelets, monocytes or plasma fibrinogen.

Platelet Aggregometry: Rabbit platelet aggregation was assayed based on the Born's turbidimetric method using a Chrono-Log optical aggregometer. Briefly, citrated blood (1:10 blood to 3.2% sodium citrate solution) was collected (6 mL) and platelet-rich plasma (PRP) was obtained by centrifugation at 110 x g for 15 min. Platelet-poor plasma (PPP) was obtained by another centrifugation of the PRP-removed blood sample at 2730

x g for 15 min and was used as the blank for aggregation. PRP was incubated for 10 min at 37 ºC and then 25 µg/mL collagen (Chrono-PAR #385 Havertown, PA) was added. The percentage of aggregation was determined 3 min after the addition of collagen using Chrono-Log Aggrolink software.

2.2.10 Statistical Analysis

Data are expressed as mean ± SEM (standard error of the mean). Comparison between the various SNAP/E2As and E2As control polymer groups were analyzed by a comparison of means using student's *t*-test. Values of $p<0.05$ were considered statistically significant for all tests.

2.3 Results and Discussion

2.3.1 Preliminary In Vitro Characterization of Various SNAP-Doped Polymer Films

SNAP doped into all of the five biomedical polymers produced homogeneous and transparent films of green color, without any observable phase separation. The 10 wt% SNAP films stored approximately 0.42 µmol of SNAP per mg polymer film (or 6 µmol/cm^2). The diffusion of SNAP into PBS from the various polymer films containing 5 and 10 wt% SNAP was monitored using UV-Vis absorption. As shown in **Figure 2.3**, which illustrates the calculated % SNAP remaining in the films, all of the SNAP diffuses out of the SG-80A and SP-60D-60 polymer films during the first day of soaking in PBS at room temperature and at 37 ºC. The SP-60D-60 polymer is hydrophilic with a water uptake of ~60 wt%, while the SG-80A is more hydrophobic, having a water uptake of ~ 6 wt% (**Table 2.1**). All of the SNAP leaves the more hydrophilic SP-60D-60 polymer during the initial 2 h of soaking, while the more hydrophobic SG-80A leaches all of the SNAP after 24 h. The diffusion of SNAP from the polymers occurs more rapidly at elevated temperatures (room temperature vs. 37 ºC) where the higher temperature allows for the polymer to more rapidly absorb water. Due to the rapid loss of the SNAP from the SP-60D-60 and SG-80A polymers, a very large initial burst of NO is observed via

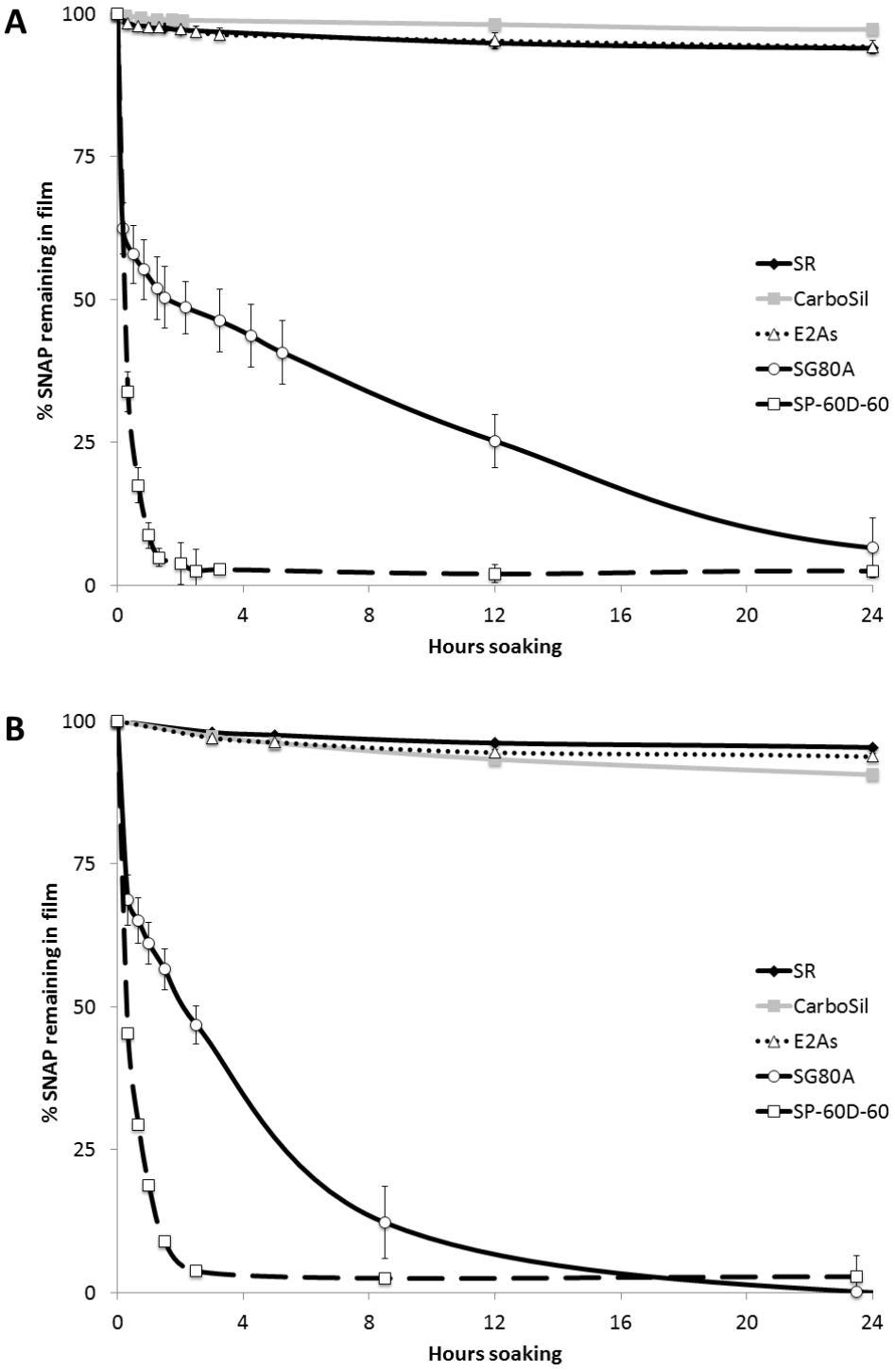

Figure 2.3. Percent of SNAP remaining in films (initially prepared with 10 wt% SNAP) after various durations of soaking in 4 mL PBS in the dark at room temperature, 22 ºC (A), or 37 ºC (B). Data are based on the difference between the amount of SNAP that leached from various polymers into the PBS, as monitored at 340 nm, and the initial amount of SNAP doped in the film. Data are the mean ± SEM (n=3).

Table 2.1. The water uptake of the 5 biomedical polymers used in this study. Polymers films (200 mg polymer) were cast in Teflon ring (d=2.5 cm) on Teflon plates. Small disks (d=0.7 cm) were cut from the parent films, weighed, and immersed in PBS for 48 h at 37 ºC. The wet films were wiped dry and weighed again. The water uptake of the polymer films are reported in weight percent as follows: water uptake (wt%) = $(W_{wet} - W_{dry})/W_{dry}$ x 100, where W_{wet} and W_{dry} are the weights of the wet and dry films, respectively.

Polymer	Water uptake [wt %]
Silicone Rubber	1.2 ± 0.3
CarboSil	1.5 ± 0.3
Elast-eon E2As	1.2 ± 0.1
Tecoflex SG80A	6.2 ± 0.7
Tecophilic SP-60D-60	64.5 ± 0.1

chemiluminescence (with NOA) during the first day of soaking (Day 0) and the films exhibit no SNAP/NO release after one day (data not shown). Therefore, these two polymers only provide a quick burst of NO/SNAP and were found not to be suitable for longer-term release of NO/SNAP.

In contrast, the silicone rubber, CarboSil, and E2As polymers exhibit significantly lower amounts of SNAP diffusing into the soaking buffer after one day (see **Figure 2.3**). For all three of these polymers, an initial burst of SNAP leaching is observed during the first day of soaking, corresponding to rapid water uptake by the polymer. This initial burst is ~10% of the total SNAP molecules incorporated into the films. Small amounts of SNAP continue to leach from these polymers during the subsequent days of soaking. Silicone rubber, CarboSil (a thermoplastic silicone-polycarbonate-urethane), and E2As (a siloxane-base polyurethane elastomer) all are hydrophobic polymers due to their high PDMS content[54, 57] and also have the lowest water uptake (see **Table 2.1**). SNAP is reported to be slightly hydrophobic.[58] Therefore, SNAP should have a preference for remaining in the more hydrophobic polymer phase. In addition, the hydrophobic property of these polymers also has a significant role in limiting the diffusion of SNAP into the buffer, due to the minimal water uptake of these polymers.

The thermal and photoinitiated NO release from the three SNAP-doped polymers was also studied by NOA measurements. Nitric oxide release can be turned on/off using the broad spectrum 100W floodlight for all 3 film types. As shown in **Figure 2.4**, there is

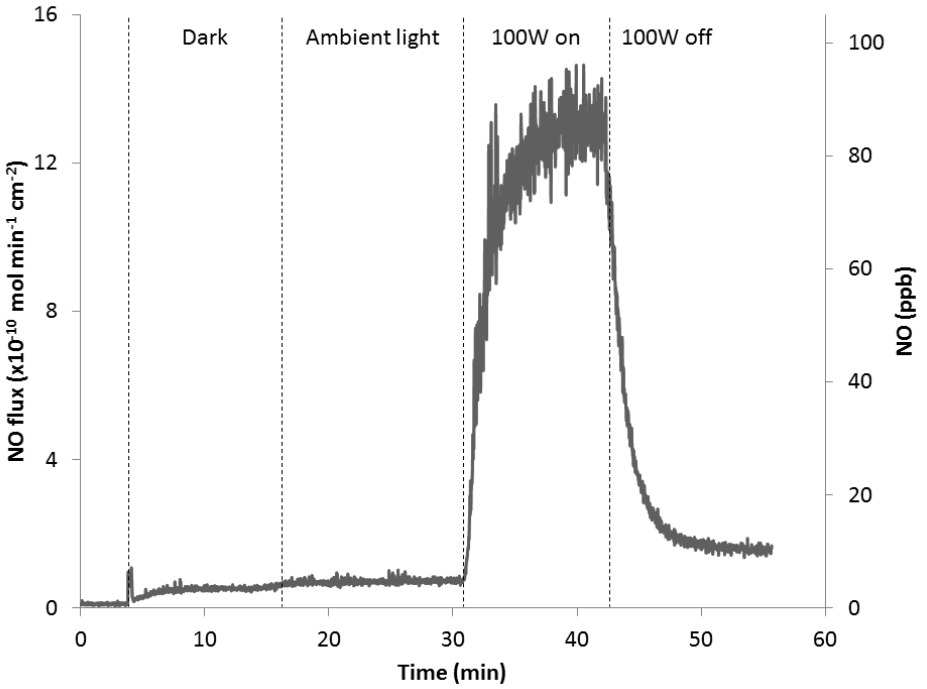

Figure 2.4. NO release behavior of 10 wt% SNAP/E2As film at 37 ºC in the dark, ambient light, and 100W floodlight.

little difference in the NO release from the films in the dark or under the ambient lab lights, since the ambient fluorescent laboratory lighting does not emit the wavelengths responsible for decomposing RSNOs (340 or 590 nm).[37] Fluorescent lights emit discrete wavelengths of light, whereas the 100W halogen floodlight is a broad spectrum light source. For all three polymers, the total NO release detected by the NOA for films continuously irradiated with the 100W floodlight is ~100% of the SNAP doped into the films. The photoinitiated NO release from these three films was examined by continuously irradiating with a 100W floodlight at 37 ºC and monitoring the NO released with the NOA (**Figure 2.5A**). The SNAP-doped E2As and CarboSil films exhibit a gradual decrease in the photo-induced NO flux over a 3 d period, while the SR-based films release NO for only 2 days under the same conditions. All three types of films incubated at 37 ºC under ambient light yielded an initial burst of NO on the first day of soaking, corresponding to release of SNAP into the solution, and on subsequent days, the NO flux is 1-2 x 10^{-10} mol cm^{-2} min^{-1}, still potentially useful to inhibit platelet function and kill bacteria.[11, 12] The NO release is most promising from the film composed of 10 wt% SNAP in E2As under the 100W floodlight. Therefore, the wt% of SNAP in E2As

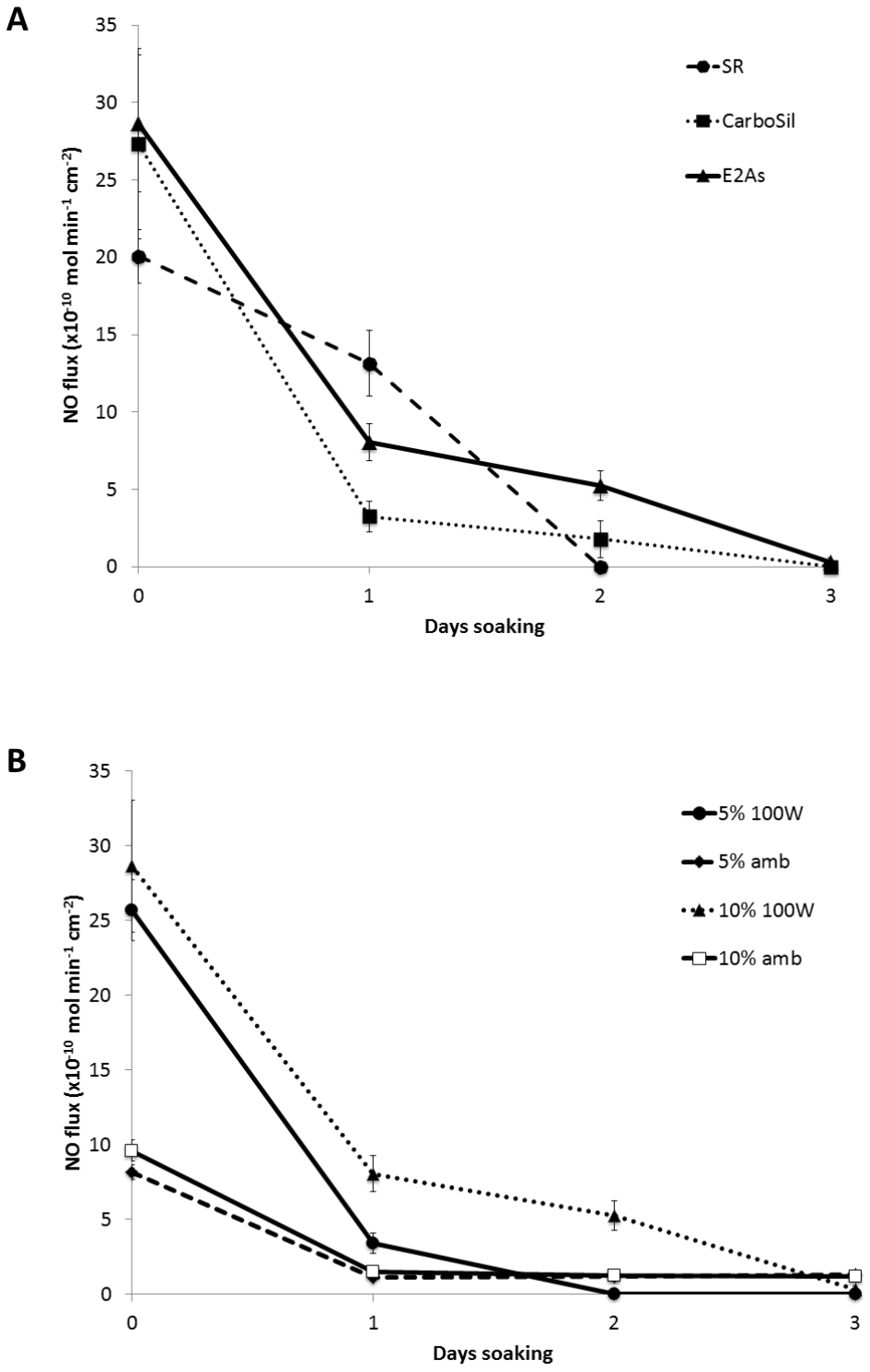

Figure 2.5. (A) NO release from 10 wt% SNAP in silicone rubber (SR), CarboSil, and Elast-eon E2As films at 37 ºC and continuously irradiated with the 100W floodlight. (B) NO release from 5 and 10 wt% SNAP in Elast-eon E2As films at 37 ºC continuously under ambient light (amb) or the 100W floodlight. Data are the mean ± SEM (n=3).

was varied and examined in more detail (**Figure 2.5B**). The NO release and SNAP leaching pattern is similar for a 5 wt% SNAP/E2As film, but the NO release takes place over a shorter time period. The biostability and biocompatibility of the Elast-eon polymer in combination with the NO release from SNAP makes this formulation most attractive for further *in vitro* studies and potential biomedical applications.

2.3.2 Long-Term NO Release of SNAP/E2As Formulation

In vitro studies were conducted with the SNAP/E2As films to examine the long-term NO release and SNAP leaching from these films. The NO release from the SNAP/E2As films over time was determined based on the amount of SNAP decomposed within the polymer phase (i.e., by measuring the SNAP remaining after dissolving the films at given time points). The initial concentration of SNAP in the 10 wt% films is 420 nmol SNAP/mg film. **Figure 2.6A** shows the UV-Vis spectra of 1.0 mM SNAP solution, a 10 wt% SNAP in E2As film redissolved in *N,N*-dimethylacetamide (DMAc), and E2As dissolved in DMAc. Due to thermal and/or photochemical decomposition of SNAP, a decrease in the 340 nm absorbance band is observed as films are soaked in PBS and the cumulative NO release based on that absorbance decrease is shown in **Figure 2.6B**. The films display an initial burst of NO during the first day of soaking (**Figure 2.3**), which corresponds to the thermal decomposition as well as diffusion of SNAP out of the film. Films soaked at room temperature have the lowest flux of NO release. However, films incubated at 37 ºC in the dark or under ambient light exhibit a higher NO release than the films at room temperature. This is due to the increased thermal decomposition of SNAP. The films that are exposed to ambient light yield essentially the same NO release profiles as the films that are soaked in the dark. Nitric oxide release from the SNAP/E2As films that are continuously irradiated with the 100W floodlight at 37 ºC only release NO for 3 d due to their higher NO fluxes that rapidly deplete the SNAP reservoir. These films can provide NO release via both a thermal and photoinitiated decomposition of SNAP.

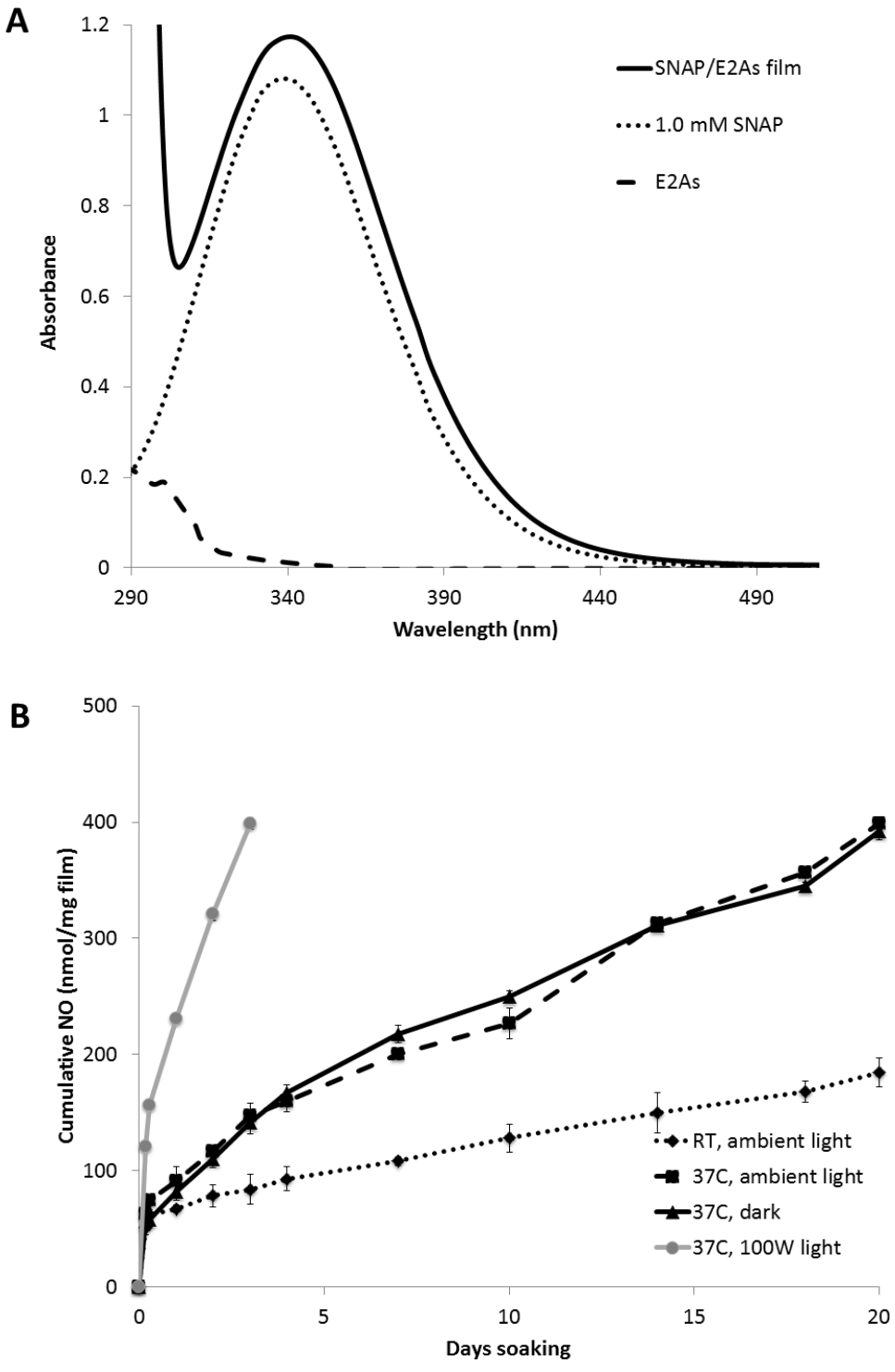

Figure 2.6. (A) UV-Vis spectra of a 10 wt% SNAP/E2As film, 1.0 mM SNAP, and E2As dissolved in *N*,*N*-dimethylacetamide (DMAc). (B) Cumulative NO release from 10 wt% SNAP/E2As films incubated in PBS under various conditions: room temperature (22 ºC) with ambient light, 37 ºC in the dark, 37 ºC under ambient light, and 37 ºC under the 100W floodlight. Data are the mean ± SEM (n=3).

In order to better understand the NO release mechanism of the SNAP/E2As coating, the SNAP diffusion into PBS was monitored over a 20 d period. As shown in **Figure 2.7A**, the films containing 10 wt% SNAP at 37 ºC exhibit an initial burst of SNAP leaching on the first day. After this initial burst, small amounts of SNAP continue

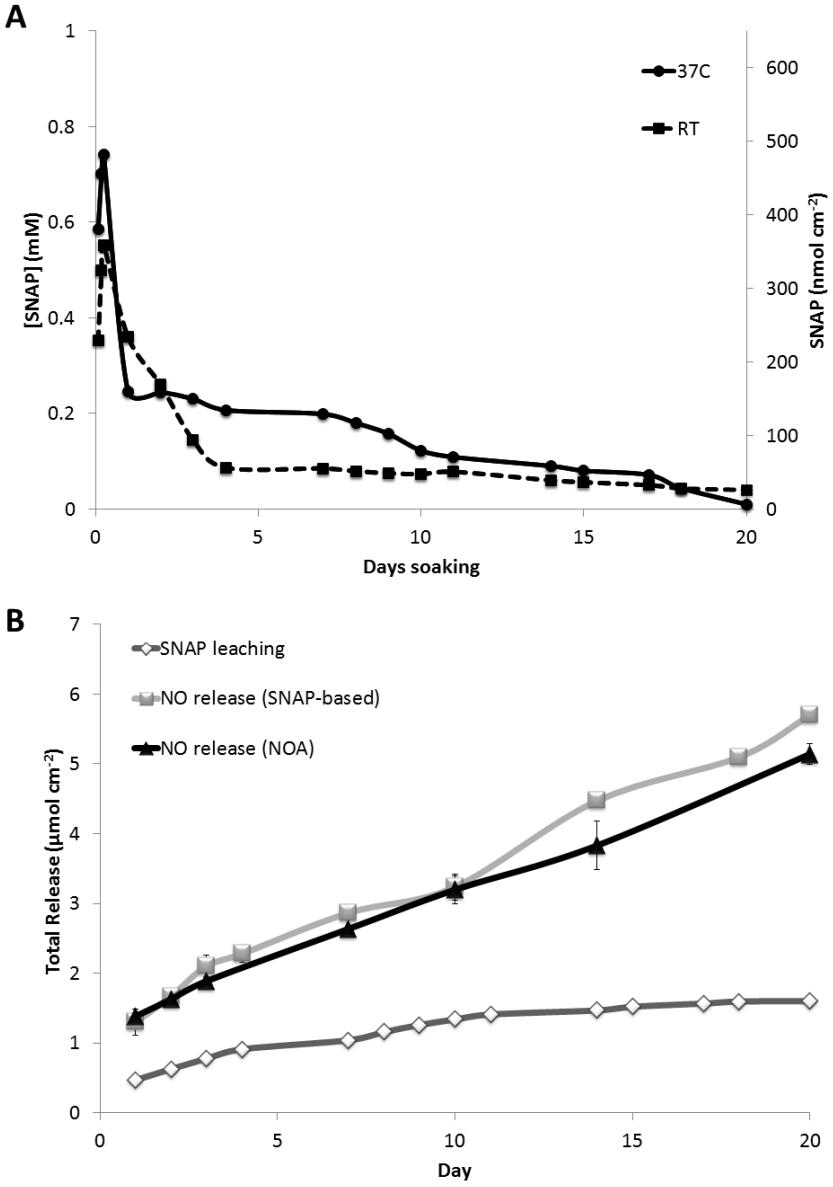

Figure 2.7. (A) Diffusion of SNAP from 10 wt% SNAP-doped E2As films soaking in 1 mL PBS in the dark, as monitored at 340 nm, at room temperature (RT, 22 ºC) or 37 ºC. (B) Comparison of the cumulative SNAP leaching and cumulative NO release (based on NOA-based or SNAP-based NO release data) from the 10 wt% SNAP-doped E2As films soaking in PBS at 37 ºC in the dark. Nitric oxide release from SNAP-doped E2As films can occur from thermal and/or photochemical decomposition of SNAP within the polymer phase, or from SNAP that leached into the aqueous phase. For the SNAP-doped E2As films, approximately 27% of the total NO release is attributed to the SNAP leaching.

to slowly diffuse from the E2As until the SNAP reservoir is nearly depleted (with still measurable amounts of SNAP leaching on day 20). The total moles of SNAP that leach from the film accounts for ca. 27% of the total NO released (as detected by NOA measurements) during the 20 d period (see **Figure 2.7B**), and thus the majority of the NO release can be attributed to the SNAP stored within the E2As film. Additionally, the effect of the number of polymer top coats on loss of SNAP was also evaluated. SNAP-doped E2As films without any top coat exhibit higher levels of SNAP diffusion into the buffer than films with at least 2 topcoats (see **Figure 2.8**). The thickness of the top coat allows control of the diffusion rate of SNAP from the polymer reservoir.

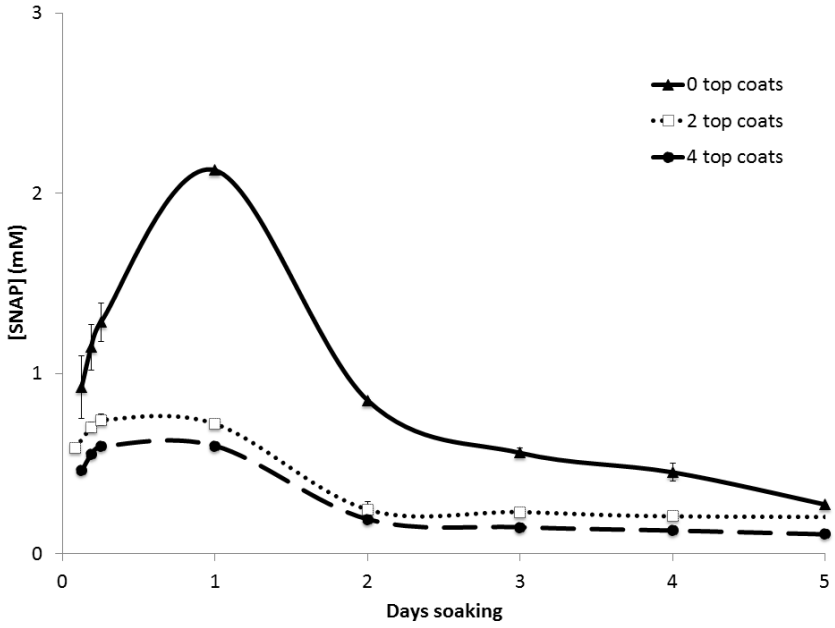

Figure 2.8. Diffusion of SNAP from 10 wt% SNAP in E2As films with 0, 2, or 4 top coats of E2As as monitored at 340 nm by UV-Vis. Films were soaked in 10 mM PBS containing 100 µM EDTA, which was replaced daily after the UV-Vis measurement, at 37ºC in the dark. Data are the mean ± SEM (n=3).

Upon loss of NO as a result of photolysis or thermal effects, SNAP decomposes into NO and an organic radical that subsequently forms the disulfide dimer of *N*-acetylpenicillamine (NAP). NAP is a well-known heavy metal chelator that is used clinically in the treatment of methyl-mercury and copper poisoning.[59-61] Indeed, NAP has been used for almost half a century.[62-65] Its medical uses have been widely taught in Medical Pharmacology courses as part of heavy metal poisoning treatments[60, 61] and it has also been used to protect against free radical induced organ injuries.[66] Hence, some slight

loss of NAP or the disulfide of NAP from the E2As polymer coatings would not likely create any toxicity issues if the proposed materials were ultimately employed for clinical applications.

2.3.3 Stability Study of the SNAP/E2As Films

The stability of SNAP doped in the E2As polymer during dry storage was also evaluated in order to ascertain the potential shelf-life of this material, as well any thermal control requirements for storage and shipping. SNAP incorporated in E2As can potentially undergo thermal or photochemical decomposition during storage, thus limiting the available NO release capacity at the time of use. Therefore, SNAP/E2As films were stored dry in the dark with desiccant at room temperature and 37 ºC. These stability studies were conducted in a similar manner as the cumulative NO release experiments, where films were dissolved in DMAc to determine the amount of SNAP remaining in the polymer at various time points (see **Figure 2.9**). Results indicate that SNAP is stable within the E2As polymer matrix after 4 months when stored at room temperature or at 37 ºC. The 10 wt% SNAP films stored in the freezer (-20 ºC) in the dark for 2 months maintain 96% of the initial SNAP species, compared to 89% for room

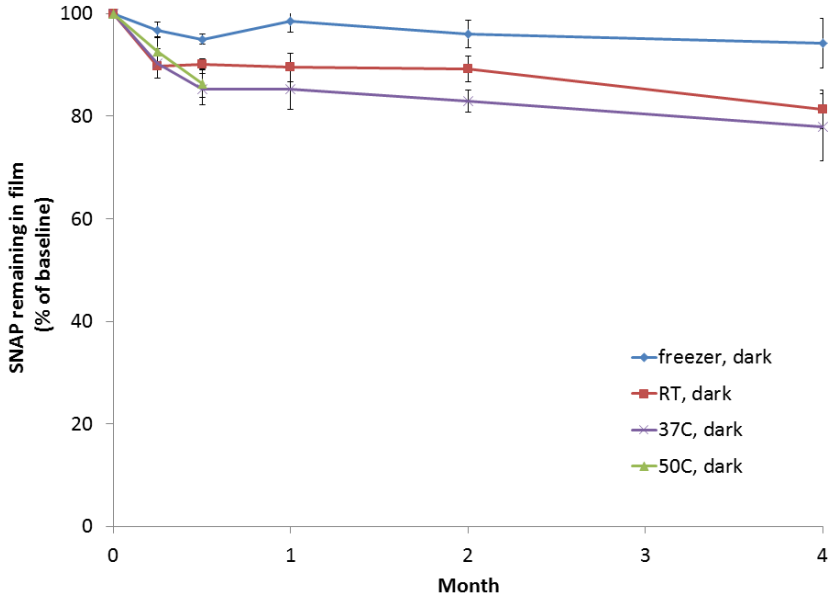

Figure 2.9. Stability of 10 wt% SNAP in E2As films stored dry with desiccant under various temperature and light conditions. Films were dissolved in DMAc to rapidly determine the amount of SNAP remaining at various times (compared to the initial level) as monitored at 340 nm by UV-Vis. Data are the mean ± SEM (n=3).

temperature and 82% for films stored at 37 ºC. Additionally, SNAP films stored at 50 ºC retained 99% of the initial SNAP after 1 d storage, indicating that the SNAP within these films will likely withstand the slightly elevated temperatures used during ethylene oxide sterilization (~12 h) that are required for clinical device applications. Tertiary RSNOs, such as SNAP, are known to have greater stability than primary RSNOs due to steric hindrance surrounding the sulfur atom.[24, 58, 67] The increased thermal stability of SNAP in combination with the stabilization effect of the E2As polymer allows provides excellent storage stability of the SNAP/E2As material.

Stability of RSNOs has been reported previously for viscous polymer matrices containing such NO donors, including poly(ethylene glycol), Pluronic F127 hydrogel, and poly(vinyl alcohol) and poly(vinyl pyrroloidone).[22, 23, 39, 40] RSNOs decompose according to the following sequence of reactions:

$$RSNO \rightarrow RS^{\cdot} + NO^{\cdot} \quad (1)$$

$$RS^{\cdot} + RSNO \rightarrow RSSR + NO^{\cdot} \quad (2)$$

$$\text{With the overall reaction: } 2RSNO \rightarrow RSSR + 2NO^{\cdot} \quad (3)$$

The viscosity of the polymer matrix provides a cage effect on the bond cleavage and radical pair recombination.[23] In addition, a viscous polymer matrix also limits the diffusion of the radical species, favoring geminate recombination to reform RSNO. Thus, the E2As polymer not only limits the diffusion of SNAP into the PBS, but it also appears to provide an additional stabilization effect to reduce the rate of SNAP decomposition.

2.3.4 SNAP/E2As Coated ECC Loops and Effects on Rabbit Hemodynamics

In order to ascertain the potential benefits of the SNAP/E2As as a thromboresistant coating, a short-term ECC study was conducted to observe the effects of NO release from this new coating on platelets and thrombus area during 4 h blood flow. The active ECC loops coated with 5 wt% SNAP in E2As (**Figure 2.10**) and control loops coated with E2As only were prepared. Five wt% SNAP was used in these tests due to the short duration of the ECC experiment. As described above, the SNAP/E2As coating has an initial burst of SNAP diffusing into solution during the first day of soaking. To reduce the effects of this burst during the short-term ECC experiments, all loops were first

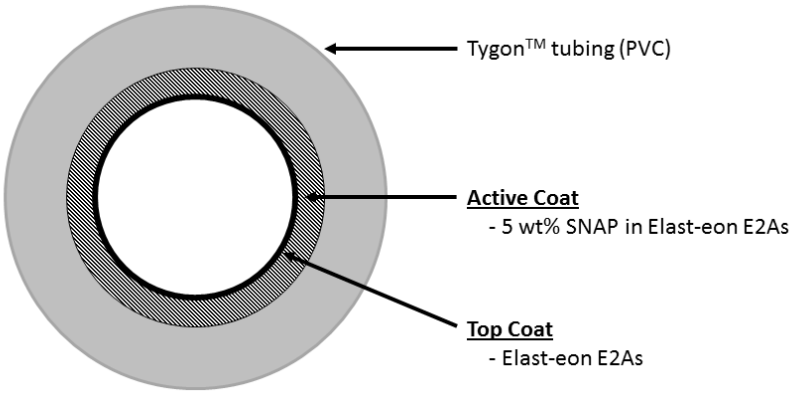

Figure 2.10. Diagram of the extracorporeal circuit (ECC) tubing coated with 5 wt% SNAP/E2As followed by a top coat of E2As.

soaked overnight in saline and the soaking solution was discarded prior to the ECC experiments. Nitric oxide released from samples of the coated ECC loops were measured with the NOA for NO release before blood exposure (after overnight soaking in saline). The NO release of the SNAP/E2As coated loops maintain an average flux of approximately 2 x 10^{-10} mol cm^{-2} min^{-1} for 4 h (at 37 ºC with ambient light). After 4 h of exposure to flowing blood, the ECC loops still exhibit a NO flux of at least 1.5 x 10^{-10} mol cm^{-2} min^{-1} for at an additional 1 h period (see **Figure 2.11**).

The hemodynamic effects of the SNAP/E2As coated ECC circuits were also monitored over the 4 h of blood exposure in the rabbit ECC model. The mean arterial pressure (MAP) dropped significantly for both SNAP/E2As and control loops within the first hour, dropping to 35±2 and 46±2 mmHg, respectively. The MAP was maintained at these levels for the 4 h by continuous IV fluid maintenance. The ECC blood flow dropped and remained at 64±5 mL/min for SNAP/E2As ECC, but maintained at baseline levels over the 4 h (76±6 mL/min) for controls. The MAP drop and slower blood flow for the SNAP/E2As circuits is likely due to the vasodilatory effects of SNAP diffusing from the coating into the blood. The heart rate is maintained over the 4 h and no significant difference was noted between the SNAP/E2As and control ECC loops, averaging 205±2 beats/min. The activated clotting time increased over the 4 h period for both SNAP/E2As and control circuits, likely due to the increase in intravascular fluids (the hemodilution effect). Similar effects on MAP and flow rate were observed with SNAP infusion.[20]

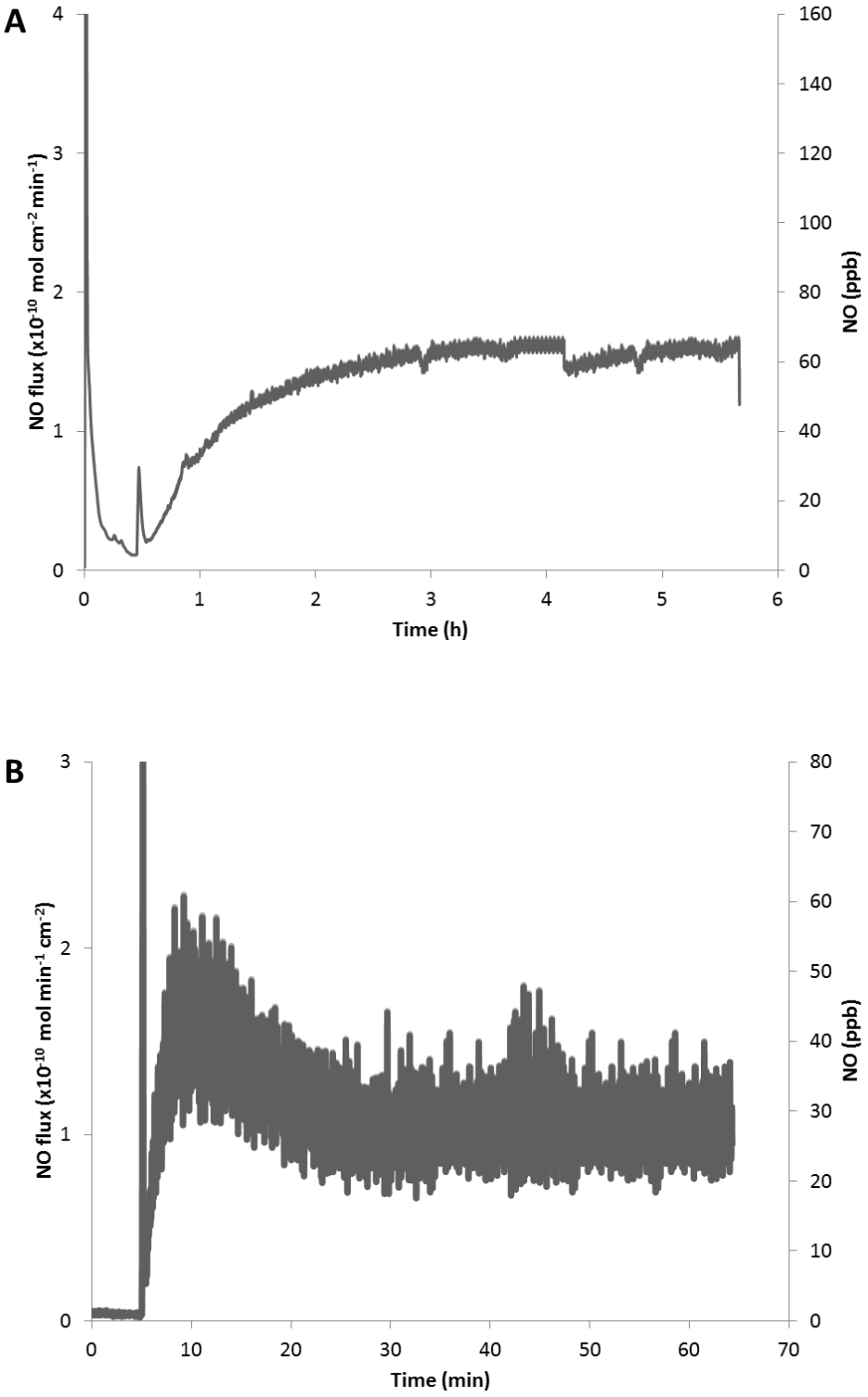

Figure 2.11. Representative NO surface flux profile from a section of ECC tubing coated with 5 wt% SNAP in E2As before (A) and after (B) blood exposure. NO release measured via chemiluminescence at 37 ºC under ambient light.

2.3.5 Effects of SNAP/E2As Coatings on Rabbit Platelet Function and Thrombus Formation

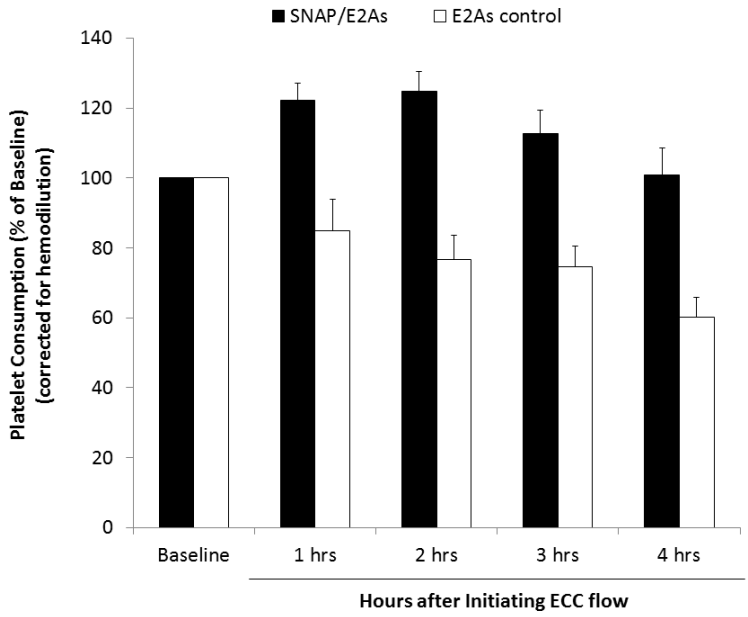

Figure 2.12. Time-dependent effects of the 5 wt% SNAP/E2As coating on platelet count (e.g. consumption) during the 4 h blood exposure in the rabbit thrombogenicity model. Data are the mean ± SEM (n=4).

Platelet activation and function throughout the 4 h ECC was assessed by recording the platelet count (**Figure 2.12**), which was corrected for hemodilution due to the added IV fluids, as well as % platelet aggregation. The baseline platelet counts ($x10^8$ platelets/mL) were 3.5±0.6 and 4.8±0.5 for the SNAP/E2As and E2As control circuits, respectively. For the SNAP/E2As circuits, the platelet count initially rose slightly and was maintained at 100±7% of baseline levels at the end of 4 h on ECC. The platelet count for control circuits exhibited a time-dependent loss in platelets, dropping to 60±6% of baseline after 4 h. The percent of platelet functional aggregation was determined by *ex vivo* collagen stimulation of PRP and measured by optical turbidity. The platelets from blood taken from circulation through the SNAP/E2As and control circuits showed similar response to collagen-stimulated platelet aggregation during the 4 h blood exposure, both maintaining 56±12% (with baseline values at 68±6%).

Plasma fibrinogen levels were maintained at baseline levels for the control circuits (**Figure 2.13A**). For the SNAP/E2As circuits, the plasma fibrinogen levels during the first hour of ECC dropped to 83% of baseline levels and remained at that level

for the 4 h ECC. This decrease in plasma fibrinogen levels can be attributed to fibrinogen binding to the surfaces, as shown by the *in vitro* fibrinogen assay (**Figure 2.13B**). Surprisingly, even with the enhanced adsorption of fibrinogen on the

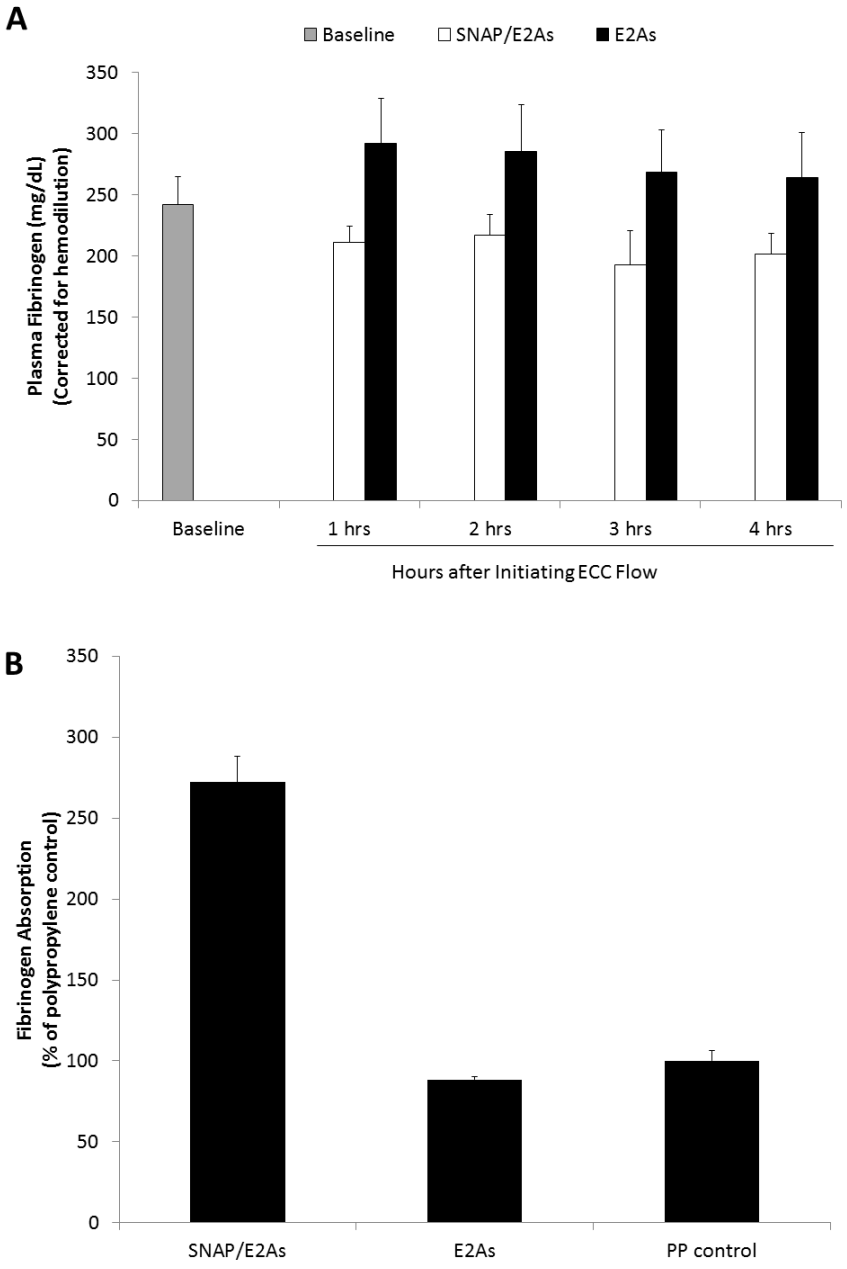

Figure 2.13. (A) Time-dependent effects of the 5 wt% SNAP/E2As coating on plasma fibrinogen during the 4 h blood exposure in the rabbit thrombogenicity model. Data are the mean ± SEM (n=4). (B) *In vitro* fibrinogen adsorption assay on the 5 wt% SNAP/E2As and E2As control coatings. Fluorescence assay in a 96-well plate that used goat anti-human fibrinogen-FITC conjugated antibody to measure the level of adsorbed human fibrinogen (3 mg/mL) on the coatings. Data are the mean ± SEM (n=24).

SNAP/E2As coatings, these materials still exhibited significantly less platelet loss than controls, suggesting that the levels of NO produced overcome the enhanced fibrinogen adsorption that would normally enhance activation of platelets. To determine the differential formation of thrombus in the thrombogenicity chamber of the ECC circuit (i.e., the 3/8 inch ID Tygon^{TM} tubing, 8 cm in length within the ECC loop), 2-dimensional (2D) image analysis was performed after 4 h of blood exposure. The thrombus area was analyzed by using Image J software and represents the 2D area of thrombus formation (cm^2) in each thrombogenicity chamber. The thrombus area was quantitated and data are shown in **Figure 2.14**. The thrombus area is significantly reduced for the SNAP/E2As circuits when compared to controls, although the E2As controls also had relatively low thrombus area, likely resulting from the enhanced intrinsic biocompatibility of the E2As polymer.[54, 55]

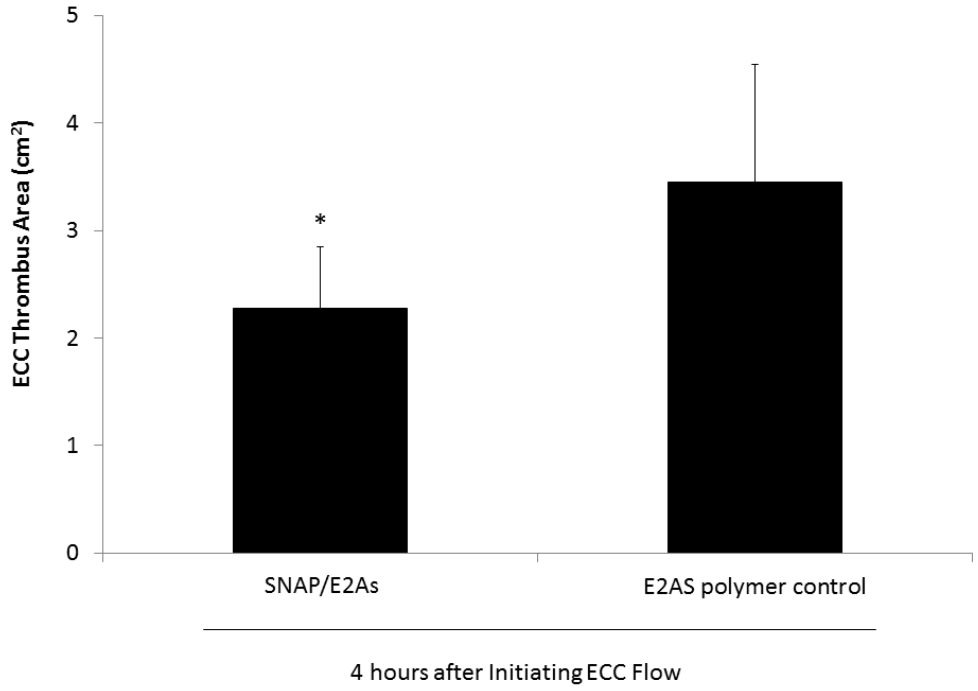

Figure 2.14. Two-dimensional representation of thrombus formation on the SNAP/E2As and control ECCs after 4 h blood exposure in the rabbit thrombogenicity model, as quantified using Image J software from NIH. Data are the mean ± SEM (n=4).

One of the effects of the new SNAP/E2As coating is the hypotension caused by the diffusion of SNAP into the blood stream, although the co-administration of intravenous fluids was able to counteract this. The ECC loops used in this study had 1

top-coat layer; however additional top coat layers could be added (see **Figure 2.8**) to limit SNAP leaching and further reduce the observed hypotensive effect. Use of a thin outer layer of a highly cross-linked polymer could also be employed to further retard the leaching of SNAP from the E2As polymer. Applications of SNAP have been reported to cause hypotension,[68, 69] hyperglycemia and impaired insulin secretion,[69] and decreased cell viability.[70-72] Endogenous thiols and superoxide dismutase will reduce many of these adverse effects. The parent thiol, *N*-acetyl-DL-penicillamine (NAP), however, has been used clinically to treat mercury poisoning[63] and cystinuria[59] with minimal side effects. Although the SNAP/E2As coatings studied here do exhibit a hypotension effect, the daily levels of SNAP delivered by the coating are well below the reported levels causing the other adverse side effects described above. Future coatings should employ the use of more lipophilic RSNOs or combine the SNAP/E2As coating with an immobilized catalyst on the inner surface of the ECC tubing to decompose the RSNO before they can enter the flowing blood, creating a fully localized delivery of the NO.

2.4 Conclusions

In this study it has been shown that the Elast-eon E2As polymer is an excellent matrix to act as reservoir for SNAP, and the resulting films can be used for the controlled release of NO and SNAP. SNAP slowly diffuses from the polymer film, and NO release from the film/coating can be initiated by light and/or thermal decomposition when blood flows through an ECC loop. Light (in the form of surgical lights, LEDs, fiber optics, etc.) could potentially be employed to administer higher doses of NO in a clinical setting. A stability study demonstrates that SNAP is quite stable within the E2As matrix, even during storage at 37 ºC for up to 4 months, demonstrating the enhanced shelf-life and potential for shipping devices made with this material without need for thermal control. Further, our finding that SNAP in the E2As also survives 50 ºC for at least one day, indicates that ethylene oxide sterilization of medical devices that utilize the SNAP/E2As coating should be possible. While the E2As polymer has excellent innate biocompatible properties on its own, incorporating SNAP into the E2As polymer matrix provides controlled delivery of NO/SNAP to further improve polymer hemocompatibility. The SNAP/E2As coated ECC loops significantly preserved platelet count and function during

4 h of ECC blood flow, while also reducing the clot area when compared to corresponding E2As coated control loops. Incorporating SNAP within Elast-eon E2As polymer films/coatings provides a simple way to locally deliver NO/SNAP, and has potential for improving the hemocompatibility of a wide variety of blood-contacting medical devices, without risk of eluting any toxic precursor, given the use of NAP already as an approved therapeutic agent.

2.5 References

1. F. C. Fang, *J Clin Invest*, **1997**, *99*, 2818-2825.

2. J.-d. Luo and A. F. Chen, *Acta Pharmacol Sin*, **2005**, *26*, 259-264.

3. J. P. Wallis, *Transfus Med*, **2005**, *15*, 1-11.

4. D. L. H. Williams, *Org Biomol Chem*, **2003**, *1*, 441-449.

5. S. H. Baek, J. A. Hrabie, L. K. Keefer, D. M. Hou, N. Fineberg, R. Rhoades and K. L. March, *Circulation*, **2002**, *105*, 2779-2784.

6. A. Chaux, X. M. Ruan, M. C. Fishbein, Y. Ouyang, S. Kaul, J. A. Pass and J. M. Matloff, *J Thorac Cardiovasc Surg*, **1998**, *115*, 604-614.

7. R. Gifford, M. M. Batchelor, Y. Lee, G. Gokulrangan, M. E. Meyerhoff and G. S. Wilson, *J Biomed Mater Res Part A*, **2005**, *75A*, 755-766.

8. B. T. Mellion, L. J. Ignarro, E. H. Ohlstein, E. G. Pontecorvo, A. L. Hyman and P. J. Kadowitz, *Blood*, **1981**, *57*, 946-955.

9. B. J. Nablo, A. R. Rothrock and M. H. Schoenfisch, *Biomaterials*, **2005**, *26*, 917-924.

10. M. W. Radomski, R. M. J. Palmer and S. Moncada, *Br J Pharmacol*, **1987**, *92*, 181-187.

11. K. L. Davis, E. Martin, I. V. Turko and F. Murad, *Annu Rev Pharmacol Toxicol*, **2001**, *41*, 203-236.

12. M. W. Vaughn, *Am J Physiol Heart Circ Physiol*, **1998**, *274*, H2163.

13. B. D. Ratner, *Biomaterials*, **2007**, *28*, 5144-5147.

14. B. D. Ratner and S. J. Bryant, *Annu Rev of Biomed Eng*, **2004**, *6*, 41-75.

15. P. N. Coneski, K. S. Rao and M. H. Schoenfisch, *Biomacromolecules*, **2010**, *11*, 3208-3215.

16. P. N. Coneski and M. H. Schoenfisch, *Polym Chem*, **2011**, *2*, 906-913.

17. V. B. Damodaran and M. M. Reynolds, *J Mater Chem*, **2011**, *21*, 5870-5872.

18. M. C. Frost and M. E. Meyerhoff, *J Biomed Mater Res Part A*, **2005**, *72A*, 409-419.

19. G. E. Gierke, M. Nielsen and M. C. Frost, *Sci Technol Adv Mat*, **2011**, *12*, 055007.

20. T. C. Major, D. O. Brant, C. P. Burney, K. A. Amoako, G. M. Annich, M. E. Meyerhoff, H. Handa and R. H. Bartlett, *Biomaterials*, **2011**, *32*, 5957-5969.

21. T. C. Major, D. O. Brant, M. M. Reynolds, R. H. Bartlett, M. E. Meyerhoff, H. Handa and G. M. Annich, *Biomaterials*, **2010**, *31*, 2736-2745.

22. S. l. M. Shishido, A. B. Seabra, W. Loh and M. Ganzarolli de Oliveira, *Biomaterials*, **2003**, *24*, 3543-3553.

23. S. M. Shishido and M. G. de Oliveira, *Photochem Photobiol*, **2000**, *71*, 273-280.

24. P. G. Wang, M. Xian, X. P. Tang, X. J. Wu, Z. Wen, T. W. Cai and A. J. Janczuk, *Chem Rev*, **2002**, *102*, 1091-1134.

25. H. Al-Sa'doni and A. Ferro, *Clin Sci (Lond)*, **2000**, *98*, 507-520.

26. N. Hogg, *Free Radic Biol Med*, **2000**, *28*, 1478-1486.

27. N. Hogg, R. J. Singh and B. Kalyanaraman, *FEBS Letters*, **1996**, *382*, 223-228.

28. E. J. Langford, A. S. Brown, R. J. Wainwright, A. J. Debelder, M. R. Thomas, R. E. A. Smith, M. W. Radomski, J. F. Martin and S. Moncada, *Lancet*, **1994**, *344*, 1458-1460.

29. M. W. Radomski, D. D. Rees, A. Dutra and S. Moncada, *Br J Pharmacol*, **1992**, *107*, 745-749.

30. E. Salas, M. A. Moro, S. Askew, H. F. Hodson, A. R. Butler, M. W. Radomski and S. Moncada, *Br J Pharmacol*, **1994**, *112*, 1071-1076.

31. G. F. P. de Souza, J. K. U. Yokoyama-Yasunaka, A. B. Seabra, D. C. Miguel, M. G. de Oliveira and S. R. B. Uliana, *Nitric Oxide-Biol Chem*, **2006**, *15*, 209-216.

32. J. Albert, M. Daleskog and N. H. Wallen, *Thromb Res*, **2001**, *102*, 161-165.

33. K. F. S. Ricardo, S. M. Shishido, M. G. de Oliveira and M. H. Krieger, *Nitric Oxide-Biol Chem*, **2002**, *7*, 57-66.

34. A. P. Dicks, H. R. Swift, D. L. H. Williams, A. R. Butler, H. H. AlSadoni and B. G. Cox, *J Chem Soc, Perkin Trans 2*, **1996**, 481-487.

35. D. J. Sexton, A. Muruganandam, D. J. McKenney and B. Mutus, *Photochem Photobiol*, **1994**, *59*, 463-467.

36. P. D. Wood, B. Mutus and R. W. Redmond, *Photochem Photobiol*, **1996**, *64*, 518-524.

37. M. C. Frost and M. E. Meyerhoff, *J Am Chem Soc*, **2004**, *126*, 1348-1349.

38. M. P. Gordge, J. S. Hothersall, G. H. Neild and A. A. N. Dutra, *Br J Pharmacol*, **1996**, *119*, 533-538.

39. A. B. Seabra, G. F. P. de Souza, L. L. da Rocha, M. N. Eberlin and M. G. de Oliveira, *Nitric Oxide-Biol Chem*, **2004**, *11*, 263-272.

40. A. B. Seabra and M. G. de Oliveira, *Biomaterials*, **2004**, *25*, 3773-3782.

41. A. B. Seabra, A. Fitzpatrick, J. Paul, M. G. De Oliveira and R. Weller, *Br J Dermatol*, **2004**, *151*, 977-983.

42. T. P. Amadeu, A. B. Seabra, M. G. De Oliveira and A. M. A. Costa, *J Eur Acad Dermatol Venereol*, **2007**, *21*, 629-637.

43. N. A. Stasko, T. H. Fischer and M. H. Schoenfisch, *Biomacromolecules*, **2008**, *9*, 834-841.

44. A. B. Seabra, R. da Silva and M. G. de Oliveira, *Biomacromolecules*, **2005**, *6*, 2512-2520.

45. A. B. Seabra, R. da Silva, G. F. P. de Souza and M. G. de Oliveira, *Artif Organs*, **2008**, *32*, 262-267.

46. A. B. Seabra, D. Martins, M. Simoes, R. da Silva, M. Brocchi and M. G. de Oliveira, *Artif Organs*, **2010**, *34*, E204-E214.

47. D. A. Riccio, P. N. Coneski, S. P. Nichols, A. D. Broadnax and M. H. Schoenfisch, *ACS Appl Mater Interfaces*, **2012**, *4*, 796-804.

48. D. A. Riccio, K. P. Dobmeier, E. M. Hetrick, B. J. Privett, H. S. Paul and M. H. Schoenfisch, *Biomaterials*, **2009**, *30*, 4494-4502.

49. R. Etchenique, M. Furman and J. A. Olabe, *J Am Chem Soc*, **2000**, *122*, 3967-3968.

50. Y. Li and P. I. Lee, *Mol Pharm*, **2009**, *7*, 254-266.

51. S. C. Puiu, Z. Zhou, C. C. White, L. J. Neubauer, Z. Zhang, L. E. Lange, J. A. Mansfield, M. E. Meyerhoff and M. M. Reynolds, *J Biomed Mater Res B Appl Biomater*, **2009**, *91B*, 203-212.

52. J. Yang, J. L. Welby and M. E. Meyerhoff, *Langmuir*, **2008**, *24*, 10265-10272.

53. B. K. Oh and M. E. Meyerhoff, *J Am Chem Soc*, **2003**, *125*, 9552-9553.

54. D. Cozzens, A. Luk, U. Ojha, M. Ruths and R. Faust, *Langmuir*, **2011**, *27*, 14160-14168.

55. A. Simmons, A. D. Padsalgikar, L. M. Ferris and L. A. Poole-Warren, *Biomaterials*, **2008**, *29*, 2987-2995.

56. I. Chipinda and R. H. Simoyi, *J Phys Chem B*, **2006**, *110*, 5052-5061.

57. P. A. Gunatillake, D. J. Martin, G. F. Meijs, S. J. McCarthy and R. Adhikari, *Aust J Chem*, **2003**, *56*, 545-557.

58. I. L. Megson, S. Morton, I. R. Greig, F. A. Mazzei, R. A. Field, A. R. Butler, G. Caron, A. Gasco, R. Fruttero and D. J. Webb, *Br J Pharmacol*, **1999**, *126*, 639-648.

59. A. Stephens and R. Watts, *Q J Med*, **1971**, *40*, 355-370.

60. C. Tiruppathi, *http://wwwuicedu/classes/pcol/pcol331/dentalpharmhandouts2006/lecture41pdf*, **2006**.

61. C. Clarckson, *http://tmedwebtulaneedu/pharmwiki/dokuphp/penicillamine_nap*, **2012**.

62. R. Gledhill and A. Hopkins, *Br J Ind Med*, **1972**, *29*, 225-228.

63. R. Kark, D. C. Poskanzer, J. D. Bullock and G. Boylen, *N Engl J Med*, **1971**, *285*, 10-16.

64. V. Parameshvara, *Br J Ind Med*, **1967**, *24*, 73-76.

65. L. Markowitz and H. H. Schaumburg, *Neurology*, **1980**, *30*, 1000-1001.

66. P. Srivastava, A. J. Arif, C. Singh and V. C. Pandey, *Pharmacol Res*, **1997**, *36*, 305-307.

67. C. E. Lin, S. K. Richardson, W. H. Wang, T. S. Wang and D. S. Garvey, *Tetrahedron*, **2006**, *62*, 8410-8418.

68. T. Rassaf, P. Kleinbongard, M. Preik, A. Dejam, P. Gharini, T. Lauer, J. Erckenbrecht, A. Duschin, R. Schulz, G. Heusch, M. Feelisch and M. Kelm, *Circ Res*, **2002**, *91*, 470-477.

69. D. McGrowder, D. Ragoobirsingh and T. Dasgupta, *Nitric Oxide-Biol Chem*, **2001**, *5*, 402-412.

70. A. A. Fatokun, T. W. Stone and R. A. Smith, *Brain Res*, **2008**, *1230*, 265-272.

71. F. Khalilmanesh and R. G. Price, *Toxicology*, **1983**, *26*, 325-334.

72. R. Zamora, K. E. Matthys and A. G. Herman, *Eur J Pharmacol*, **1997**, *321*, 87-96.

CHAPTER 3

S-Nitroso-*N*-acetylpenicillamine (SNAP)-Doped Elast-eon Catheters Reduce Thrombosis and Bacterial Adhesion in a Long-Term Animal Model

3.1 Introduction

Blood-material interaction is critical to the success of implanted medical devices such as intravascular catheters, vascular grafts, stents, and extracorporeal life support circuits.[1, 2] Two common factors that can cause complications with blood-contacting devices are thrombosis and infection. As soon as blood comes in contact with these foreign surfaces, platelets adhere and become activated, forming thrombus within hours. Clinical use of catheters range from acute catheters placed in operating rooms, emergency rooms, and intensive care units (ICUs) (typically for up to 7 d), to permanent catheters for long-term nutrition and pacemaker leads (months to years). Complications due to thrombosis and infection can result in extended hospital stay, increased healthcare costs, and even patient death. Thrombus formation on catheters decreases their patency and functional lifetime. Venous thrombosis has been detected by Doppler imaging in 33% of intensive care unit patients.[3] Infection is another significant problem, where there are 1.7 million Healthcare Associated Infections that result in 99,000 deaths per year in the United States.[4] In addition, up to 40% of all indwelling catheters become infected.[5] An estimate 80,000 catheter-related bloodstream infections occur in patients within ICUs, resulting in as many as 28,000 deaths per year.[6]

Over the last 50 years, much has been learned about surface-induced thrombosis and many different strategies to create hemocompatible materials have been also been reported.[1, 7-9] Some of the surface modifications to improve hemocompatibility include

hydrophilic or hydrophobic surfaces, zwitterionic polymers, and immobilized heparin (as discussed in Chapter 1). However, in a clinical setting many devices still require the use of systemic anticoagulation (e.g., heparin) to avoid device failure due to thrombosis.[10] Long-term use of systemic anticoagulation is not desirable because it can have adverse side effects such as hemorrhage, thrombocytopenia, and thrombosis.[11] Catheters with antimicrobial coatings (e.g., containing silver compounds or antibiotics) are available, but are not completely effective at preventing infection and biofilm formation and also do not address complications associated with activation of platelets.[5, 12] A recent study reported that catheters coated with a silver alloy had a similar infection rate as control catheters.[13] Antibiotic resistant bacterial strains are becoming more common in the hospital setting.[14, 15] Further, bacteria have the ability to form biofilms (communities of bacterial encased in a self-synthesized extracellular matrix) that protect the bacteria from antiseptics, antibiotics, and the host's defense system.[16-19] Biofilm formation decreases the effectiveness of many antibiotics because they cannot penetrate the biofilm matrix, making the infections difficult to eradicate.[20]

Nitric oxide (NO)-releasing polymers are one approach that has a great potential to improve the hemocompatibility of blood-contacting devices such as catheters. Radomski et al. first described NO as a potent vasodilator secreted by the normal endothelium that has the ability to inhibit platelet adhesion and aggregation to the blood vessel wall.[21, 22] Nitric oxide is a natural inhibitor of platelet activation that is release from healthy endothelial cells at a flux into the blood stream of 0.5 -4.0 x 10^{-10} mol cm^{-2} min^{-1}.[23] In addition, NO that is released within the sinus cavities and by neutrophils/macrophages functions as a potent natural antimicrobial agent.[24, 25] Nitric oxide is known to have broad-spectrum antibacterial properties, where both gram-positive and gram-negative bacteria can be killed.[26] Therefore, NO-releasing polymers have the advantage that they could be used to create dual-functioning catheters that would possess both antithrombotic and antiseptic properties.

A wide variety of nitric oxide (NO)-releasing polymers have been reported and investigated for their potential biomedical applications.[24, 27-29] NO-releasing polymers have preserved platelet count and reduced thrombus formation when tested in a rabbit model of extracorporeal circulation (ECC) thrombogenicity.[30-34] *S*-nitrosothiol-modified

xerogels significantly reduced adhesion of platelets and bacteria (*Pseudomonas aeruginosa*) when tested *in vitro*.[35, 36] Diazeniomdiolate-doped poly(lactic-*co*-glycolic acid)-based films exhibited antibiofilm properties against both gram-positive (*Staphylococcus aureus*) and gram-negative (*Escherichia coli*) bacteria when tested using a drip-flow bioreactor over a 7 d period.[37] Despite the promising results reported in the literature, many of these NO-releasing polymers have not been clinically applied due to instability of the S-NO group during storage or sterilization, significant leaching of unbound NO donors, or difficult methods to covalently bind the NO donor to the polymer.[30, 38] For example, *S*-nitrosothiol-modified polyesters were effective at reducing platelet adhesion/activation and had antimicrobial effect against *Staphylococcus aureus* and the multi-drug resistant *Pseudomonas aeruginosa* strains, but the NO release capability was significantly influenced by ethylene oxide sterilization.[39, 40] In addition, most of the NO-releasing materials reported to date have been tested *in vitro* or in short-term animal models for their hemocompatibility properties, so testing these materials in long-term animal models would be beneficial to evaluate more clinically relevant situations.

As described in Chapter 2, the new SNAP-doped Elast-eon E2As polymer formulation has encouraging properties, in terms of its long-term NO release, enhanced shelf-life stability, and its ability to preserve platelets and reduce thrombus during the 4 h extracorporeal circulation, that could make clinical applications feasible.[30] In this study, catheters were fabricated with the SNAP/E2As polymer using a dip coating method. The NO release from these catheters was monitored over a 20 d period under physiological conditions (37 ^{o}C, dark). Another key hurdle for potential clinical applications is the ability of the NO-releasing materials to withstand sterilization. The effect of ethylene oxide (EO) sterilization on the SNAP/E2As catheters was also evaluated. Finally, the SNAP/E2As catheters were assessed for their ability to reduce thrombosis and bacterial adhesion after 7 d intravascular implantation in sheep.

3.2 Materials and Methods

3.2.1 Materials

N-Acetyl-DL-penicillamine (NAP), sodium chloride, potassium chloride, sodium phosphate dibasic, potassium phosphate monobasic, ethylenediaminetetraacetic acid (EDTA), tetrahydrofuran (THF), sulfuric acid and *N*,*N*-dimethylacetamide (DMAc) were purchased from Sigma-Aldrich (St. Louis, MO). Methanol, hydrochloric acid and sulfuric acid were obtained from Fisher Scientific (Pittsburgh, PA). Elast-eon^{TM} E2As was obtained from AorTech International, plc (Scoresby, Victoria, Australia). All aqueous solutions were prepared with 18.2 MΩ deionized water using a Milli-Q filter (Millipore Corp., Billerica, MA). Phosphate buffered saline (PBS), pH 7.4, containing 138 mM NaCl, 2.7 mM KCl, 10 mM sodium phosphate, 100 μM EDTA was used for all *in vitro* experiments.

3.2.3 SNAP Synthesis Protocol

SNAP was synthesized using a modified version of a previously reported method. Briefly an equimolar ratio of NAP and sodium nitrite was added to a 1:1 mixture of water and methanol containing 2 M HCl and 2 M H_2SO_4. After 30 min of stirring, the reaction vessel was cooled in an ice bath to precipitate the green SNAP crystals. The crystals were collected by filtration, washed with water, and allowed to air dry. The reaction mixture and resulting crystals were protected from light at all times.

3.2.3 Preparation of Intravascular Catheters

Catheters were prepared by dip coating polymer solutions on 18 cm long stainless steel mandrels of 2.0 mm diameter (purchased from McMaster Carr). The E2As control catheter solution consisted of E2As dissolved in THF (150 mg/mL). Thirty-five coats of the E2As solution was applied on the mandrel by dip coating at an interval of 2 min between each coat. The SNAP-doped E2As catheters had a trilayer configuration, E2As top/base coats and a SNAP-containing active layer. The top/base coat solution consisted of E2As dissolved in THF (150 mg/mL). The active solution was made up of 10 wt% SNAP and 90 wt% E2As dissolved in THF with overall total concentration of 150

mg/mL. Trilayer catheters were prepared by dip coating 5 base coats of E2As solution, 25 coats of active solution, and 5 top coats of E2As solution. All catheters were allowed to dry overnight under ambient conditions, protected from light. Cured catheters were removed from the mandrels and dried under vacuum for 48 h. Catheters had an i.d. of 2.08 ± 0.06 mm and o.d. of 3.30 ± 0.12 mm, as measured with a Mitutoyo digital micrometer.

3.2.4 NO Release Measurements

Nitric oxide released from the catheters was measured using a Sievers chemiluminescence Nitric Oxide Analyzer (NOA), model 280 (Boulder, CO). A sample was placed in 4 mL PBS buffer at 37 ºC. Nitric oxide liberated from the sample was continuously swept from the headspace of the sample cell and purged from the buffer with a nitrogen sweep gas and bubbler into the chemiluminescence detection chamber. The flow rate was set to 200 mL/min with a chamber pressure of 5.4 Torr and an oxygen pressure of 6.0 psi. Catheters were incubated in 4 mL of PBS buffer, pH 7.4, at 37 ºC and tested for NO release at various time points. Buffer was replaced every day. After the 7 d chronic animal study, a section of the implanted NO release catheters were tested for NO release post-blood exposure. For dry vs. humidity experiments, a catheter sample was placed in a dry NOA sample cell incubated at 55 ºC. Humidity was introduced by injecting PBS buffer into the cell, with the catheter sample suspended in the air above the buffer. The relative humidity in the sample cell was measured using a Fieldpiece PRH2 psychrometer.

3.2.5 Effect of Ethylene Oxide (EO) Sterilization

The SNAP-doped E2As catheters were sterilized by ethylene oxide (EO) at the University of Michigan Hospital sterilization facility. Briefly, the EO sterilization procedure consists of the following steps, all at 54 ºC: humidity and conditioning (1 h, 40-80% humidity); EO gas exposure (2-3 h, 40-80% humidity); and exhaust/aeration (14 h). Catheters were tested for the wt% SNAP content before and after EO sterilization by UV-Vis analysis. Catheter pieces were weighed and dissolved in *N*,*N*-dimethylacetamide (DMAc) for rapid determination of SNAP by UV-Vis (absorbance at 340 nm). UV-Vis

spectra were recorded in the wavelength range of 200-700 nm using a UV-Vis spectrophotometer (Lambda 35, Perkin-Elmer, MA) at room temperature. The molar absorption coefficient for SNAP in DMAc at 340 nm was determined to be: ε_{SNAP}=1025 M^{-1} $cm^{-1.}$

3.2.6 Catheter Implantation in Sheep Model

Sheep catheter implantation protocol: All animals received care compliant with the "Principles of Laboratory Animal Care" formulated by the National Society for Medical Research and the "Guideline for the Care of Use of Laboratory Animals" prepared by the National Academy of Sciences and published by the NIH. This study was approved by the University of Michigan Committee on Use and Care of Animals. Five adult sheep (Valley View Farms, Dexter, MI) were utilized in the large animal model. All experiments were performed under sterile conditions. Sheep experiments were performed under general anesthetic. Propofol (APP Pharmaceuticals LLC, Schaumburg, IL) (1 mg/kg) was used for induction followed by isoflurane (Peramal Health Car Limited, Andhra Pradesh, India) (0.1-4%) anesthetic for maintenance. A small 2-3 cm incision was created overlying the jugular vein. The right and left jugular veins were then isolated and either control (E2As) or experimental (SNAP/E2As) cannulas were placed under direct visualization. Small 1-2 cm vertical and transverse incisions were created over the right and left jugular veins. Cannulas were then placed using a modified Seldinger technique with one cannula either control (E2As) or experimental (SNAP/E2As) placed in either the right or left jugular vein. The skin was then re-approximated using skin staples.

Post-operative recovery protocol: Sheep were recovered from anesthesia after the catheter placements and returned to animal housing. The sheep remained in animal housing throughout the remainder of the experiment. Necropsy was performed on day 7. Sheep were anesthetized using the same anesthetic protocol described above. The right and left jugular veins were dissected along their length and isolated. Sheep were heparinized using approximately 100-150 IU/kg bolus dose and activated clotting time of >200 s was confirmed. The jugular veins were then ligated and opened longitudinally. Catheters were removed and placed in sterile saline for further analysis.

Catheter evaluation: After explanting, the catheters were rinsed in sterile saline solution. Pictures were taken of the exterior of the whole catheter using a Nikon L24 digital camera. Catheter sections (1 cm) were cut for NO release testing and bacterial adhesion measurements. To quantitate the viable bacteria on the surfaces of the catheters, a 1 cm piece was cut longitudinally and was homogenized in 1 mL sterile PBS buffer. The resulting homogenate was serially diluted in sterile PBS. Triplicate aliquots of each dilution (10 µL) of each dilution were plated on LB agar plates. The agar plates were incubated at 37 ºC for 24 h followed by calculation of colony forming units per catheter surface area (CFU/cm^2).

3.3 Results and Discussion

3.3.1 In Vitro NO Release from Catheters and Effects of Ethylene Oxide Sterilization

As discussed in Chapter 2, the SNAP-doped E2As polymer has many properties that make it desirable for various biomedical applications, including long-term NO release, stability during storage, and ability to preserve platelets during short-term extracorporeal circulation.[30] In this study, catheters were prepared with the SNAP-doped E2As polymer using a dip coating method and a trilayer configuration shown in **Figure 3.1**. The top and base coats of E2As were employed to reduce any initial burst of NO

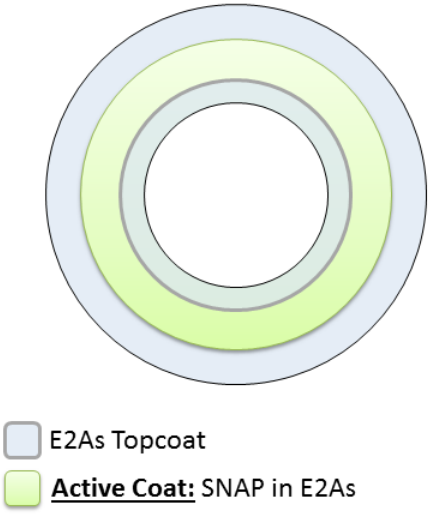

Figure 3.1. Schematic of SNAP-doped E2As catheters with a trilayer configuration.

from the leaching of SNAP. There is little concern regarding the low levels of SNAP leaching typically observed from the SNAP/E2As polymer, since the parent thiol (NAP) is clinically used to treat heavy metal poisoning.[41-44] Hence, the small amounts of SNAP, NAP, or NAP disulfide that could diffuse from the catheter into the blood would not likely create any toxicity issues. The NO release from SNAP/E2As catheters was monitored using the NOA over a 20 d period (**Figure 3.2**). The catheters exhibited a higher level of NO release upon first exposure to physiological conditions (soaked in PBS at 37 ºC) on Day 0. The initial water uptake of the polymer and leaching of SNAP on the outer surface of the catheters contributes to the higher level of NO release observed during this initial test period. However, as shown, the SNAP/E2As catheters continue to release physiological levels of NO (> 0.5 x 10^{-10} mol cm^{-2} min^{-1}) for up to 20 d. The NO release from the catheters approaches the lower end of the normal endothelium range, which may still prove beneficial to reduce thrombosis and bacterial adhesion.

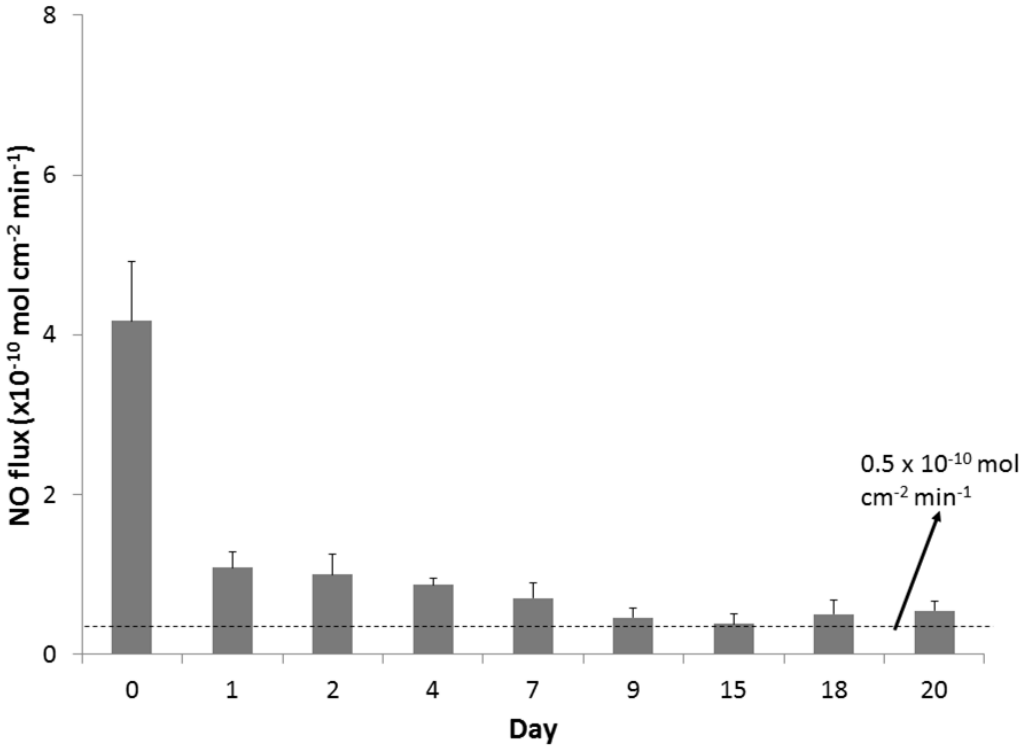

Figure 3.2. NO release from SNAP/E2As catheters under physiological conditions (soaking in PBS buffer at 37 ºC in the dark). Data represents the mean ± SEM (n=5).

In order for medical devices, such as the SNAP/E2As catheters, to be used clinically they must be able to withstand sterilization and still retain their NO-releasing properties. Ethylene oxide (EO) sterilization is one common method used to sterilize medical devices. This method is recommended for heat-sensitive devices over other sterilization techniques (e.g., autoclave). The SNAP/E2As were also evaluated for their ability to withstand the EO sterilization process. One cm sections of the SNAP/E2As catheter were EO sterilized by the University of Michigan Hospital sterilization facility. Precautions were taken to minimize any excessive exposure to light, so that only the effects of the EO sterilization process were observed. The SNAP/E2As catheters (before and after EO) were dissolved in DMAc to quantitate the wt% SNAP by UV-Vis. The catheters that had been EO sterilized had 89% of the original SNAP, as shown in **Figure 3.3**, and the NO release profile was not significantly affected. During the EO sterilization process, the SNAP/E2As catheters were not only exposed to the EO gas, but also were

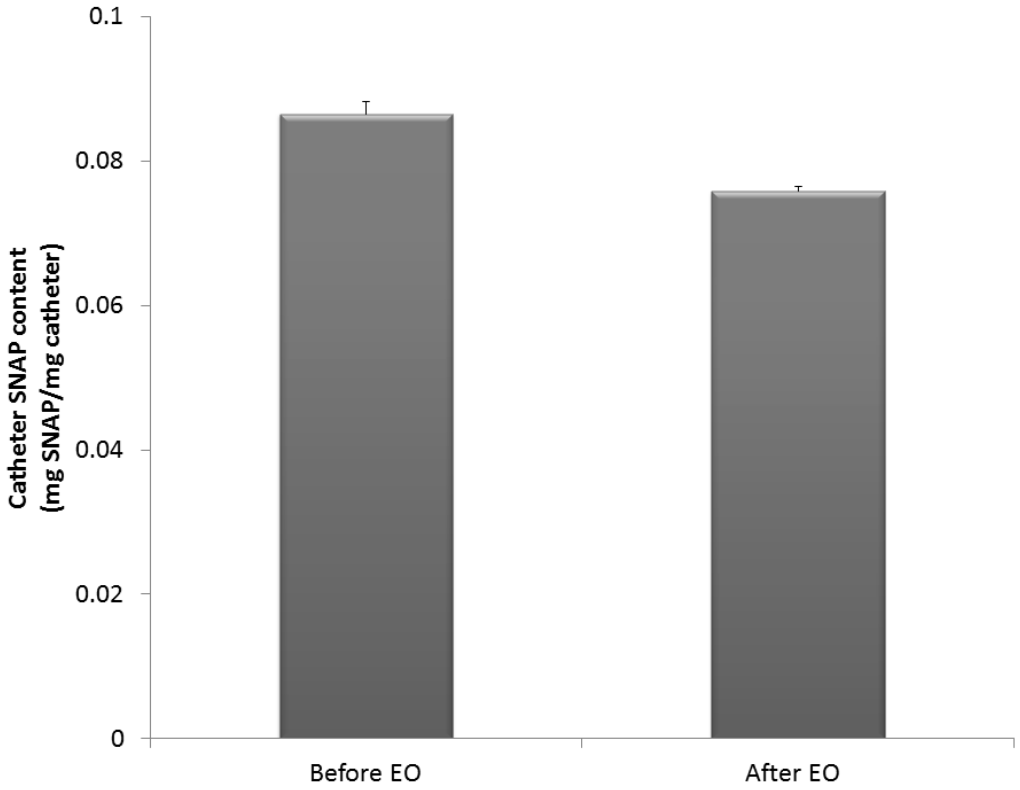

Figure 3.3. The SNAP content (mg SNAP/mg catheter) of catheters before and after ethylene oxide (EO) sterilization. Data represents the mean ± SEM (n=4).

exposed to elevated temperatures (54 ºC) and humidity (40-80 %RH). The NO release from catheter sections was observed with the NOA under dry and humid conditions at 55 ºC. As shown in **Figure. 3.4**, the NO release from the catheters is low under dry conditions, but dramatically increased upon exposure to humidity (~ 50% RH). This demonstrates that the NO loss observed during EO sterilization may, in part, be caused by the humidity exposure. This loss of SNAP could be significantly reduced if sterilized under dry conditions.

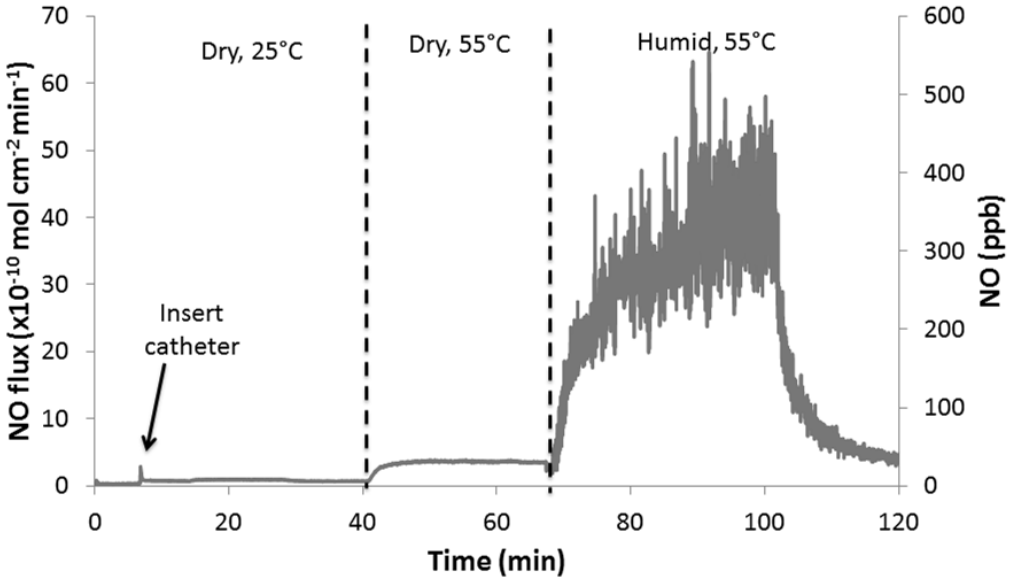

Figure 3.4. Representative NO release from SNAP/E2As catheters under various conditions: dry and room temperature (25 ºC); dry and 55 ºC; and humid (~50 %RH) and 55 ºC.

3.4 Evaluation of Thrombus Formation and Bacterial Adhesion on Catheters in 7 d Sheep Model

The catheters were implanted for 7 d in the jugular veins of sheep (1 SNAP/E2As catheter and 1 E2As control catheter per animal). Following catheter implantation, sheep were monitored closely for changes in behavior, weight, appearance, and activity level. All the sheep recovered rapidly from the surgical procedure and returned to normal activity level. At the time of catheter explantation, precautions were taken to remove the catheter from the vessel without disrupting the catheter surface. The vessel was cut longitudinally to carefully remove the whole catheter. The catheter was briefly rinsed in

sterile saline solution. Any residual thrombus on the catheter was photographed. Explanted catheters were systematically cut into 1 cm sections starting at the distal tip for post-implantation NO release measurements and bacterial adhesion testing.

Surface thrombi on the explanted catheters were photographed and the degree of thrombus area was quantitated using Image J imaging software from National Institutes of Health (Bethesda, MD). **Figure 3.5A,** shows representative images of the clot

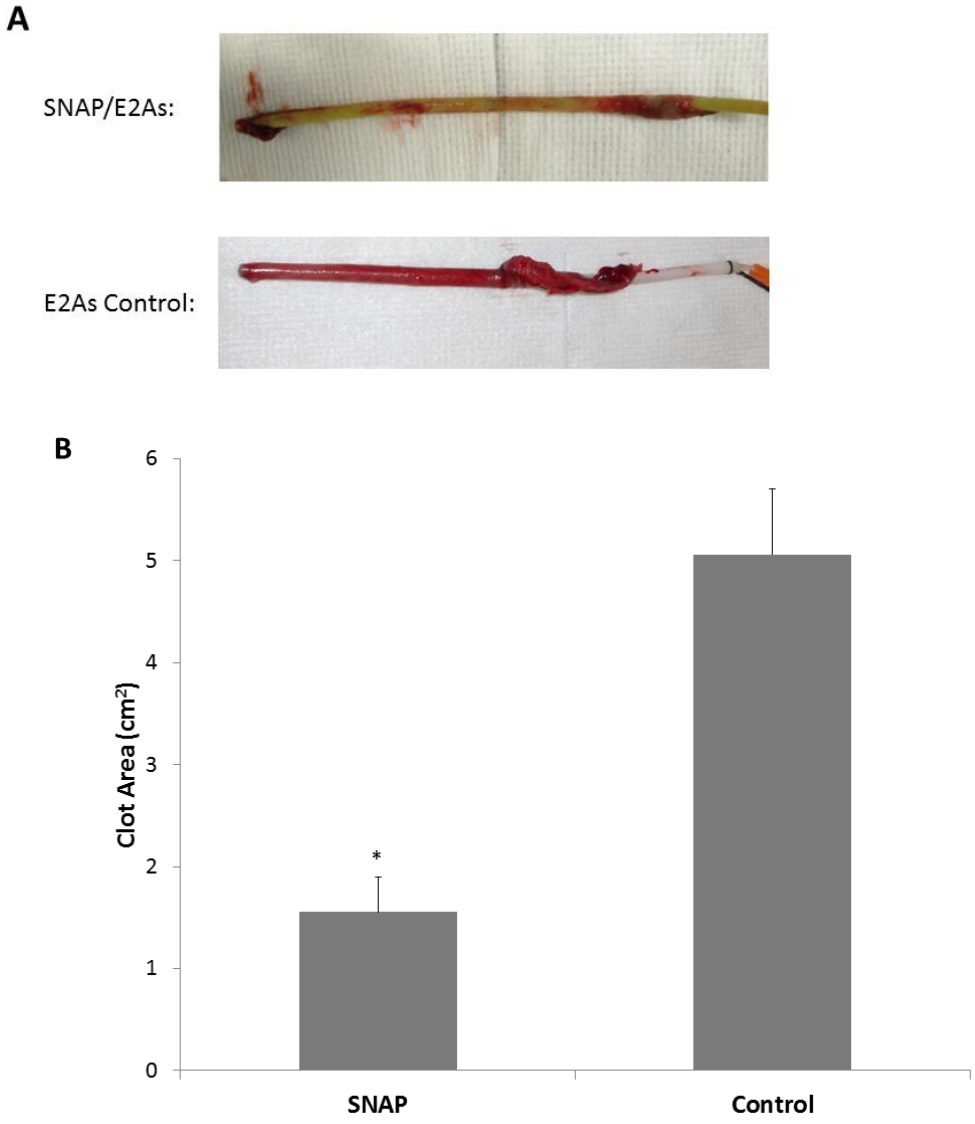

Figure 3.5. Representative images of SNAP/E2As and E2As control catheters after 7 d implantation in sheep veins (A). Two-dimensional representation of thrombus formation on the SNAP/E2As and E2As control catheters after 7 d implantation in sheep veins (B). Data represents the mean ± SEM (n=5). * = $p < 0.05$, SNAP/E2As vs. E2As control.

formation on the exterior of SNAP/E2As and control catheters. These thrombi area measurements were quantitated and, as shown in **Figure 3.5B**, the thrombus area of the SNAP/E2As catheters was significantly reduced compared to the control catheters, 1.56 ± 0.34 and 5.06 ± 0.64 cm^2, respectively.

One cm catheter section in 1 mL sterile PBS was homogenized to detach the bacteria from the inner and outer catheter surfaces and cultured as described in experimental section above. The bacterial colonies were counted the following day and are represented as CFU/cm^2 in **Figure 3.6**. A 1.0 log reduction (90% reduction) in bacterial adhesion was observed for SNAP/E2As catheters as compared to the controls. Post-implanted catheters had a NO flux of 0.6 ± 0.1 x 10^{-10} mol cm^{-2} min^{-1} on the day of explantation, which is at the lower end of the normal range of NO from the endothelium.[23] This data is consistent with previously reported animal data, where it was shown that NO release is not compromised due to blood exposure.[31, 33] The hemocompatibility of these catheters likely could be further improved by exploring methods to increase the NO flux from the SNAP/E2As polymer.

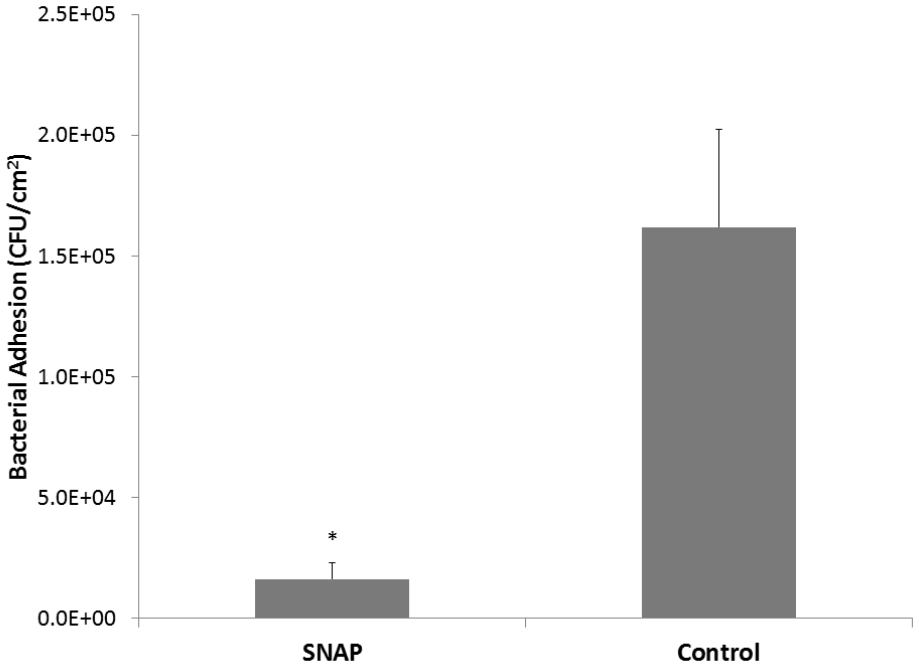

Figure 3.6. Bacterial adhesion on SNAP/E2As and E2As control catheters after 7 d implantation in sheep veins. Data represents the mean ± SEM (n=5). * = $p < 0.05$, SNAP/E2As vs. E2As control.

3.4 Conclusions

Nitric oxide-releasing materials have many potential biomedical applications. In this study, the SNAP-doped E2As polymer was used to fabricate catheters and evaluated for its hemocompatibility properties in a sheep model. The SNAP-doped E2As catheters release physiological levels of NO (> 0.5 x 10^{-10} mol cm^{-2} min^{-1}) for up to 20 d. The ability of the SNAP/E2As polymer to withstand ethylene oxide sterilization, maintaining ca. 89% of the original SNAP, was observed. The SNAP/E2As catheter significantly reduces the amount of thrombus and bacterial adhesion, in comparison to control catheters, after 7 d of intravascular implantation in sheep. This study demonstrates the potential of the SNAP/E2As polymer in clinical applications to improve the hemocompatibility and antimicrobial properties of catheters and other medical devices, even for longer-term implantation periods.

3.5 References

1. B. D. Ratner, *Biomaterials*, **2007**, *28*, 5144-5147.

2. E. S. Wiener, P. McGuire, C. J. Stolar, V. C. Albo, A. R. Ablin, D. L. Betcher, A. L. Sitarz, J. D. Buckley, M. D. Krailo and C. Versteeg, *J Pediatr Surg*, **1992**, *27*, 155-164.

3. P. A. Dillon and R. P. Foglia, *J Pediatr Surg*, **2006**, *41*, 1582-1587.

4. A. Vertes, V. Hitchins and K. S. Phillips, *Anal Chem*, **2012**, *84*, 3858-3866.

5. A. L. Casey and T. S. Elliott, *Br J Nurs*, **2010**, *19*, 78.

6. N. P. O'Grady, M. Alexander, E. P. Dellinger, J. L. Gerberding, S. O. Heard, D. G. Maki, H. Masur, R. D. McCormick, L. A. Mermel and M. L. Pearson, *Clin Infect Dis*, **2002**, *35*, 1281-1307.

7. C. Werner, M. F. Maitz and C. Sperling, *J Mater Chem*, **2007**, *17*, 3376-3384.

8. A. G. Kidane, H. Salacinski, A. Tiwari, K. R. Bruckdorfer and A. M. Seifalian, *Biomacromolecules*, **2004**, *5*, 798-813.

9. C. Salvagnini, **2002**, *295*, 995-1033.

10. A. M. Gaffney, S. M. Wildhirt, M. J. Griffin, G. M. Annich and M. W. Radomski, *BMJ*, **2010**, *341*.

11. T. M. Robinson, T. S. Kickler, L. K. Walker, P. Ness and W. Bell, *Crit Care Med*, **1993**, *21*, 1029-1034.

12. S.-h. Hsu, H.-J. Tseng and Y.-C. Lin, *Biomaterials*, **2010**, *31*, 6796-6808.

13. C. V. Gould, C. A. Umscheid, R. K. Agarwal, G. Kuntz, D. A. Pegues and H. I. C. P. A. Committee, *Infect Control Hosp Epidemiol*, **2010**, *31*, 319-326.

14. M. A. Fischbach and C. T. Walsh, *Science*, **2009**, *325*, 1089-1093.

15. G. Taubes, *Science*, **2008**, *321*, 356.

16. J. W. Costerton, Z. Lewandowski, D. E. Caldwell, D. R. Korber and H. M. Lappin-Scott, *Annu Rev Microbiol*, **1995**, *49*, 711-745.

17. L. Hall-Stoodley, J. W. Costerton and P. Stoodley, *Nature Rev Microbiol*, **2004**, *2*, 95-108.

18. G. O'Toole, H. B. Kaplan and R. Kolter, *Annu Rev Microbiol*, **2000**, *54*, 49-79.

19. M. R. Parsek and P. K. Singh, *Annu Rev Microbiol*, **2003**, *57*, 677-701.

20. C. Fux, J. Costerton, P. Stewart and P. Stoodley, *TIM*, **2005**, *13*, 34-40.

21. M. W. Radomski and S. Moncada, in *Mechanisms of Platelet Activation and Control*, Springer, 1993, pp. 251-264.

22. M. W. Radomski, R. M. Palmer and S. Moncada, *Biochem Biophys Res Commun*, **1987**, *148*, 1482-1489.

23. M. W. Vaughn, *American Journal of Physiology-Heart and Circulatory Physiology*, **1998**, *274*, H2163-H2176.

24. G. M. Halpenny and P. K. Mascharak, *Anti-Infective Agents in Medicinal Chemistry (Formerly `Current Medicinal Chemistry - Anti-Infective Agents)*, **2010**, *9*, 187-197.

25. J.-J. Rouby, *Am J Respir Crit Care Med*, **2003**, *168*, 265-266.

26. R. Raulli, G. McElhaney-Feser, J. Hrabie and R. Cihlar, *Rec Res Devel Microbiol* **2002**, *6*, 177-183.

27. A. W. Carpenter and M. H. Schoenfisch, *Chem Soc Rev*, **2012**, *41*, 3742-3752.

28. M. C. Frost, M. M. Reynolds and M. E. Meyerhoff, *Biomaterials*, **2005**, *26*, 1685-1693.

29. M. C. Jen, M. C. Serrano, R. van Lith and G. A. Ameer, *Adv Funct Mater*, **2012**, *22*, 239-260.

30. E. J. Brisbois, H. Handa, T. C. Major, R. H. Bartlett and M. E. Meyerhoff, *Biomaterials*, **2013**, *34*, 6957-6966.

31. T. C. Major, D. O. Brant, M. M. Reynolds, R. H. Bartlett, M. E. Meyerhoff, H. Handa and G. M. Annich, *Biomaterials*, **2010**, *31*, 2736-2745.

32. G. M. Annich, J. P. Meinhardt, K. A. Mowery, B. A. Ashton, S. I. Merz, R. B. Hirschl, M. E. Meyerhoff and R. H. Bartlett, *Crit Care Med*, **2000**, *28*, 915-920.

33. H. Handa, E. J. Brisbois, T. C. Major, L. Refahiyat, K. A. Amoako, G. M. Annich, R. H. Bartlett and M. E. Meyerhoff, *Journal of Materials Chemistry B*, **2013**, *1*, 3578-3587.

34. H. Handa, T. C. Major, E. J. Brisbois, K. A. Amoako, M. E. Meyerhoff and R. H. Bartlett, *Journal of Materials Chemistry B*, **2014**, *2*, 1059-1067.

35. D. A. Riccio, K. P. Dobmeier, E. M. Hetrick, B. J. Privett, H. S. Paul and M. H. Schoenfisch, *Biomaterials*, **2009**, *30*, 4494-4502.

36. D. A. Riccio, P. N. Coneski, S. P. Nichols, A. D. Broadnax and M. H. Schoenfisch, *ACS Applied Materials & Interfaces*, **2012**, *4*, 796-804.

37. W. Cai, J. Wu, C. Xi and M. E. Meyerhoff, *Biomaterials*, **2012**, *33*, 7933-7944.

38. J. M. Joslin, S. M. Lantvit and M. M. Reynolds, *ACS Applied Materials & Interfaces*, **2013**, *5*, 9285-9294.

39. A. B. Seabra, R. Da Silva, G. F. P. De Souza and M. G. De Oliveira, *Artif Organs*, **2008**, *32*, 262-267.

40. A. B. Seabra, D. Martins, M. Simoes, R. da Silva, M. Brocchi and M. G. de Oliveira, *Artif Organs*, **2010**, *34*, E204-E214.

41. C. Clarckson, *http://tmedwebtulaneedu/pharmwiki/dokuphp/penicillamine_nap*, **2012**.

42. V. Parameshvara, *Br J Ind Med*, **1967**, *24*, 73-76.

43. C. Tiruppathi, *http://wwwuicedu/classes/pcol/pcol331/dentalpharmhandouts2006/lecture41pdf*, **2006**.

44. M. Blanusa, V. M. Varnai, M. Piasek and K. Kostial, *Curr Med Chem*, **2005**, *12*, 2771-2794.

CHAPTER 4

Improving Diazeniumdiolate-Based Nitric Oxide (NO) Delivery with Poly(lactic-*co*-glycolic acid) (PLGA) Additives for Blood-Contacting Device Applications

4.1. Introduction

The hemocompatibility of blood-contacting medical devices (e.g., extracorporeal circuits, catheters, stents, grafts, etc.) is still a challenge, despite decades of research.[1-3] Thrombosis is one of the primary problems associated with clinical application of blood contacting materials. For example, extracorporeal circulation (ECC) includes a wide variety of devices, from short-term hemodialysis and cardiopulmonary bypass (several hours), to extracorporeal life support (ECLS) (days to weeks).[4] The most common complications with ECLS devices are bleeding (7-34%) and thrombosis (8-17%).[5] In a clinical setting, these extracorporeal devices require the use of systematic anticoagulation (e.g., heparin) to avoid device failure.[6] Systemic infusion of anticoagulants, such as heparin, is known to be the cause of hemorrhage and thrombocytopenia.[7] Despite these complications, heparin is still used as the standard in anticoagulation therapy for patients on ECC.

Biomaterial related thrombosis is a complex process, where the initial biological response when blood comes in contact with a foreign surface is protein adsorption, which is followed by platelet adhesion and activation, leading to thrombus formation. Over the last 50 years much has been learned about foreign surface-induced thrombosis and attempts to prevent it with systemic anticoagulation and surface modifications. Surface modifications have included using pure, very smooth silicone rubber[8] or polyurethane,[9] pre-exposure of the surfaces to albumin[10] or other coating proteins,[11] and surface binding

of heparin in an ionic[12] as well as a covalent fashion.[13] Despite a thorough understanding of the mechanisms of blood–surface interactions and decades of bioengineering research effort, the ideal non-thrombogenic prosthetic surface remains an unsolved problem.[14]

One approach to improve the hemocompatibility of a surface is to prevent platelet adhesion and activation, which is desirable for improving clinical outcomes. In 1993 Radomski and Moncada[15] described nitric oxide (NO) as one of two potent vasodilators secreted by normal endothelium that has the ability to inhibit platelet adhesion and aggregation to the blood vessel wall. The amount of NO released from normal and stimulated endothelium has been estimated to between 0.5-4.0 $x10^{-10}$ mol cm^{-2} min^{-1}.[16] Nitric oxide has been extensively studied for its inhibitory effects on circulating platelet and monocyte activation that leads to aggregation and ultimately initiation of thrombosis.[17-20] Hence, one potential strategy to decrease the level or completely avoid systemic heparinization is to develop coatings that mimic the endothelium with respect to NO release at physiological levels. A wide range of NO donors such as *S*-nitrosothiols,[21, 22] N-hydroxy-N-nitrosoamines,[23] N-diazeniumdiolates[24, 25] and nitrosyl metal complexes[26] have also been studied over the past decade, as a means to release NO either by systemic infusion[27] or locally released from a polymer surface (to mimic the NO release from normal endothelium).[28] Despite the promising potential of NO-releasing materials, their development has been hindered due to challenges in prolonging the NO release beyond a few days.

Diazeniumdiolates (also called NONOates) have been one of the most widely studied NO donors, that release NO through proton[29] or thermal[30] driven mechanisms. Prior work has shown that NO can be emitted from the NO donor compound, diazeniumdiolated dibutylhexanediamine (DBHD/N_2O_2), when this species is incorporated into hydrophobic polymer films.[28, 31] While DBHD/N_2O_2 is an excellent donor for incorporation into polymers to create NO release coatings, the loss of NO from this molecule creates free lipophilic amine species within the polymer that react with water, thereby increasing the pH within the organic polymer phase which effectively turns off the NO production before a significant fraction of the total NO payload has been released.[31] In earlier work, tetrakis-(p-chlorophenyl)-borate was employed as an additive to maintain a low enough pH within the organic polymer phase and to promote a

sustained NO flux.[28, 31] However, this additive did not enable the release of the entire payload of NO from the polymer coatings and was also found to be cytotoxic towards endothelial and smooth muscle.[32]

The work presented herein focuses on a new approach to address this pH control problem, and hence greatly prolong the NO release from DBHD/N_2O_2-doped polymers. This novel method involves the use of poly(lactide-co-glycolide) (PLGA) species as additives to help stabilize the pH within the organic phase polymeric coatings (**Figure 4.1**). The addition of PLGA can be used to control the flux of NO emitted from polymers

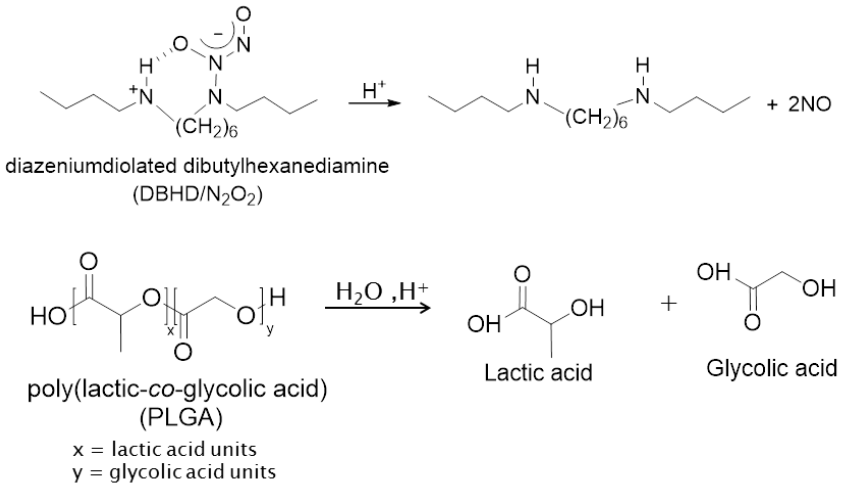

Figure 4.1. Reactions of diazeniumdiolated dibutylhexanediamine (DBHD/N_2O_2) and poly(lactic-co-glycolic acid) (PLGA).

containing diazeniumdiolate species by helping to control the pH within the polymer phase.[33, 34] PLGA is a biodegradable and biocompatible polymer[35-37] that can be used as an additive to sustain the NO flux for a prolonged period by the slow formation of lactic and glycolic acid within the base polymer layer of the coating. Ester linkages of the PLGA are slowly hydrolyzed as small amounts of water penetrate the polymer from the surrounding aqueous environment to generate lactic and glycolic acid within the polymer matrix.[38, 39] The presence of this continuous acid production reaction compensates for the increase in pH from generation of organo-ammonium hydroxide (reaction of liberated free amines from DBHD with water in the polymer film) from the NO release reaction, thereby maintaining a greater rate of NO release for longer periods of time.

In the literature there are reports of two main strategies that utilize PLGA to deliver NO from diazeniumdiolate species. The first strategy is dispersing the NO donor compound within the PLGA matrix, creating a completely biodegradable NO release material. Yoo et al. employed PLGA microparticles with an NO donor (diethylenetriamine diazeniumdiolate (DETA NONOate), a low molecular weight diazeniumdiolate) within to deliver NO for a very short 6 h period.[40] In another study, Cai et al. studied *in vitro* effects of NO-releasing PLGA films on biofilm formation.[41] In this study the authors dispersed the NO donor compound in a completely hydrolysable PLGA matrix; however, due to the toxicity concerns of the product amine, leaching is a potential limitation of these films. In the second strategy, Zhou and Meyerhoff have shown that PLGA has the potential to act as a proton donor to enhance the release of NO from a polymer material that had covalently linked diazeniumdiolate groups for a relatively short 20 h period.[33] Although these approaches have had some limited success, prolonging the NO release still remains one of the great challenges preventing use of NO-releasing materials in clinical application.

In this study, various PLGAs are investigated for their potential to be used as an additive in poly(vinyl chloride)/dioctyl sebacate (PVC/DOS) and Elast-econ E2As polymers to control NO release from a lipophilic diazeniumdiolate (DBHD/N_2O_2) species added to the organic phase of the coating. The effects of the PLGA end group chemistry (either free carboxylic acid or ester end group) and hydrolysis rate on the NO release profiles are compared. The hydrolysis rate of the PLGA is primarily determined by the copolymer ratio, the nature of the end group (e.g., free acid or ester), and molecular weight. Further, incorporation of pH indicators in the coatings provides a means to correlate the NO release with the observed pH changes within the PVC/DOS matrix.

In addition, preservation of platelets and reduced thrombus area in a rabbit model of ECC with NO release coatings using DBHD/N_2O_2 doped poly(vinyl chloride)/dioctyl sebacate (PVC/DOS) as the base polymer has been reported.[28, 42] However, the inherent hemocompatiblity properties of the base polymers used in combination with NO release can have a direct effect on the ultimate efficacy in preventing thrombus formation. In this study, the degree of platelet consumption and thrombus formation is also compared for two biomedical grade polymers PVC/DOS and E2As in a rabbit thrombogenicity

model using an arterio-venous (A-V) shunt. Further, the PVC/DOS- and E2As-based NOrel polymers are coated on ECC circuits and evaluated in the rabbit model. These new PLGA-doped NOrel coatings could provide a breakthrough for achieving sustained preservation of circulating platelets, an important goal for longer-term ECC situations, such as ECMO, or other blood-contacting devices (e.g., catheters, vascular grafts, etc.).

4.2 Materials and Methods

4.2.1 Materials

Tygon™ poly(vinyl chloride) (PVC) tubing was purchased from Fisher Healthcare (Houston, TX). Tecoflex SG-80A was obtained from Lubrizol Advanced Materials Inc. (Cleveland, OH). Elast-Eon™ E2As was a product of AorTech International, plc (Scoresby, Victoria, Australia). High molecular weight poly(vinyl chloride) (PVC), dioctyl sebacate (DOS), anhydrous tetrahydrofuran (THF), anhydrous acetonitrile, bromothymol blue, bromocresol green, sodium chloride, potassium chloride, sodium phosphate dibasic, and potassium phosphate monobasic were purchased from Sigma-Aldrich Chemical Company (St. Louis, MO). Various poly(D,L-lactide-co-glycolide) materials, including 5050DLG1A, 5050DLG7E, and 6536DLG7E, were obtained from SurModics Pharmaceuticals Inc. (Birmingham, AL). *N,N'*-Dibutyl-1,6-hexanediamine (DBHD) was purchased from Alfa Aesar (Ward Hill, MA). DBHD/N_2O_2 was synthesized by treating DBHD with 80 psi NO gas purchased from Cryogenic Gases (Detroit, MI) at room temperature for 48 h, as previously described.[31] Phosphate buffered saline (PBS), pH 7.4, containing 138 mM NaCl, 2.7 mM KCl, 10 mM sodium phosphate, was used for all *in vitro* experiments.

4.2.2 Preparation of NOrel Films for NO Release and pH Studies

As mentioned earlier, the main focus of this work is to use PLGA as an additive in the PVC/DOS and E2As polymer matrices to prolong the NO release from a lipophilic DBHD/N_2O_2 species (**Figure 4.1**). In this study, 5050DLG1A (1-2 wk hydrolysis rate), 5050DLG7E (1-2 mo hydrolysis rate), and 6535DLG7E (3-4 mo hydrolysis rate) PLGAs were used. These product names identify polymer mole ratio, polymer type, inherent

viscosity and the end group designation (ester or acid). For example, 5050DLG7E stands for: 50 mole% DL-lactide, 50 mole% glycolide, 0.7dL/g and 'E' for an ester end group (Table 1). The hydrolysis rate of the PLGA is primarily determined by the copolymer ratio, end group, and molecular weight (as determined from the inherent viscosity).

A variety of NO-releasing (NOrel) film formulations were prepared using the solvent evaporation method in order to optimize the NO release duration. The NOrel films were prepared with either the 2:1 PVC/DOS or E2As as the base polymer. The amount of DBHD/N_2O_2 was kept at a constant 25 wt% of the active layer for all the films. A variety of NO-releasing films with a total weight of 800 mg in 5 mL THF, and were cast in Teflon rings (d = 2.5 cm). For example, 10 wt% PLGA + 25 wt% DBHD/N_2O_2 in 2:1 PVC/DOS were prepared with 80 mg PLGA, 200 mg DBHD/N_2O_2, 173 mg DOS and 347 mg PVC in 5 mL THF. The NO-releasing films were cast and cured for 2 d under nitrogen. Disks (d = 0.9 cm) were cut from the parent NO-releasing film and a topcoat of the respective polymer was added. Top coats were employed for three main reasons: 1) to prevent leaching of DBHD/N_2O_2; 2) to neutralize the surface charge; and 3) to yield a smoother finish to the surface. The PVC/DOS-based films were dip coated 8 times using the top coating solution (375 mg DOS, 750 mg PVC in 15 mL THF) in 10 min intervals. The E2As-based films were dip coated 4 times using the top coating solution (550 mg E2As in 7.5 mL THF). Top coated films were dried under nitrogen conditions for 1 d to minimize the loss of NO due to ambient moisture. Similarly, control films were also prepared using solvent evaporation followed by top coating as described above. The 10 wt% PLGA control film solution consisted of 80 mg PLGA, 240 mg DOS and 480 mg PVC in 5 mL THF. The 25 wt% DBHD/N_2O_2 control film (without PLGA) consisted of 200 mg DBHD/N_2O_2, 200 mg DOS, and 400 mg PVC in 5 mL THF. The final films had a total thickness of ~1000 μm including a topcoat of ~200 μm, which were measured using a Mitutoyo digital micrometer (Metron Precision Inc.).

For the pH studies, the films were prepared as described above with the exception of adding given pH indicators to the active layer solution. The pH indicators, bromocresol green (BG5) or bromothymol blue (BB7), were present in the active layer casting solution at 0.025 wt%. Photos of the pH films were taken each day with Nikon

L24 digital camera to monitor the change in pH as indicated by the color of the incorporated pH indicators.

4.2.3 Acid Content of PLGA

The acid number, which is a measure of the initial acid content of the PLGA and is directly related to the free carboxylic acid functionalities, was determined by a previously reported titration method.[43] Briefly, approximately 50 mg of PLGA was dissolved in 10 mL of a 1:1 mixture of acetone and THF. This solution was immediately titrated with 0.01 N KOH in methanol to a stable pink endpoint. Phenolphthalein in methanol (0.1 wt%) was used as the indicator for the titration. Titrations were performed in triplicate.

4.2.4 Preparation of NOrel Coated ECC loops

The ECC configuration employed in the *in vivo* rabbit study was previously described.[28, 42, 44, 45] Briefly, the ECC consisted of a 16-gauge and 14-gauge IV polyurethane angiocatheters (Kendall Monoject Tyco Healthcare Mansfield, MA), two 16 cm in length ¼ inch inner diameter (ID) Tygon™ tubing and an 8 cm length of 3/8 inch ID Tygon™ tubing that created a thrombogenicity chamber where thrombus could form more easily due to more turbulent blood flow.

Base polymer coated control ECCs: Polymer control loops were coated with E2As or 2:1 PVC/DOS solutions. All the control loops contained 2 coats of the polymer/THF solution (2500 mg in 15 mL).

NOrel coated ECCs: NOrel loops were prepared with E2As or PVC/DOS coating containing 25 wt% DBHD/N_2O_2 as the NO donor, and 10 wt% 5050DLG7E PLGA additive. The PVC/DOS-based NOrel solution consisted of 770 mg PVC, 385 mg DOS, 180 mg PLGA and 450 mg DBHD/N_2O_2 in 10 mL THF to obtain a slightly cloudy dispersion of the diazeniumdiolate in the solution. The PVC/DOS top coat solution was prepared using 181 mg PVC, 362 mg DOS plasticizer and 10 mL THF. The E2As-based NOrel solution was prepared by dissolving 1600 mg E2As and 250 mg PLGA in 15 mL THF. DBHD/N_2O_2 (625 mg) was then dispersed within the polymer cocktail by sonication for 30 min to obtain a slightly cloudy dispersion of the diazeniumdiolate in the

solution. The E2As top coat solution consisted of 2500 mg E2As dissolved in 15 mL THF.

The Tygon tubing was first coated with 2 layers of the NOrel solution, followed by 1 coat of the top coat solution. The circuitry was filled with each solution, which was then removed. All ECC circuitry were allowed to air dry for 1 h between each coat. The completely coated ECC was assembled together using THF, starting with the 16-gauge angiocatheter, one 15 cm length ¼ inch ID tubing, the 8 cm length thrombogenicity chamber, the second 15 cm length ¼ inch ID tubing and finally the 14-gauge angiocatheter (**Figure 4.2**). The angiocatheters were interfaced with tubing using two

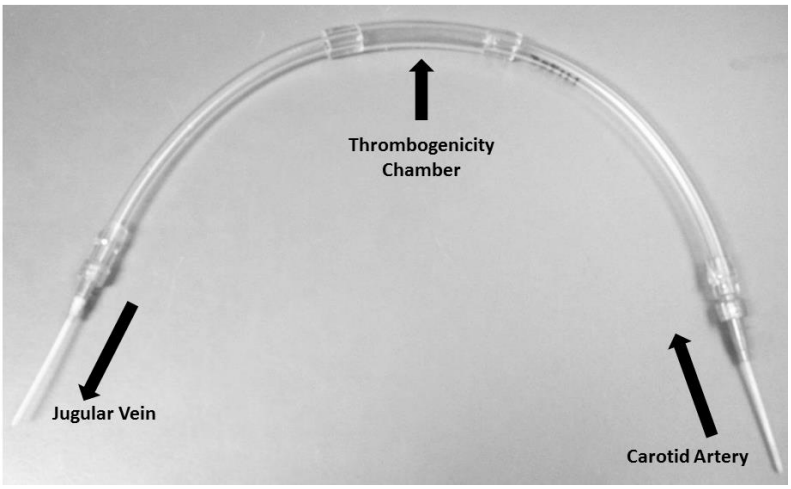

Figure 4.2. Schematic of the assembled extracorporeal circulation (ECC) loop, depicting the blood flow direction and thrombogenicity chamber.

luer-lock PVC connectors. The assembled ECC loops were dried for 20 min under ambient conditions and then under vacuum for 48 h, to minimize the negative effects of ambient moisture on the coating. The configuration for both NO-releasing and control ECCs had a total thickness of approximately 150–200 μm., much thinner than the free standing multilayer films described above.

4.2.5 NO Release Measurements

Nitric oxide released from the films was measured using a Sievers chemiluminescence Nitric Oxide Analyzer (NOA), model 280 (Boulder, CO). The chemiluminiscence nitric oxide analyzer (NOA) is considered the gold standard for detecting NO and is widely used to measure NO release from materials.[28, 31, 41, 46, 47] The

major advantage of using the NOA is that the most troublesome interferents such as nitrites and nitrates are not transferred from the sample vessel to the reaction cell; thus, NO selectivity is enhanced.[48, 49] A sample of the film was placed in 4 mL PBS buffer at 37 ºC. Nitric oxide liberated from the film was continuously swept from the headspace of the sample cell and purged from the buffer with a nitrogen sweep gas and bubbler into the chemiluminescence detection chamber. The flow rate was set to 200 mL/min with a chamber pressure of 5.4 Torr and an oxygen pressure of 6.0 psi. Films were incubated in 4 mL of PBS buffer at 37 ºC for a 2 week period and tested for NO release at various time points. Buffer was replaced every day to prevent saturation of NO. In addition, a uniform segment was cut from the coated ECC loop and was tested for 4 h *in vitro* for NO release in PBS buffer prior to blood exposure. After the surgery, a section of the ECC loop was tested for NO release in PBS buffer post blood exposure.

4.2.6 The Rabbit Thrombogenicity Model

Rabbit thrombogenicity model protocol: The animal handling and surgical procedures were approved by the University Committee on the Use and Care of Animals in accordance with university and federal regulations. A total of 28 New Zealand white rabbits (Myrtle's Rabbitry, Thompson's Station, TN) were used in this study. All rabbits (2.5-3.5 kg) were initially anesthetized with intramuscular injections of 5 mg/kg xylazine injectable (AnaSed® Lloyd Laboratories Shenandoah, Iowa) and 30 mg/kg ketamine hydrochloride (Hospira, Inc. Lake Forest, IL).

Maintenance anesthesia was administered via isoflurane gas inhalation at a rate of 1.5-3% via mechanical ventilation which was done via a tracheotomy and using an A.D.S. 2000 Ventilator (Engler Engineering Corp. Hialeah, FL). Peek inspiratory pressure was set to 15 cm of H_2O and the ventilator flow rate set to 8 L/min. In order to aid in maintenance of blood pressure stability, IV fluids of Lactated Ringer's were given at a rate of 10 mL/kg/h. For monitoring blood pressure and collecting blood samples, the rabbits' right carotid artery was cannulated using a 16-gauge IV angiocatheter (Jelco®, Johnson & Johnson, Cincinnati, OH). Blood pressure and derived heart rate were monitored with a Series 7000 Monitor (Marquette Electronics Milwaukee, WI). Body temperature was monitored with a rectal probe and maintained at 37 ºC using a water-

jacketed heating blanket. Prior to placement of the arteriovenous (AV) custom-built extracorporeal circuits, the rabbit left carotid artery and right external jugular vein were isolated and baseline hemodynamics as well as arterial blood pH, pCO_2, pO_2, and total hemoglobin were measured using an ABL 825 blood-gas analyzer. In addition, baseline blood samples were collected for platelet and total white blood cell (WBC) counts which were measured on a Coulter Counter Z1 (Coulter Electronics Hialeah, FL). Activated clotting times (ACT) were monitored using a Hemochron Blood Coagulation System Model 801 (International Technidyne Corp. Edison, NJ).

After baseline blood measurements, the custom-built ECC was placed into position by cannulating the left carotid artery for ECC inflow and the right external jugular vein for ECC outflow. The flow through the ECC was initiated by unclamping the arterial and venous sides of ECC and blood flow in circuit was monitored with an ultrasonic flow probe and flow meter (Transonic HT207 Ithaca, NY). Animals were not systemically anticoagulated during the experiments.

Blood sampling: Rabbit whole blood samples were collected in non-anticoagulated 1 mL syringes for ACT, 3.2% sodium citrate vacutainers (Becton, Dickinson. Franklin Lakes, NJ) in 3 mL volumes for cell counts and 1 mL syringes containing 40 U/mL of sodium heparin (APP Pharmaceuticals, LLC Schaumburg, IL) for blood-gas analysis. Following the initiation of ECC blood flow, blood samples were collected every hour for 4 h for *ex vivo* measurements. Samples were used within 2 h of collection to avoid any activation of platelets, monocytes, or plasma fibrinogen.

Determination of thrombus area: After 4 h on ECC, the circuits were clamped, removed from animal, rinsed with 60 mL of saline, and drained. Any residual thrombus in the larger tubing of ECC (i.e., thrombogenicity chamber) was photographed and the degree of thrombus image was quantitated using Image J imaging software from National Institutes of Health (Bethesda, MD). Prior to euthanasia, all animals were given a dose of 400 U/kg sodium heparin to prevent necrotic thrombosis. The animals were euthanized using a dose of Fatal Plus (130 mg/kg sodium pentobarbital) (Vortech Pharmaceuticals Dearborn, MI). All animals underwent gross necropsy after being euthanized, including examination of the lungs, heart, liver and spleen for any signs of thromboembolic events.

4.2.7 Statistical Analysis

Data are expressed as mean ± SEM (standard error of the mean). Comparison of ECC results between the various NOrel and control polymer groups were analyzed by a one-way ANOVA with a multiple comparison of means using Student's *t*-test. Values of $p<0.05$ were considered statistically significant for all tests.

4.3 Results and Discussion

4.3.1 In Vitro NO Release from PVC/DOS- or E2As-Based Films Containing DBHD/N_2O_2 in with Various PLGA Additives

The diazeniumdiolate species investigated here, DBHD/N_2O_2, decomposes to generate NO primarily by a proton-driven mechanism.[31] A tetrakis-(p-chlorophenyl)-borate derivative was used previously as a lipophilic additive counteranion to stabilize the pH within NO-releasing polymers prepared with DBHD/N_2O_2.[31] However, the borate derivative is not an ideal additive because of its toxicity.[32] In this study, PLGA additives with varying hydrolysis rates were used as a replacement of the borate derivative to act as a proton donor source to control the NO release from DBHD/N_2O_2-doped PVC and Elast-eon E2As coatings. It is well known that, in the presence of water, the ester bonds in PLGA hydrolyze to yield lactic and glycolic acids, and that PLGA is a widely used biodegradable/biocompatible polymer that has been approved by FDA for numerous products.[50]

The films used in this study had a two layer configuration: an active coat (containing the NO donor, DBHD/N_2O_2, and PLGA additive) and a top coat. The active coat consisted of the base polymer (PVC/DOS or E2As) doped with 25 wt% DBHD/N_2O_2 and various amounts of the PLGA additive. The top coat consisted of the base polymer, either PVC/DOS in 2:1 ratio or E2As, without any additives. The 2:1 ratio of PVC/DOS was selected because, as demonstrated by Reynolds et al.,[31] PVC films containing DBHD/N_2O_2 with a 2:1 ratio of PVC/DOS had a more prolonged NO release when compared to 1:1 or 1:2 ratio of PVC/DOS. Increasing the DOS content of the polymer increases the water uptake, resulting in a higher initial burst of NO release. The top coats of the base polymer were employed for three main reasons indicated above in

the Materials and Methods Section. In this study, PLGAs with various hydrolysis rates were compared for their effects on NO release: 5050DLG1A (1-2 week hydrolysis rate), 5050DLG7E (1-2 month hydrolysis rate), and 6535DLG7E (3-4 month hydrolysis rate).

It has been previously reported that DBHD/N_2O_2 within PVC films without an additive releases NO, producing the corresponding diamine, DBHD, that raises the pH within the polymer film slowing and eventually stopping the NO release in 1-2 d.[31] Use of a PLGA additive promotes a more sustained NO release. As shown in **Figure 4.3A**, DBHD/N_2O_2 in PVC/DOS with 5050DLG1A as the additive had an initial burst of NO due to high proton activity, but the NO release quickly diminished over a 10 d period. In contrast, the PVC films prepared with the 5050DLG7E additive had a more consistent NO flux with no initial burst of NO, and this enabled the NO release to be prolonged for a 14 d period. Not only does the 5050DLG1A hydrolyze and produce acid monomers more quickly than the 5050DLG7E, but it has a higher initial acid content (compared to the ester-capped PLGA) (**Table 4.1**). The higher acid content and faster hydrolysis rate of the 5050DLG1A directly correlates to the high initial burst and greater initial NO fluxes which quickly depletes the DBHD/N_2O_2 reservoir.

Table 4.1. Analytical information for the 5050DLG1A, 5050DLG7E, and 6535DLG7E PLGA additives.

PLGA	Copolymer Ratio (^{1}H NMR) (Lactide:Glycolide)*	Acid number (mg KOH/g PLGA)	Inherent viscosity* (dL/g)	Molecular weight (GPC)*	
				M_w (kDa)	PDI
5050DLG1A	52:48	60.4 ± 2.5	0.08	4.1	2.1
5050DLG7E	51:49	2.4 ± 0.8	0.65	106	1.6
6535DLG7E	65:35	1.4± 0.5	0.78	121	1.6

* Information provided in Analytical Report from Lakeshore Biomaterials.

From **Figure 4.3A** it is apparent that the 5050DLG7E additive films exhibit little or no initial burst of NO and release the NO for a prolonged time period. In order to optimize the film formulation containing 5050DLG7E, the amount of PLGA was varied. In **Figure 4.3B**, the amount of DBHD/N_2O_2 is kept constant at 25 wt%, while the 5050DLG7E PLGA amount is varied from 5-30 wt%. The 5 wt% 5050DLG7E films are

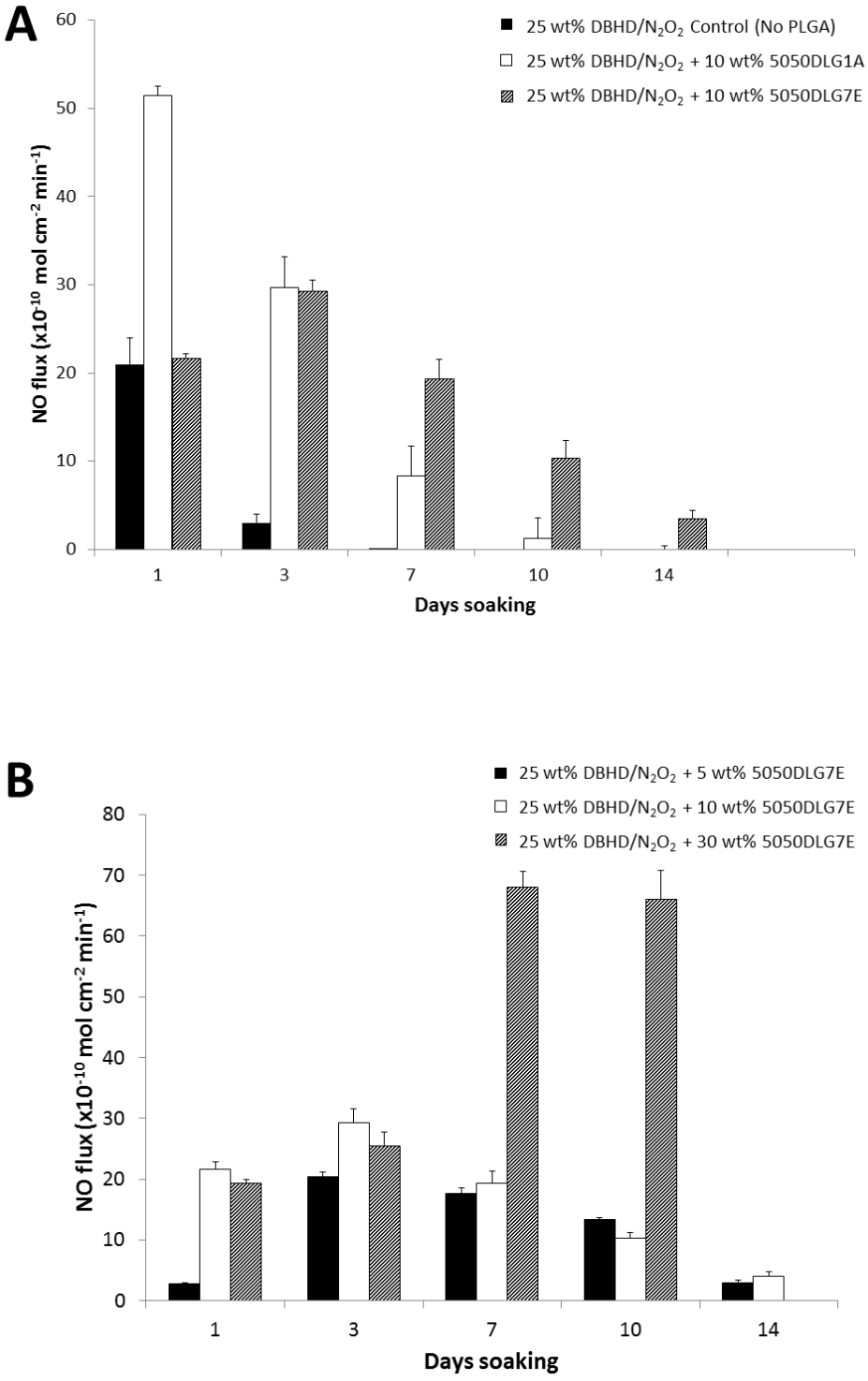

Figure 4.3. NO release profiles of PVC/DOS films doped with 25 wt% DBHD/N_2O_2 and no PLGA (control), 10 wt% 5050DLG1A, or 10 wt% 5050DLG7E additives (A). NO release profiles of PVC/DOS films doped with 25 wt% DBHD/N_2O_2 and 5, 10, or 30 wt% 5050DLG7E (B). The data are means ± SEM (n=4).

shown to release NO for 14 d; however, the fluxes were quite low for the first few days of soaking. These low fluxes indicate that the 5 wt% PLGA is not adequate to compensate for the pH increase due to production of free DBHD diamine within the film. Increasing the 5050DLG7E to 30 wt% yields films that exhibit high fluxes from days 7-10 due to the increased amount of acid monomers being produced, resulting in complete depletion of the NO reservoir before day 14. The ideal NO release coating has a consistent NO release, with little variation in the NO flux from day-to-day under physiological conditions. The films with 10 wt% 5050DLG7E had little variation in the NO flux until days 10-14, while the 5 wt% and 30 wt% films gave fluxes that were either low or very high. From this data one can conclude that using 10 wt% 5050DLG7E PLGA gives the more constant and sustained NO release profile. Based on our calculations, approximately 85% of the theoretical NO is recovered from PVC/DOS films doped with 10 wt% 5050DLG7E and 25 wt% DBHD/N_2O_2. The 15% of the theoretical NO that is lost during coating preparation and curing is likely due to the residual acid monomers present in the PLGA and thermal NO release at room temperature. This loss of NO is difficult to avoid during the coating and curing processes.

As shown in **Figure 4.4**, similar NO release profiles and trends are observed for the E2As-based films doped with 25 wt% DBHD/N_2O_2 and various PLGA additives. The PLGA additives can prolong the NO release from the E2As-based films, in comparison to films without any PLGA additive (**Figure 4.4A**). The high residual acid content of the 5050DLG1A is responsible for the initial burst and short release of NO, while the ester-capped PLGA (5050DLG7E) prolongs the NO release for up to 14 d (with smaller day-to-day variations in the NO flux). The E2As-based films were further evaluated for their NO release with two different ester-capped PLGAs (5050DLG7E and 6535DLG7E). As shown in **Figure 4.4B**, the 5 wt% 5050DLG7E and 6535DLG7E films are shown to release NO for 14 d; however, the fluxes were quite low indicating that the 5 wt% PLGA is not adequate to compensate for the pH increase due to production of DBHD diamine within the film. Increasing the PLGAs to 25 wt% yield films that exhibit high fluxes on days 1-3 due to the increased amount of acid monomers being produced, resulting in complete depletion of the NO reservoir by day 14. No significant difference between the films containing the 10wt% of the 5050DLG7E and 6535DLG7E PLGA

additives is observed. This similarity can be attributed to the fact that films are only tested for the initial 2 week period, whereas these PLGAs have much longer hydrolysis

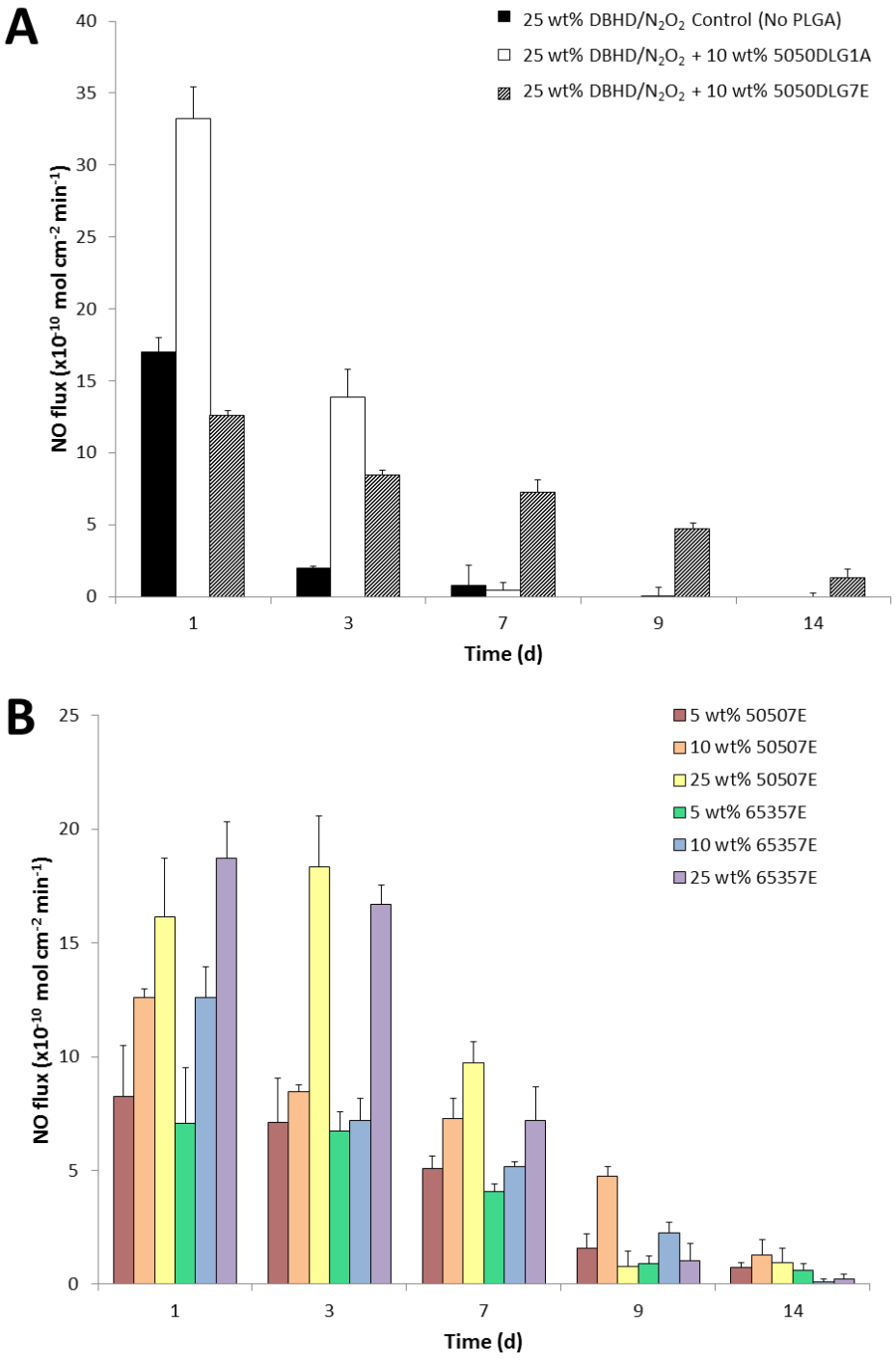

Figure 4.4. NO release profiles of E2As films doped with 25 wt% DBHD/N_2O_2 and no PLGA (control), 10 wt% 5050DLG1A, or 10 wt% 5050DLG7E PLGA additives (A). NO release profiles of E2As doped 25 wt% DBHD/N_2O_2 and 5, 10, or 25 wt% 5050DLG7E or 6535DLG7E PLGA additives (B). The data are means ± SEM (n=4).

timeframes. In addition, these PLGAs are being doped into hydrophobic polymers (with water uptake < 8%), which likely slows the hydrolysis rates even further. These results demonstrate the ability to fine-tune the NO release profile with various PLGA additives, to match with the NO release needed for particular applications.

4.3.2 Correlating NO Release and pH Change in the Films

At 37 ºC, incubation of DBHD/N_2O_2 films in PBS enables NO to be released through a proton driven mechanism and the diamine DBHD product formed increases the pH within the PVC film. The pH increase causes the NO release rate to decrease and eventually cease completely, without delivering the entire NO payload. In contrast, using PLGA as an additive in appropriate proportion helps ensure that the DBHD/N_2O_2 is the limiting reagent and the entire NO payload is eventually released. PLGA continues to hydrolyze creating a more acidic environment essential for NO release. Hydrolysis of PLGA takes place simultaneously with NO release, balancing the pH of the film in a pH range that favors NO release. However, the key to optimizing the NO release from these formulations is balancing the rates of PLGA hydrolysis with the rate of DBHD amine production.

It is challenging to measure the rate constant of diazeniumdiolate decomposition and PLGA hydrolysis, since one reaction directly effects the other. That is, the formation of the diamine causes the coating to become basic, which will further catalyze (increase rate of) the PLGA hydrolysis. Therefore, the rate constants for the two reactions will change over time, and be somewhat dependent on another. Hence, it is not possible to assess the kinetics of each independently. Studying the pH changes within the polymer matrix, via the addition of pH indicator dyes, allows for qualitative correlation between the pH changes and NO release profile. Studying the pH changes within the polymer matrix as a function of time provides a means to further support the hypothesis that the addition of PLGA to the PVC films derives its benefit via control of the polymer phase pH. In previous work, Chromoionophore II (9-dimethylamino-5-[4-(16-butyl-2,14-dioxo-3,15-dioxaeicosyl)phenylimino]benzo[a]phenoxazine) was doped into a PVC/DOS film with DBHD/N_2O_2. However, this pH indicator only demonstrated the mechanism whereby this matrix becomes more basic over time without any detailed correlation to the

observed NO release rate.[31] The pH within pure PLGA matrices has been studied previously using confocal microscopy with an acidic pH sensitive probe Lysosensor yellow/blue.[38] In the present study, doping the films with simple pH indicator dyes allows a convenient and inexpensive way to visualize the pH changes that occur throughout the 14 d incubation period. The amount of dye added to the films is crucial, as too little dye will prevent visual interpretation, while too much dye will compete with the DBHD/N_2O_2 reaction. As shown in **Figure 4.5**, bromothymol blue (BB7) has a pH transition range of 6-7 and bromocresol green (BG5) of 4-5, where yellow is acidic and blue indicates basic conditions.

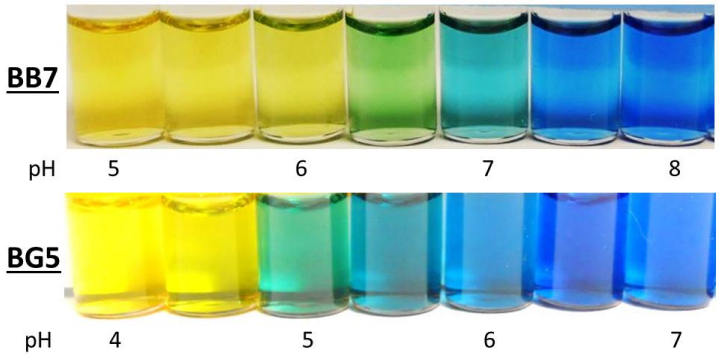

Figure 4.5. Comparison of color changes of bromocresol green (BG5) and bromothymol blue (BB7) in PBS buffer at various pH values.

The PVC/DOS-based films containing DBHD/N_2O_2 (without PLGA additive) and the pH indicator dyes initially have a basic environment (see **Figure 4.6A**). This basic environment is maintained throughout the incubation time period. This demonstrates that without an additive, the pH in the DBHD/N_2O_2 only films remains basic (from free

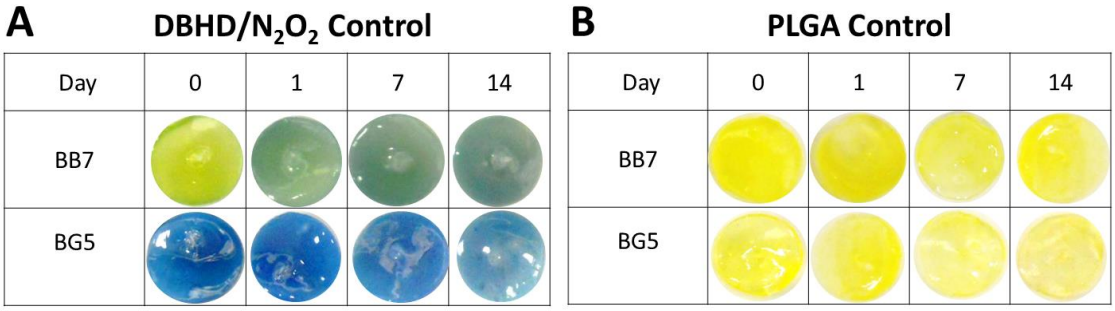

Figure 4.6. Comparison of color changes of BG5 and BB7 doped with 25 wt% DBHD/N_2O_2 in PVC/DOS (A). Comparison of color changes of BG5 and BB7 doped with 10 wt% of 5050DLG7E PLGA in PVC/DOS matrix (B). All films were incubated at 37 ºC for 14 d in PBS buffer.

DBHD within the DBHD/N_2O_2 preparation) and prevents any further NO release. The dyes were also added to the PVC/DOS films doped with PLGA (without any DBHD/N_2O_2), and all showed an acidic environment (see **Figure 4.6**). Similar results are observed for the corresponding E2As-based control films.

In contrast, the films doped with 10 wt% 5050DLG1A and 25 wt% DBHD/N_2O_2 release NO for 10 d, but exhibit a burst of NO on the first day of soaking. As shown in **Figure 4.7A**, the pH indicators in these 5050DLG1A-doped films indicate an initial acidic environment (pH ~5-6). This initial acidic environment correlates to the observed large NO burst on day 1, caused by the high residual acid content in the 5050DLG1A (**Table 4.1**). After 1 d of soaking, the PVC/DOS film doped with 5050DLG1A and BB7 dye indicates an increase in pH (color change from yellow to green). This increase of pH is due to the high flux of NO that occurs (**Figure 4.3A**) thereby producing significant amounts of the free DBHD amine within the film during a short period of time. By days 7-10, the NO flux diminishes significantly, during which time both dyes gradually

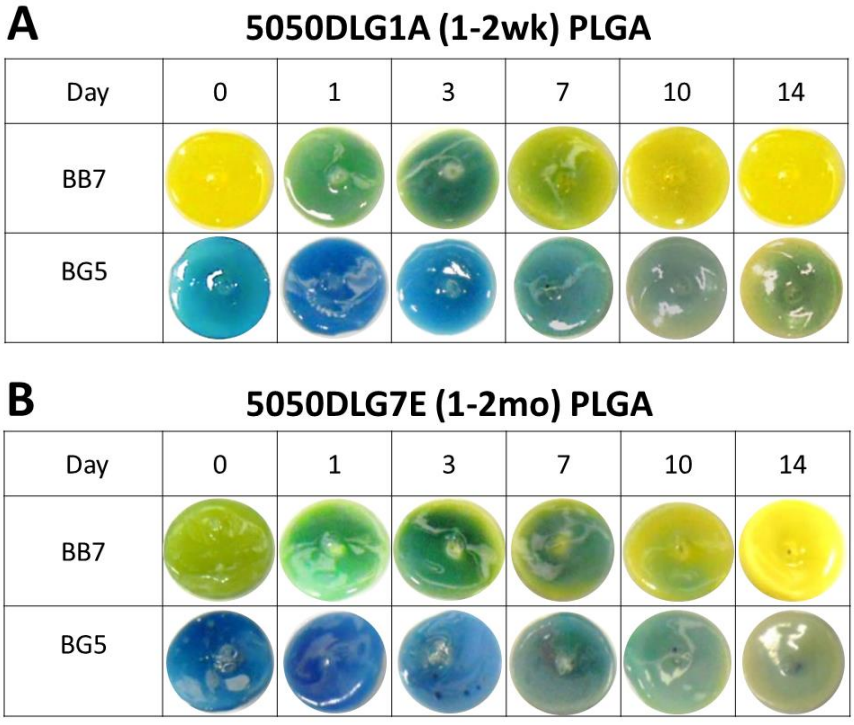

Figure 4.7. Comparison of color changes of BG5 and BB7 doped with 25 wt% DBHD/N_2O_2 and 10 wt% of 5050DLG1A PLGA in PVC/DOS polymer matrix (A). Comparison of color changes of BG5 and BB7 doped with 25 wt% DBHD/N_2O_2 and 10 wt% of 5050DLG7E PLGA in PVC/DOS polymer matrix (B). All films were incubated at 37 ºC for 14 d in PBS buffer.

indicate a decrease in film pH (films turned green and then yellow), an indication that the DBHD/N_2O_2 reservoir has been depleted as the PLGA continues to hydrolyze, recreating an acidic environment.

Additionally, as reported above, NO release profiles of the PVC/DOS-based films doped with ester-capped PLGA (5050DLG7E) films yield the best balance between the hydrolysis rate of PLGA and NO release from DBHD/N_2O_2, providing a prolonged NO release profile. The pH indicators show (**Figure 4.7B**) that these films also are initially acidic, but less acidic than the 5050DLG1A films. In fact, the 5050DLG7E polymer possesses a much lower acid content and therefore slower hydrolysis rate in comparison to the films containing the 5050DLG1A polymer additive (**Table 4.1**); therefore, no initial burst of NO is observed. This lower initial acid content is crucial to prolonging the NO release from these films. The films containing ester-capped PLGAs (5050DLG7E PLGA and 6535DLG7E) exhibit little color change until days 10-14, when they begin to become more acidic. This demonstrates that the acid production rate (from the PLGA hydrolysis) and DBHD amine production rate is closely balanced within these films, explaining the consistency of the pH and NO release from day-to-day. These films also turned yellow by day 14, indicating the depletion of the NO reservoir.

Similar trends in pH changes are observed for the E2As-based films (**Figure 4.8**). As shown in **Figure 4.8A**, the E2As films doped with 5050DLG1A have a more acidic pH, corresponding to the high initial burst of NO on the first day of soaking. Films become more basic (green) as the NO is released and the diamine forms. As the NO reservoir becomes depleted, the films become acidic (yellow) as the PLGA continues to hydrolyze. In contrast, the E2As films doped with the ester-capped PLGA (5050DLG7E) have less significant changes in the organic phase pH until days 10-14 when the NO reservoir is depleted (**Figure 4.8B**). This more steady organic phase pH results in the more consistent day-to-day NO release observed (**Figure 4.4A**).

Although a direct comparison in the colors cannot be made between the PVC/DOS- and E2As-based films (due to the pKa values of the pH indicator dyes varying in different polymer matrices), the general trends in pH changes can be observed and correlated with the NO release profile. In short, the use of pH indicators within the films provides further evidence that the ester-capped PLGAs, especially the 5050DLG7E

PLGA, exhibits a hydrolysis rate that balances the decomposition rate of the DBHD/N_2O_2, producing the optimum pH and concomitant prolonged NO release/flux profile.

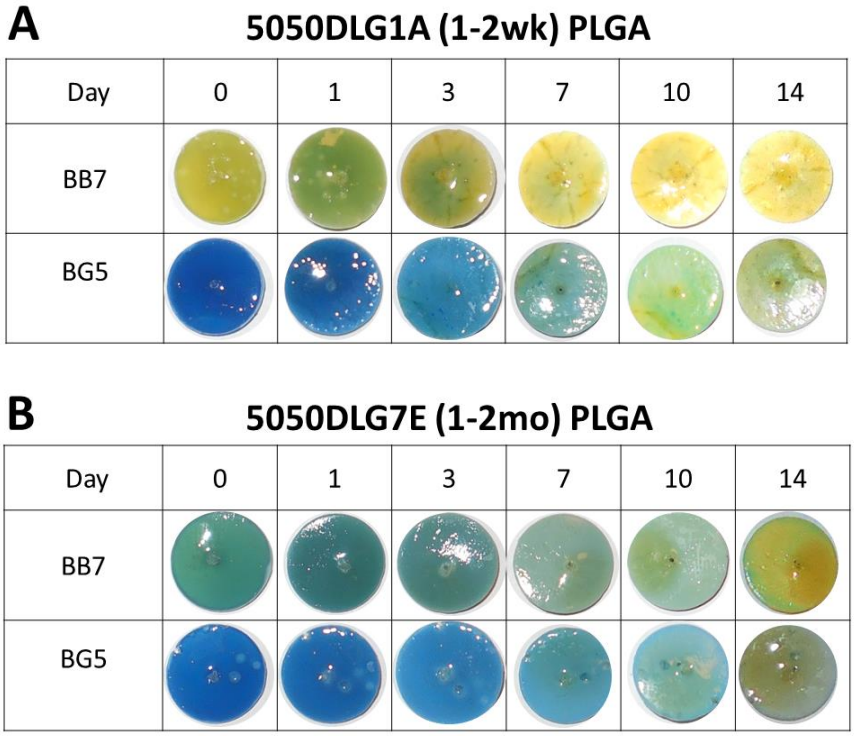

Figure 4.8. Comparison of color changes of BG5 and BB7 doped with 25 wt% DBHD/N_2O_2 and 10 wt% of 5050DLG1A PLGA in E2As polymer films (A). Comparison of color changes of BG5 and BB7 doped with 25 wt% DBHD/N_2O_2 and 10 wt% of 5050DLG7E PLGA in E2As polymer films (B). All films were incubated at 37 ºC for 14 d in PBS buffer.

4.3.3 Comparison of Hemodynamic Effects of PVC/DOS and E2As Control Polymers in ECC Rabbit Model

The hemocompatibility of PVC/DOS and E2As polymer coatings was compared using the 4 h rabbit thrombogenicity model. The goal of this comparison was to choose the polymer with the best hemocompatible properties to be combined with the NO release chemistry for optimizing NOrel coatings for extracorporeal circulation testing in rabbits. Polymers were coated on the ECC tubings as described in Section 4.2.4 (**Figure 4.9**). Platelet preservation during exposure of the coated ECC surfaces to flowing blood was assessed by measuring the platelet count every hour. Platelet count was used as one of the parameters to assess the hemocompatibility of the surface because the decrease in the

platelet count over time indicates the activation of platelets on the tubing surface.[28, 42, 51]

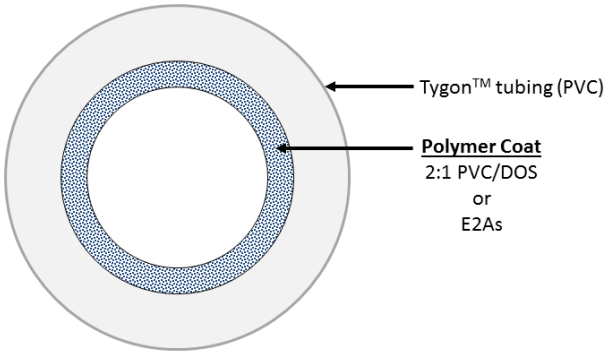

Figure 4.9. Diagram of the extracorporeal circuit (ECC) tubing coated with the base polymers (PVC/DOS or E2As).

Platelet count was corrected for any hemodilution due to any IV infusion of fluids into the rabbits. Only 1 out of 5 loops coated with E2As clotted before the end of the 4 h experiment, whereas, of 3 out 4 PVC/DOS loops clotted. As shown in **Figure 4.10A**, at the end of 4 h, both polymer coatings exhibited a time dependent loss in platelets, however, 58 ± 3% of platelets were preserved for E2As ECCs whereas, animals tested with PVC/DOS exhibited a more significant loss in platelets count (46 ± 3%).

To ascertain the differential of the thrombus in the thrombogenicity chambers (i.e., the 3/8" Tygon 8 cm in length within the ECC loop) of the coated ECCs, a two dimensional analysis was performed after 4 h of blood exposure. NIH Image J imaging software was used to calculate the representative 2-D thrombus area (cm^2) in each tubing chamber.[28, 42, 44, 45] As shown in **Figure 4.10B**, the thrombus area of the E2As polymer coated ECC was significantly lower than the PVC/DOS (5.2 ± 0.3 and 6.7 ± 0.3, respectively). Based on the platelet count and clot area, the E2As polymer was found to have enhanced intrinsic hemocompatible properties compared to the PVC/DOS. The preservation of platelet count and reduced clot area can be attributed to the fact that the E2As polymer binds to albumin more strongly than fibrinogen, which likely aids in passivating the surface.[52] It is widely accepted fact that protein adsorption is the first event that occurs upon surface-blood contact.[53] Fibrinogen is a key protein in the coagulation cascade that rapidly adsorbs to foreign surfaces and binds to activated platelets. Fibrinogen contains multiple binding sites for platelet integrin $\alpha_{IIb}\beta_3$ (GPIIbIIIa).[54, 55] These fibrinogen-$\alpha_{IIb}\beta_3$ interactions play a significant role in platelet

adhesion, activation and aggregation that ultimately leads to a clot formation.[55] Platelets can bind to both albumin and fibrinogen, however albumin can significantly reduce the platelet adhesion in comparison to fibrinogen coated surfaces.[56] The fact that E2As

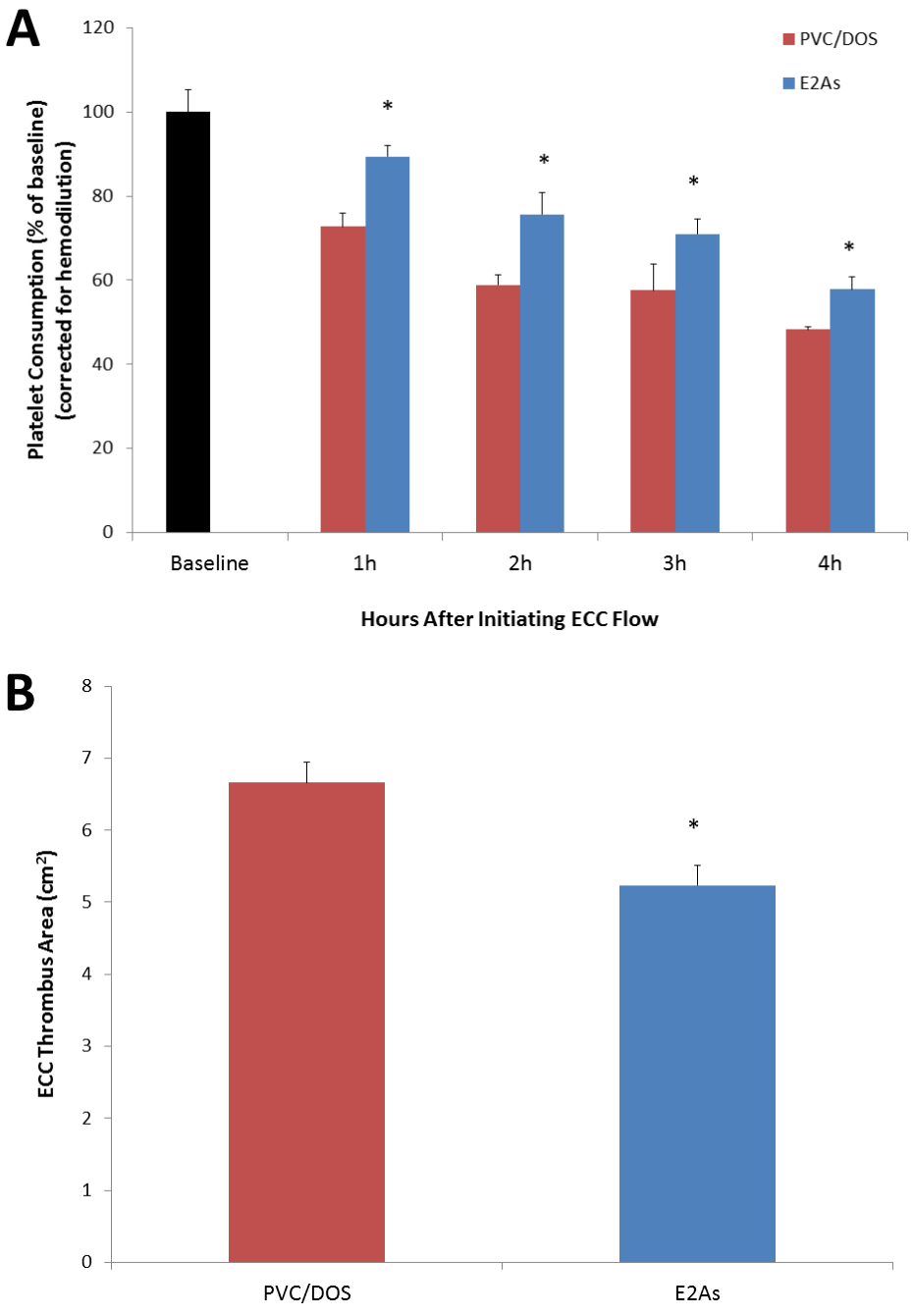

Figure 4.10. (A) Comparison of time-dependent effects of base polymer coated ECC loops on platelet consumption. (B) Quantitation of thrombus area as calculated with NIH Image J software using a 2D representation of thrombus. The data are means ± SEM. * = $p < 0.05$, PVC/DOS vs. E2As.

polymer adsorbs albumin more strongly than fibrinogen indicates its potential in passivating the blood contacting surfaces though this mechanism.[52] Our hypothesis is that by combining the E2As polymer (with excellent intrinsic hemocompatibility properties) with NO release will further improve the overall hemocompatibility of such coatings than can be achieved by use of either approach alone.

4.3.4 Nitric Oxide Release from PVC/DOS- and E2As-Based NOrel Coatings in ECC and Effects on Rabbit Hemodynamics, Platelet Function, and Thrombus Formation

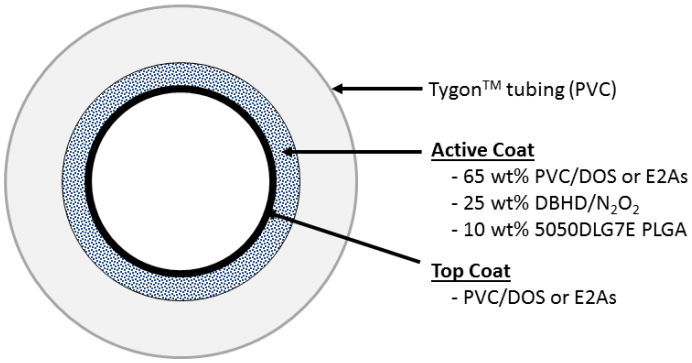

Figure 4.11. Diagram of the extracorporeal circuit (ECC) tubing coated with the PVC/DOS- or E2As-based NO-releasing polymer containing 25 wt% DBHD/N_2O_2 and 10 wt% 5050DLG7E PLGA.

ECC circuits coated (**Figure 4.11**) on the inner walls with the PVC/DOS- and E2As-based polymers containing the 10 wt% 5050DLG7E PLGA and 25 wt% DBHD/N_2O_2 were tested for NO release flux, pre- and post-4 h rabbit blood exposure. These optimized coating materials continuously releases NO under physiological conditions at levels that exceeds the physiological NO release from endothelial cells (0.5-4 x 10^{-10} mol cm^{-2} min^{-1}).[57] The NOrel coated ECCs exhibited a slight burst of NO upon initial exposure to the PBS and 37 ºC that lasted ~ 30 min. Therefore, the ECC loops were first soaked with PBS for 30 min prior to the rabbit experiments in order to reduce the effects of this burst. The NO release from the PVC/DOS- and E2As-based NOrel ECC circuits show a sustained NO flux of approximately 11 x 10^{-10} mol cm^{-2} min^{-1} and 6 x 10^{-10} mol cm^{-2} min^{-1}, respectively, for 4 h, as measured using the chemiluminescence NO analyzer (**Figure 4.12**). After 4 h of blood flow, the NO flux was found to be 10 x 10^{-10} mol cm^{-2} min^{-1} (PVC/DOS) and 5 x 10^{-10} mol cm^{-2} min^{-1} (E2As) post-blood

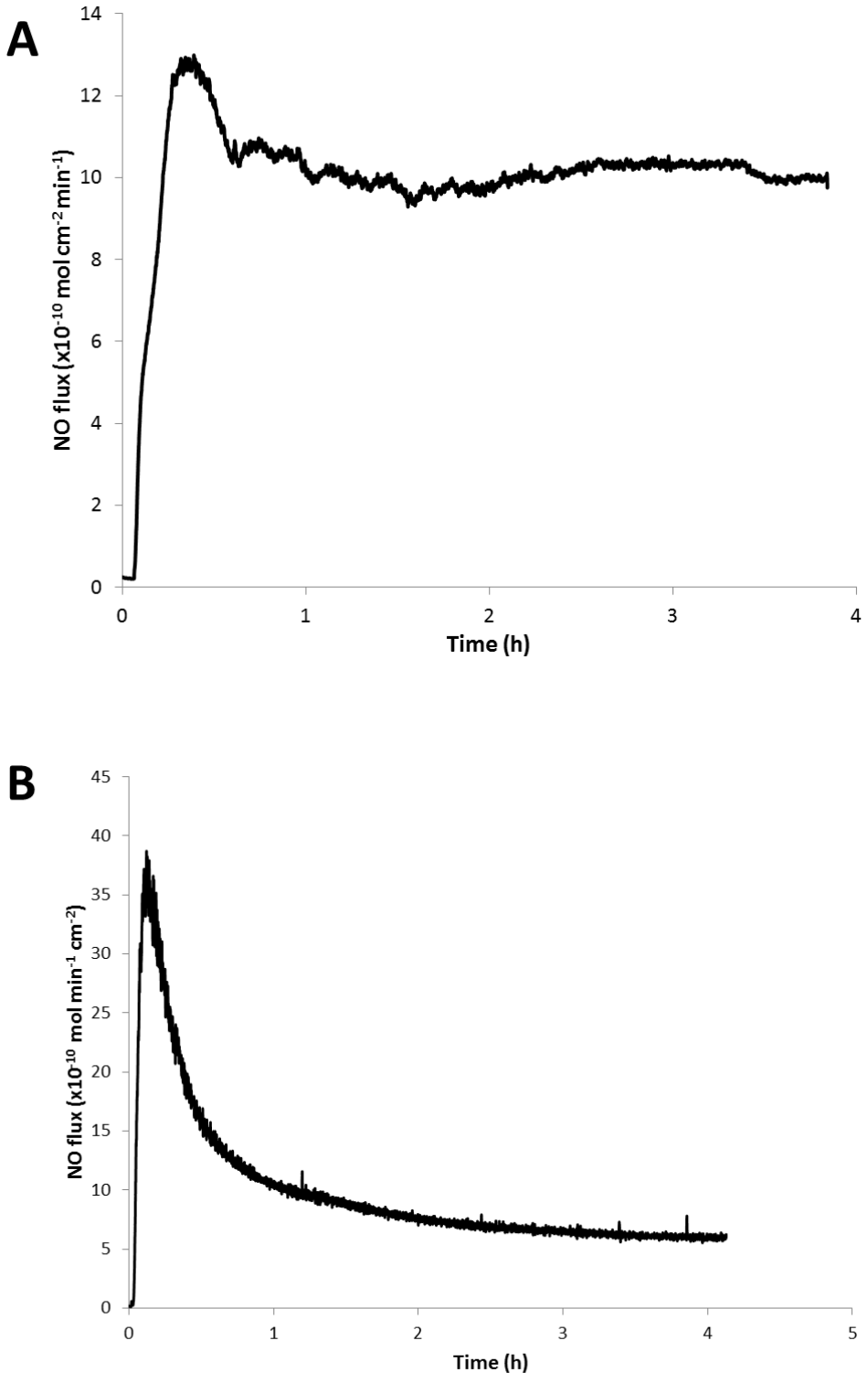

Figure 4.12. Representative NO release profile of PVC/DOS-based (A) and E2As-based (B) ECC coatings doped with 25 wt% DBHD/N_2O_2 and 10 wt% 5050DLG7E as measured in PBS using chemiluminescence.

exposure. The fact that the blood environment does not alter the kinetics of the NO release from the coating agrees well with the previously reported data for various NO release circuits.[28] Further, given the prolonged NO release capability of the new coatings being tested, applications in much longer-term extracorporeal or other biomedical applications would be possible.

No significant difference in the mean arterial pressure (MAP) of the animals on the NOrel vs. control circuits was noted, with pressures averaging 45±5 mm Hg for both types of circuits. Heart rates for the NOrel and control ECC groups were unchanged over the 4 h time period. The ECC blood flow was maintained at approximately 110 mL/min for the NOrel circuits over the 4 h animal test period. However, for the control circuits, the blood flow dropped from the initial 110 mL/min to approximately 75 mL/min in the first one hour for the control circuits, and then further dropped to 60 mL/min over the next 3 h period. Intravascular fluids were maintained at 10 mL/kg/min to maintain the blood flow in both NOrel and control circuits. The NOrel and control ECC loops have the same inner diameter (which remains static due to the rigidity of the tubing) and therefore maintains the integrity of the coating, hence having no effect on the blood flow rates. Monitoring the flow rate is a means to measure the time at which the ECC circuits has completely clotted. Since the control ECC loops often clotted, this blocked the blood flow through the tubing, thus the flow rates decreased. The activation clotting time for blood obtained from the test animals increases over the 4 h period for both NOrel and control coated circuits. As noted in previous studies,[28] this behavior can be attributed to the increase in intravascular fluids and concomitant hemodilution effect.

4.3.5 Effects of PVC/DOS- and E2As-Based NOrel Coatings on Platelet Consumption and Thrombus Formation in the Rabbit Model

The short-term 4 h rabbit ECC model was used to observe the effects of the NOrel coating on platelet count and clotting. Platelet consumption throughout the 4 h ECC was assessed by recording the platelet count, which was corrected for hemodilution due to the added IV fluids. For the PVC/DOS-based ECC circuits, 4 out of 7 control circuits clotted within 3 h, whereas all the 7 NOrel coated circuits remained patent after 4 h. All 5 of the E2As-based NOrel circuits survived the 4 h experiment, whereas for the E2As controls

only 1 out of 5 loops clotted during the 4 h ECC run. The animals tested with the PVC/DOS-based NOrel polymer coated ECCs showed 79 ± 11% preservation of the platelet count over the course of the 4 h blood contact period, whereas animals tested with the PVC/DOS control polymer ECCs exhibited a time-dependent loss in platelet count (54 ± 6 %). For the E2As-based NOrel circuits, the platelet count rose slightly above the baseline value during the first hour, likely due to the release of reserve platelets from the spleen. The platelet count returned to the baseline level during the second hour and was maintained at an average of 97 ± 10% of baseline levels at the end of the 4 h experiments. The platelet count for E2As control circuits showed a time-dependent loss in platelets dropping to 58 ± 3% of baseline after 4 h (**Figure 4.13**).

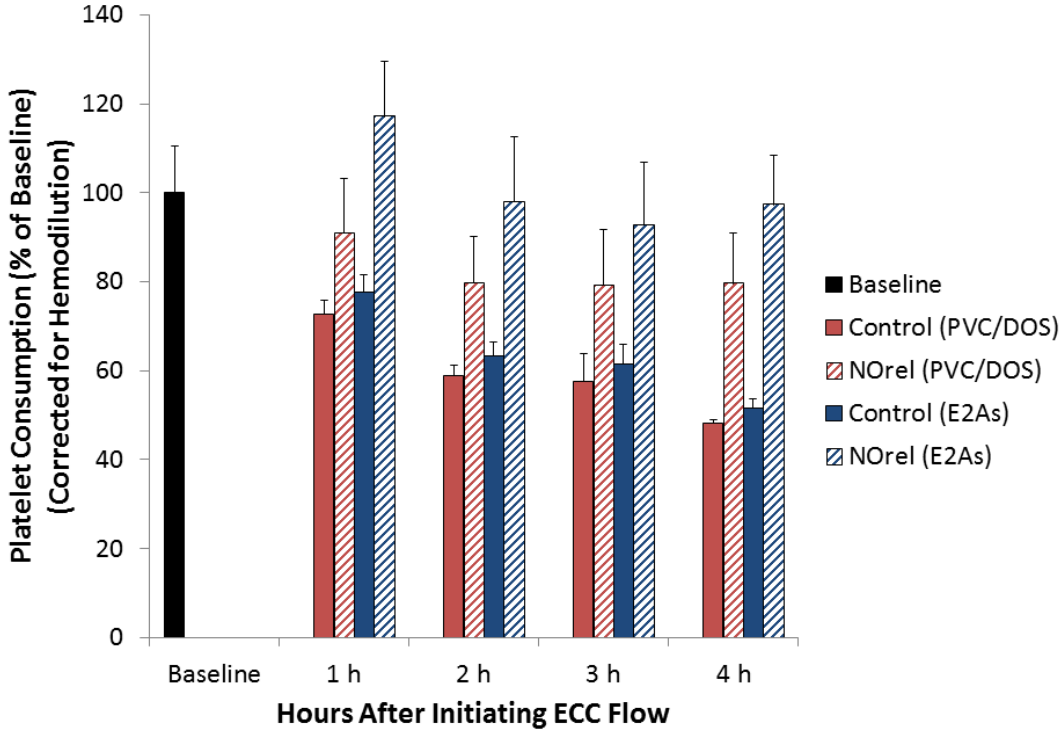

Figure 4.13. Time-dependent effects of PVC/DOS control, PVC/DOS-based NOrel, E2As control, and E2As-based NOrel coatings on rabbit platelet count. The data are means ± SEM.

As previously described, Image J software was used to calculate the 2D representative thrombus area (cm^2) in each thrombogenicity chamber after 4 h of blood exposure. **Figures 4.14A and B**, show representative images of the control and NOrel circuits, respectively, after 4 h blood flow in the rabbit ECC model. The thrombi area measurements were quantitated and, as shown in **Figure 4.14C**, the thrombus area of the

PVC/DOS-NOrel polymer ECC was significantly reduced compared to the PVC/DOS control polymer ECCs (1.5 ± 0.5 and 6.5 ± 0.4 cm^2, respectively). A similar trend is observed for the E2As-based control and NOrel circuits, with clot areas of 5.2 ± 0.3 cm^2 and 0.9 ± 0.3 cm^2, respectively. For an A-V shunt procedure, the lungs are the first main filter for the blood. After the 4 h experimental period, the lungs were evaluated for accumulated thromboemboli. The control ECCs rabbit lungs appeared to have more emboli accumulated in the lower lobes of both lungs then any of the NOrel ECC rabbit lungs.

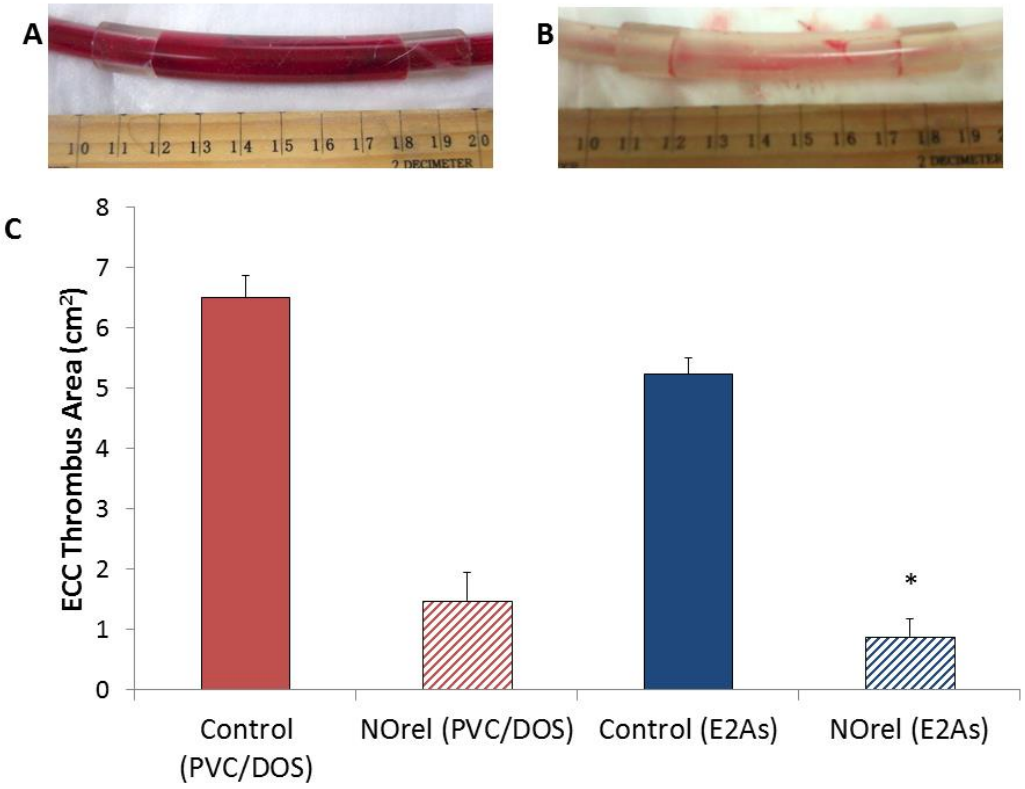

Figure 4.14. Evaluation of thrombus area on PVC/DOS- and E2As-based Control and NOrel coated ECC loops after 4 h blood exposure in rabbit thrombogenicity model. The 2D representation of thrombus quantitated using NIH Image J software. The data are means ± SEM. * = $p < 0.05$, PVC/DOS-based NOrel vs. E2As-based NOrel.

Using the DBHD/N_2O_2 chemistry in PVC/DOS polymer an NO flux of approximately 10 – 15 x 10^{-10} mol cm^{-2} min^{-1} is needed to prevent clotting and maintain ~80% of baseline platelet count in extracorporeal circulation.[28, 42, 44] However, with the appropriate polymer, such as E2As, an NO flux of only 6 x 10^{-10} mol cm^{-2} min^{-1} is

sufficient to prevent platelet activation, reduce clot area, and is able to maintain 97% of baseline platelet count at the end of 4 h.

4.4 Conclusions

This study demonstrates that PLGA polymers can be used as an additive within polymer matrices (PVC/DOS and E2As) containing lipophilic diazeniumdiolate species. The high residual acid content and fast hydrolysis rates of acid-capped PLGA additives results in high initial bursts of NO. The NO release from DBHD/N_2O_2-doped PVC and E2As was extended to 14 d by using ester-capped PLGAs. By using various pH indicators it is shown that the hydrolysis rates of specific PLGA species employed can control the NO release properties by influencing the steady-state pH within the polymer films. The inherent hemocompatibility properties of the base polymers (Elast-Eon E2As and PVC/DOS) was also compared in the ECC model, and E2As was found to be superior in prevention of preservation of platelets and reduced thrombus formation. Further, it was demonstrated that nitric oxide release from E2As and PVC/DOS coatings containing a diazeniumdioloate NO donor and PLGA additive on the inner walls of the ECC circuits was able to further attenuate the activation of the platelets, while maintaining their functionality, and reduce clot area (vs. control ECC circuits without NO release) in a 4 h ECC rabbit model. The E2As-based NOrel circuits preserved platelets at a higher level than PVC-based NOrel circuits (97% and 80% of baseline, respectively). After 4 h of blood flow, the E2As-based NOrel circuits also had a significantly lower thrombus area than the PVC-based NOrel circuits. This study demonstrated that the inherent hemocompatibility properties of the base polymer can also influence the efficiency of the NO release coatings. These encouraging results demonstrate that E2As-based NOrel materials have great potential to improve the hemocompatibility of both short- and potentially long-term blood contacting devices such as catheters, vascular grafts, stents and other extracorporeal life support devices, such as long-term ECMO.[58]

4.5 References

1. B. D. Ratner, *Biomaterials*, **2007**, *28*, 5144-5147.

2. D. C. Sin, H. L. Kei and X. Miao, *Expert Rev Med Devices*, **2009**, *6*, 51-60.

3. M. Ranucci, A. Balduini, A. Ditta, A. Boncilli and S. Brozzi, *Ann Thorac Surg*, **2009**, *87*, 1311-1319.

4. M. M. Reynolds and G. M. Annich, *Organogenesis*, **2011**, *7*, 42-49.

5. *Extracorporeal Life Support Organization (ELSO) Extracorporeal Life Support (ECLS) registry report international summary*, **2010**.

6. A. M. Gaffney, S. M. Wildhirt, M. J. Griffin, G. M. Annich and M. W. Radomski, *BMJ*, **2010**, *341*.

7. T. M. Robinson, T. S. Kickler, L. K. Walker, P. Ness and W. Bell, *Crit Care Med*, **1993**, *21*, 1029-1034.

8. T. Kolobow, E. W. Stool, P. K. Weathersby, J. Pierce, F. Hayano and J. Suaudeau, *Trans Am Soc Artif Intern Organs*, **1974**, *20A*, 269-276.

9. M. Szycher, *J Biomater Appl*, **1988**, *3*, 297-402.

10. L. H. Edmunds, Jr., *ASAIO J*, **1995**, *41*, 824-830.

11. P. Didisheim, *ASAIO J*, **1994**, *40*, 230-237.

12. W. S. Kim and H. Jacobs, *Blood Purificat*, **1996**, *14*, 357-372.

13. O. Larm, R. Larsson and P. Olsson, *Biomater Med Devices Artif Organs*, **1983**, *11*, 161-173.

14. B. D. Ratner, *J Biomater Sci Polym Ed*, **2000**, *11*, 1107-1119.

15. M. W. Radomski and S. Moncada, *Adv Exp Med Biol*, **1993**, *344*, 251-264.

16. M. W. Vaughn, L. Kuo and J. C. Liao, *Am J Physiol*, **1998**, *274*, H2163-H2176.

17. J. S. Isenberg, M. J. Romeo, C. Yu, C. K. Yu, K. Nghiem, J. Monsale, M. E. Rick, D. A. Wink, W. A. Frazier and D. D. Roberts, *Blood*, **2008**, *111*, 613-623.

18. B. L. Nguyen, M. Saitoh and J. A. Ware, *Am J Physiol - Heart C*, **1991**, *261*, H1043-H1052.

19. Y. Sato, Y. Hiramatsu, S. Homma, M. Sato, S. Sato, S. Endo and Y. Sohara, *J Thorac Cardiovasc Surg*, **2005**, *130*, 346-350.

20. A. K. Zimmermann, H. Aebert, A. Reiz, M. Freitag, M. Husseini, G. Ziemer and H. P. Wendel, *ASAIO J*, **2004**, *50*, 193-199.

21. G. F. P. de Souza, J. K. U. Yokoyama-Yasunaka, A. B. Seabra, D. C. Miguel, M. G. de Oliveira and S. R. B. Uliana, *Nitric Oxide*, **2006**, *15*, 209-216.

22. A. B. Seabra, G. F. P. de Souza, L. L. da Rocha, M. N. Eberlin and M. G. de Oliveira, *Nitric Oxide*, **2004**, *11*, 263-272.

23. T. A. Alston, D. J. Porter and H. J. Bright, *J Biol Chem*, **1985**, *260*, 4069-4074.

24. G. M. Annich, J. P. Meinhardt, K. A. Mowery, B. A. Ashton, S. I. Merz, R. B. Hirschl, M. E. Meyerhoff and R. H. Bartlett, *Crit Care Med*, **2000**, *28*, 915-920.

25. M. H. Schoenfisch, K. A. Mowery, M. V. Rader, N. Baliga, J. A. Wahr and M. E. Meyerhoff, *Anal Chem*, **2000**, *72*, 1119-1126.

26. G. B. Richter-Addo and P. Legzdins, *Oxford, University Press: New York*, **1992**.

27. W. J. Paulus, P. J. Vantrimpont and A. M. Shah, *Circulation*, **1994**, *89*, 2070-2078.

28. T. C. Major, D. O. Brant, M. M. Reynolds, R. H. Bartlett, M. E. Meyerhoff, H. Handa and G. M. Annich, *Biomaterials*, **2010**, *31*, 2736-2745.

29. K. M. Davies, D. A. Wink, J. E. Saavedra and L. K. Keefer, *J Am Chem Soc*, **2001**, *123*, 5473-5481.

30. H. Zhang, G. M. Annich, J. Miskulin, K. Osterholzer, S. I. Merz, R. H. Bartlett and M. E. Meyerhoff, *Biomaterials*, **2002**, *23*, 1485-1494.

31. M. M. Batchelor, S. L. Reoma, P. S. Fleser, V. K. Nuthakki, R. E. Callahan, C. J. Shanley, J. K. Politis, J. Elmore, S. I. Merz and M. E. Meyerhoff, *J Med Chem*, **2003**, *46*, 5153-5161.

32. B. Wu, *PhD Dissertation, University of Michigan, Ann Arbor*, **2009**.

33. Z. Zhou and M. E. Meyerhoff, *Biomacromolecules*, **2005**, *6*, 780-789.

34. S. Kaul, B. Cercek, J. Rengstrom, X.-P. Xu, M. D. Molloy, P. Dimayuga, A. K. Parikh, M. C. Fishbein, J. Nilsson, T. B. Rajavashisth and P. K. Shah, *J Am Coll Cardiol*, **2000**, *35*, 493-501.

35. C. E. Holy, S. M. Dang, J. E. Davies and M. S. Shoichet, *Biomaterials*, **1999**, *20*, 1177-1185.

36. L. Lu, S. J. Peter, M. D. Lyman, H. L. Lai, S. M. Leite, J. A. Tamada, S. Uyama, J. P. Vacanti, R. Langer and A. G. Mikos, *Biomaterials*, **2000**, *21*, 1837-1845.

37. S. J. Siegel, J. B. Kahn, K. Metzger, K. I. Winey, K. Werner and N. Dan, *Eur J Pharm Biopharm*, **2006**, *64*, 287-293.

38. A. Ding and S. Schwendeman, *Pharm Res*, **2008**, *25*, 2041-2052.

39. A. Shenderova, A. G. Ding and S. P. Schwendeman, *Macromolecules*, **2004**, *37*, 10052-10058.

40. J. W. Yoo, J. S. Lee and C. H. Lee, *J Biomed Mater Res A*, **2010**, *92A*, 1233-1243.

41. W. Cai, J. Wu, C. Xi and M. E. Meyerhoff, *Biomaterials*, **2012**.

42. E. J. Brisbois, H. Handa, T. C. Major, R. H. Bartlett and M. E. Meyerhoff, *Biomaterials*, **2013**, *34*, 6957-6966.

43. D. H. Na and P. P. DeLuca, *Pharm Res*, **2005**, *22*, 736-742.

44. H. Handa, T. C. Major, E. J. Brisbois, K. A. Amoako, M. E. Meyerhoff and R. H. Bartlett, *J Mater Chem B Mater Biol Med*, **2014**, *2*, 1059-1067.

45. H. Handa, E. J. Brisbois, T. C. Major, L. Refahiyat, K. A. Amoako, G. M. Annich, R. H. Bartlett and M. E. Meyerhoff, *Journal of Materials Chemistry B*, **2013**, *1*, 3578-3587.

46. S. M. Lantvit, B. J. Barrett and M. M. Reynolds, *J Biomed Mater Res A*, **2013**.

47. K. M. Miranda, T. Katori, C. L. Torres de Holding, L. Thomas, L. A. Ridnour, W. J. McLendon, S. M. Cologna, A. S. Dutton, H. C. Champion, D. Mancardi, C. G.

Tocchetti, J. E. Saavedra, L. K. Keefer, K. N. Houk, J. M. Fukuto, D. A. Kass, N. Paolocci and D. A. Wink, *J Med Chem*, **2005**, *48*, 8220-8228.

48. E. M. Hetrick and M. H. Schoenfisch, in *Annual Review of Analytical Chemistry*, 2009, pp. 409-433.

49. P. N. Coneski and M. H. Schoenfisch, *Chem Soc Rev*, **2012**, *41*, 3753-3758.

50. S. P. Schwendeman, *Crit Rev Ther Drug*, **2002**, *19*, 73-98.

51. E. J. Brisbois, H. Handa, T. C. Major, R. H. Bartlett and M. E. Meyerhoff, *Biomaterials*, **2013**.

52. D. Cozzens, A. Luk, U. Ojha, M. Ruths and R. Faust, *Langmuir*, **2011**, *27*, 14160-14168.

53. L.-C. Xu and C. A. Siedlecki, *Langmuir*, **2009**, *25*, 3675-3681.

54. A. Agnihotri, P. Soman and C. A. Siedlecki, *Colloids Surf B Biointerfaces*, **2009**, *71*, 138-147.

55. M. A. Hussain, A. Agnihotri and C. A. Siedlecki, *Langmuir*, **2005**, *21*, 6979-6986.

56. B. Sivaraman and R. A. Latour, *Biomaterials*, **2011**, *32*, 5365-5370.

57. M. W. Vaughn, L. Kuo and J. C. Liao, *Am J Physiol - Heart C*, **1998**, *274*, H2163-H2176.

58. W. C. Oliver, *Semin Cardiothorac Vasc Anesth*, **2009**, *13*, 154-175.

CHAPTER 5

Optimized Polymeric Film-Based Nitric Oxide Delivery Inhibits Bacterial Growth in a Mouse Burn Wound Model

5.1 Introduction

Bacterial infection and biofilm formation is a significant problem with a variety of biomedical devices that can lead to complications, increased medical costs, and increased morbidity.[1] Indwelling medical devices are responsible for more than one million hospital acquired infections, resulting in 99,000 deaths per year in the United States.[2, 3] Another significant area of infection is in wounds. More than one million burn injuries are reported annually in the US,[4] resulting in 3,500 deaths per year.[5] Complications of wound infection are also significant and include delayed wound healing, tissue necrosis, spread of infection to the bloodstream and other organs, and transmission of wound-associated bacteria to other patients in hospitals.[6] Treatment of these infections often includes antibiotics and other antimicrobial agents, such as silver.[7] However, these materials often fail to prevent the infection and there is a growing concern for their use due to the emergence of bacterial resistance to antibiotics and antimicrobial agents.[7-9] Recent findings have also suggested that silver delays the wound-healing process and may have serious cytotoxic effects.[10] *Acinetobacter baumannii* is one such bacterial strain that has developed extensive antimicrobial resistance, and it also forms biofilms that are resistant to host defenses and antimicrobial treatment.[11] *A. baumannii* has been named a "new enemy"[12] due to large outbreaks in intensive care units[13-17] and also is a dominant organism isolated from wound infections (e.g., troops injured in Afghanistan and Iraq).[11, 18, 19]

Among its many biological roles, nitric oxide (NO) is known as a potent antimicrobial agent and an accelerant to the wound healing process.[1] Nitric oxide is endogenously synthesized by nitric oxide synthase enzymes (NOS): endothelial (eNOS), neuronal (nNOS), and inducible (iNOS). The iNOS is capable of producing high levels of NO[20] and micromolar concentrations of NO are known to have cytotoxic effects.[21-23] Reactive oxygen species (such as superoxide (O_2^-), hydrogen peroxide (H_2O_2), and hydroxyl radical (OH)) and reactive nitrogen species (such as NO, N_2O_3, and peroxynitrite ($OONO^-$)) are generated by the iNOS and phagocyte oxidase pathways and are responsible for the antimicrobial effects observed due to their interactions with thiols, proteins, DNA, and lipids.[20] The broad-spectrum antibacterial properties of NO against a wide range of microbes have been demonstrated, showing that both gram-positive and gram-negative bacteria can be killed.[24] In addition, bacteria have the ability to form biofilms (communities of bacteria encased in a self-synthesized extracellular matrix), which is one of the mechanisms that bacteria use to survive in adverse environments.[25-28] Indeed, formation of biofilms protects bacteria from antiseptics, antibiotics, and host defenses, making the infections difficult to eradicate.[29] Evidence suggests that biofilms also play a role in wound infections, which may explain the chronic nature of many wounds infections and their resistance to antimicrobial therapy.[30] Low nM concentrations of NO have been shown to be efficient at dispersing biofilms of various bacterial strains.[31-34] Therefore, NO-releasing materials have great potential in biomedical applications, especially to reduce the risk of infection, promote wound healing, and improve biocompatibility of implantable medical devices.[34-37]

Due to the potential benefits of NO release, a wide variety of NO-releasing polymers have been reported in the literature, and many of these are summarized in a recent review by Carpenter and Schoenfisch.[38] Materials with short durations of NO release may have potential wound healing applications due to the ease of replacing the material periodically throughout the wound healing process. The NO released from these materials may also decrease the risks of infected wounds, thereby reducing the wound healing time and repair chronic wounds.[39] Gaseous nitric oxide treatments and NO-releasing materials have been used topically and shown to increase dermal blood flow, increase reepithelialization and angiogenesis, and accelerate wound repair; however,

some of these studies have been conducted with uninfected wounds.[40-44] Previous studies have shown NO can be released from polymer films doped with diazeniumdiolate dibutylhexanediamine (DBHD/N_2O_2), which releases NO through proton or thermal driven mechanisms.[45-48] However, the loss of NO from DBHD/N_2O_2 creates free lipophilic amine species within the polymer that react with water, thereby increasing the pH within the polymer phase and effectively turning off the NO release. In Chapter 4, poly(lactic-co-glycolic) acid was used as an additive to promote and prolong the NO release from poly(vinyl chloride) films doped with DBHD/N_2O_2.[48, 49] The ester linkages of the PLGA will hydrolyze in the presence of water, producing lactic and glycolic acids that can act as proton sources to promote the NO release from DBHD/N_2O_2-doped polymers. PLGAs can have varying hydrolysis rates, which is primarily determined by the copolymer ratio, the end group chemistry (either a free carboxylic acid or ester end group), and molecular weight. Lactate has been shown to enhance angiogenesis and accelerate wound healing,[50] so any lactic acid monomers that leach from the NO-releasing patches may also prove beneficial. Previous work with DBHD/N_2O_2-based films have primarily utilized hydrophobic polymers (e.g., PVC) as the base polymer.[45, 48] In this study, we compared the effects of the base polymer, in terms of their water uptake property, on the NO release from polymer films doped with DBHD/N_2O_2 and PLGA. The optimal formulation was then utilized to create NO-releasing patches (and corresponding controls) that were applied to partial thickness scald burn wounds in a mouse model that were infected with *A. baumannii* to observe effects of such NO release patches on bacterial growth and TGF-β levels in the wounds after 24 h.

5.2 Materials and Methods

5.2.1 Materials

Tecoflex SG-80A and Tecophilic SP-60D-20 were purchased from Lubrizol Advanced Materials Inc. (Cleveland, OH). Anhydrous tetrahydrofuran (THF), anhydrous acetonitrile, sodium chloride, potassium chloride, sodium phosphate dibasic, and potassium phosphate monobasic were products of Sigma-Aldrich Chemical Company (St. Louis, MO). Poly(D,L-lactide-co-glycolide) 5050DLG1A (1-2 week hydrolysis rate),

5050DLG7E (1-2 month hydrolysis rate), and 6535DLG7E (3-4 month hydrolysis rate) were obtained from SurModics Pharmaceuticals Inc. (Birmingham, AL). N,N'-Dibutyl-1,6-hexanediamine (DBHD) was purchased from Alfa Aesar (Ward Hill, MA). DBHD/N_2O_2 was synthesized by treating DBHD with 80 psi NO gas purchased from Cryogenic Gases (Detroit, MI) at room temperature for 48 h, as previously described.[45] Phosphate buffered saline (PBS), pH 7.4, containing 138 mM NaCl, 2.7 mM KCl, and 10 mM sodium phosphate was used for all *in vitro* experiments.

5.2.2 Preparation of NO-Releasing Films and Patches

The focus of this study was to compare the effects of polymer water uptake on the NO release properties from DBHD/N_2O_2 and PLGA-doped within these base polymers (SG-80A or SP-60D-20). The PLGA additives used were 5050DLG1A (1-2 week hydrolysis rate), 5050DLG7E (1-2 month hydrolysis rate), and 6535DLG7E (3-4 month hydrolysis rate). The product names identify the copolymer ratio, inherent viscosity (used to determine the molecular weight), and the end group type (acid or ester), which are the main factors that determine the hydrolysis rate of the PLGA. For example, the 5050DLG7E is a PLGA with 50 mol% DL-lactide, 50 mol% glycolide, an inherent viscosity of 0.7 dLg^{-1}, and has an ester end group ('E'). A variety of NO-releasing films were prepared via a solvent evaporation method using either SG-80A or SP-60D-20 polyurethanes as the base polymer, while keeping the amount of DBHD/N_2O_2 and PLGA constant at 25 wt% and 10 wt%, respectively. NO-releasing films consisting of 25 wt% DBHD/N_2O_2, 10 wt% PLGA, and 65 wt% polyurethane were prepared by dissolving 80 mg PLGA, 200 mg DBHD/N_2O_2, and 520 mg polyurethane in 5 mL THF. This solution was cast in Teflon rings (dia. = 2.5 cm) and cured under ambient conditions for 2 d. Disks (dia. = 0.9 cm) were cut from the parent films and dip-coated 4 times in a top-coat solution (550 mg of the respective polyurethane in 7.5 mL THF).

The patches for the *in vivo* studies were prepared in a similar manner and consisted of SG-80A doped with 25 wt% DBHD/N_2O_2 and 10 wt% 5050DLG1A. The active layer of the NO-releasing patches were prepared by dissolving 1300 mg SG-80A, 200 mg 5050DLG1A, and 500 mg DBHD/N_2O_2 in 20 mL THF. This solution was cast in a Teflon mold (5 cm x 6 cm) and dried under ambient conditions overnight. The control

patches were prepared in a similar manner with 5050DLG1A and DBHD amine (non-diazeniumdiolate) in the active layer. The control active layer consisted of 1410 mg SG-80A, 200 mg 5050DLG1A, and 390 mg DBHD amine dissolved in 20 mL THF. The patches were dip coated 4 times using the corresponding top-coating solution (750 mg SG-80A in 20 mL THF).

All films and patches were dried under ambient conditions overnight after the top-coating, followed by vacuum drying for 48 h. The final films and patches had a total thickness of ~1000 μm (~600 μm active layer and ~200 μm top-coat), as measured using a Mitutoyo digital micrometer (Metron Precision, Inc.).

5.2.3 Polymer Water Uptake

SG-80A and SP-60D-20 polymer films were prepared by the solvent casting method. Polymer solutions consisting of 200 mg polymer dissolved in 5 mL THF were cast in Teflon rings (d = 2.5 cm). Disks (d = 0.9 cm) were cut from the parent films, weighed, and immersed in PBS buffer for 48 h at 37 °C. The wet films were wiped dry and weighed again. The water uptake of the polymer films are reported in weight percent as follows: water uptake (wt%) = $((W_{wet} - W_{dry})/W_{dry}) \times 100$, where W_{wet} and W_{dry} are the weights of the wet and dry films, respectively.

5.2.4 NO Release Measurements

Nitric oxide released from the NO release patches was measured using a Sievers chemiluminescence Nitric Oxide Analyzer (NOA) 280 (Boulder, CO). Films were placed in the sample vessel immersed in PBS (pH 7.4). Nitric oxide was continuously purged from the sample vessel and swept from the headspace using a N_2 sweep gas into the chemiluminescence detection chamber. Patches for the *in vivo* studies were wrapped in a moist Kim wipe and Tegaderm dressing (which was replaced daily to mimic the moist environment of the wound) and tested for *in vitro* NO release at 37 °C.

5.2.5 In Vitro Zone Inhibition Test

Overnight LB (Luria Bertani) broth grown *A. baumannii* ATCC 17978 culture was washed with 1 × PBS buffer three times by centrifugation, and was then resuspended

in 1 × PBS buffer to make a final cell concentration of approximately 10^5 CFU/mL. For the zone of inhibition, 50 µL of the 10^5 CFU/mL solution was plated onto LB agar plates. NO-releasing and control patches (1 cm x 1 cm square) were placed on the agar plates and incubated at 37°C for 24 h. The zone of inhibition was made by estimating the inhibition zone as circles and measuring the distance from the edge of the sample to the nearest bacterial colony. All the experiments were conducted in triplicate.

5.2.6 Partial Thickness Scald Burn Model in Mice

Mouse burn model: The animal handling and surgical procedures used in this study were approved by the University Committee on the Use and Care of Animals (UCUCA) in accordance with university and federal regulations. A total of 9 female pathogen-free C57BL/6 mice (Harlan, Indianapolis, IN), 9-10 weeks old, weighing ~17-23 grams each were used in this study. Mice were housed in standard cages at the University's Unit for Laboratory Animal Medicine Facility and were allowed to acclimate for 7 d after delivery prior to the experiment. The animals were kept on a 12 h light cycle and were provided with rodent chow (LabDiet 5001, PMI Int'l., Richmond, IN) and water *ad libitum* throughout the study. Pentobarbital (Nembutal, Ovation Pharmaceuticals,Inc., Deerfield, IL, manufactured by Hospira, Lake Forest, IL) was administered intraperatonially (50 mg/kg IP) for anesthesia. The eyes of the animals were covered with sterile Altalube (Altaire Pharmaceuticals, Aquebogue, NY). During the study, all mice were singly housed and all received 0.1 mg/kg buprenorphine (Buprenex; Reckitt Benckiser Pharmaceuticals Inc., Richmond, VA) subcutaneously (SQ) twice daily for post-burn pain control.

The skin over the lumbrosacral and back region of the mice was clipped using a 35-W model 5-55E electrical clipper (Oyster-Golden A-S, Head no.80, blade size 50). To create the burn, anesthetized mice were placed in an insulated, custom-made mold that exposes only the lumbrosacral and back region that is approximately 30% of the total body area (calculated using Meeh's formula[51]). Partial thickness burns were achieved by exposure of the skin to 60 °C water for 18 s. The burn was then wiped with sterile gauze. The burn sites were immediately inoculated with *A. baumannii* bacteria (200 µL of 10^6 CFU/mL) and covered with Tegaderm dressing (3M, Minneapolis, MN). The mice were

returned to cages in a 37 ºC incubator until fully ambulatory. Each mouse was given a 1 mL injection of 5% Dextrose and Lactated Ringer's Injection (Baxter) IP and another 500 µl injection SQ on the back of its hind leg.

Application of NO release and control patches: The *A. baumannii* infection was allowed to grow in the wounds for a 24 h period prior to the application of the patches. The mice were divided into 3 groups receiving the following treatments: control (DBHD + PLGA patch), NO-releasing patch, and control (no patch). NO release and control patches were soaked in sterile saline for approximately 15 min before attachment. The Tegaderm dressing was removed, patches were applied to the wounds, and fresh Tegaderm was used to cover and hold the patch in place on the wound. The Tegaderm was removed and replaced for mice that did not receive the patch treatment.

Tissue collection: At the time-point for tissue harvest (24 h after NO release and control patch application) the mice were given IP injections of pentobarbital (100 mg/kg) and exsanguinated followed by a bilateral pneumothorax. Skin samples were collected for bacterial counts, slides/staining, and mRNA isolation for TGF-β PCR. For the bacterial counts, skin tissue samples were excised and weighed, homogenized in 2 mL of PBS for 30 s, and cultured to determine the number of living *A. baumannii* microorganisms. Plate counting was conducted with LB agar plates.

The relative TGF-β mRNA levels were determined using TGF-β1 and GAPDH primers previously reported.[52, 53] The skin samples were immediately frozen in liquid nitrogen and stored overnight at -80 ºC. Samples were thawed briefly and homogenized in TRizol (Invitrogen, Carlsbad, CA) and RNA was extracted according to the manufacturer's instructions. RNA (2 µg) was utilized to make cDNA using the ABI High Capacity cDNA Reverse Transcription Kit (Applied Biosystems, Foster City, CA). Two hundred ng of cDNA was used to perform PCR with iQ SYBRGreen Supermix (Bio-Rad, Hercules, CA) on an Eppendorf Mastercycler epgradient S realplex 4 thermocycler (Eppendorf North America, Hauppauge, NY). After an initial denaturation for 2 min at 95 ºC, samples were subjected to 50 cycles of 95 ºC for 20 s, annealing at 60 ºC for 30 s, and extension at 72 ºC for 20 s.

5.3 Results and Discussion

5.3.1 In Vitro NO Release Measurements from Films and Patches

Diazeniumdiolates are a group of widely studied NO donor molecules that release NO through proton or thermal driven mechanisms.[46-48] Previous studies have shown NO can be released from polymer films doped with DBHD/N_2O_2.[45, 48] Poly(lactic-co-glycolic) acid additives have been shown recently help promote and prolong the NO release from poly(vinyl chloride) films doped with DBHD/N_2O_2.[48] The ester linkages of the PLGA will hydrolyze in the presence of water, producing lactic and glycolic acids that can act as a proton source to sustain the NO release from DBHD/N_2O_2-doped polymers (see Chapter 4). Previous work with DBHD/N_2O_2 films have primarily utilized hydrophobic polymers (e.g., PVC) as the base polymer;[45, 48] however, in this study we compared the effects of the base polymer, in terms of its water uptake property, on the NO release from combined DBHD/N_2O_2 and PLGA-doped films. In order to measure the water uptake of the two base polymers used in this study, films of the polymers were cast without any additives. The water uptake was then determined by the weight difference of the polymer film before and after soaking in PBS at 37 ºC for 48 h. As shown in **Table 5.1**, the Tecoflex SG-80A polymer is more hydrophobic and has a significantly lower water uptake than the Tecophillic SP-60D-20.

Table 5.1. The water uptake of SG-80A and SP-60D-20 polyurethanes. Polymer films were weighed before and after soaking in PBS for 48 h at 37 ºC. The water uptake of the polymer films are reported in weight percent as follows: water uptake (wt%) = (W_{wet} –W_{dry})/W_{dry} x 100, where W_{wet} and W_{dry} are the weights of the wet and dry films, respectively.prior to immersing in PBS for 48 h at 37 ºC. The wet films were wiped dry and weighed again.

Polymer	Water uptake (wt%)
SG80A	6.2 ± 0.7
SP-60D-20	22.5 ± 1.1

The NO-releasing films and patches used in this study were prepared using a two layer configuration, top-coat and active coat, as shown in **Figure 5.1**. The active coat was doped with 25 wt% DBHD/N_2O_2 and 10 wt% PLGA (either 5050DLG1A,

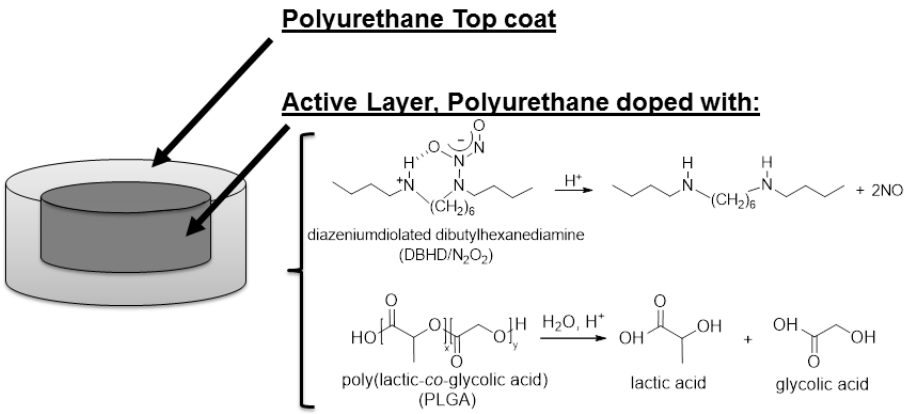

Figure 5.1. Diagram of the polyurethane (SG-80Aor SP-60D-20) based films/patches consisting of an active layer, doped with a lipophilic DBHD/N_2O_2 and PLGA additive, and a top coat of the corresponding polyurethane.

5050DLG7E, or 6535DLG7E). The NO release from these films was measured using a chemiluminescene NO analyzer at 37 ºC while immersed in PBS buffer. The films doped with 5050DLG1A have a significant burst of NO during the first day of soaking (see **Figure 5.2**). This high initial burst can be attributed to the higher residual acid content

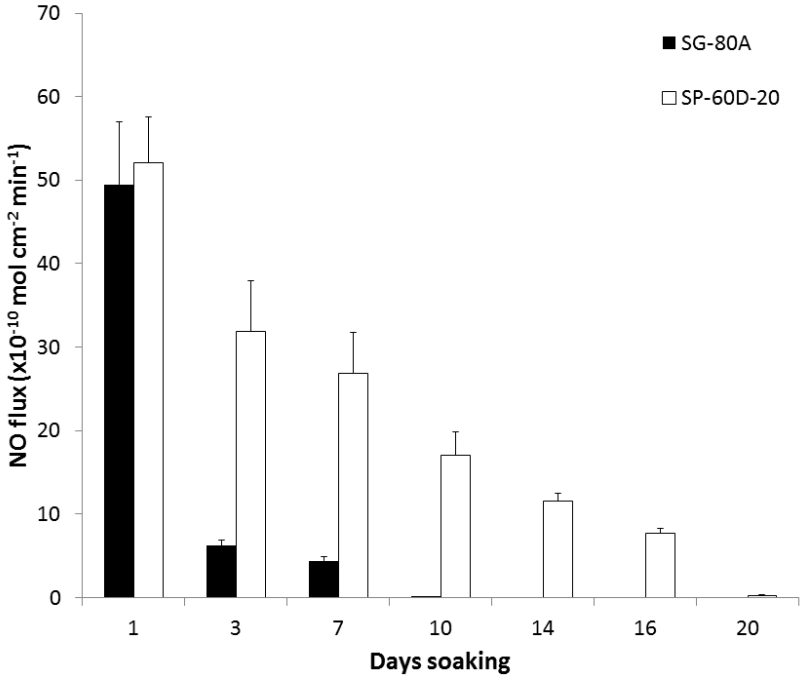

Figure 5.2. NO surface flux from SG-80A and SP-60D-20 films doped with 25 wt% DBHD/N_2O_2 and 10 wt% 5050DLG1A (1-2 week hydrolysis rate) PLGA additives. Films were incubated in PBS buffer at 37 ºC during the testing period. The data are means ± SEM (n=3).

(from the carboxylic end groups and residual monomers). The NO release rapidly decreases by day 3 for the SG-80A films, due to the low water uptake of this polymer, which slows the PLGA hydrolysis rate. The films made with SP-60D-20 continue to release higher levels of NO for up to 16 d. SP-60D-20 has a higher water uptake, which continues to allow water to diffuse into the film and promote PLGA hydrolysis and NO release. In contrast, the films doped with the ester-capped PLGAs (either 5050DLG7E or 6535DLG7E) do not exhibit an initial burst during the first day (**Figures 5.3 and 5.4**). The SP-60D-20 based films have higher NO release that has a longer duration than the corresponding SG-80A based films. This trend is most noticeable in the films doped with PLGAs that have lower hydrolysis rates (5050DLG1A and 5050DLG7E). The higher water uptake of the SP-60D-20 polymer facilitates the PLGA hydrolysis, which then continues to promote NO release.

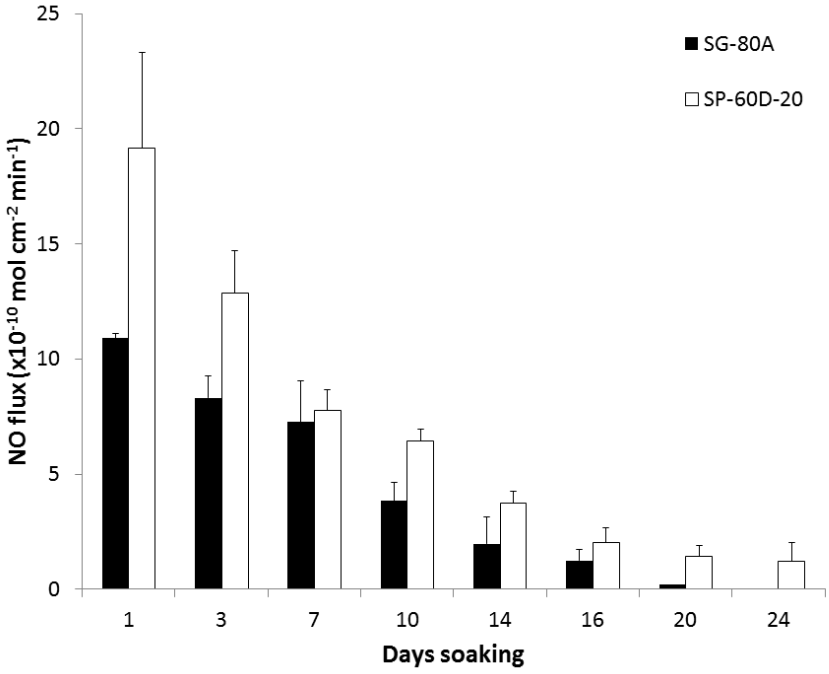

Figure 5.3. NO surface flux from SG-80A and SP-60D-20 films doped with 25 wt% DBHD/N_2O_2 and 10 wt% 5050DLG7E (1-2 month hydrolysis rate) PLGA additives. Films were incubated in PBS buffer at 37 ºC during the testing period. The data are means ± SEM (n=3).

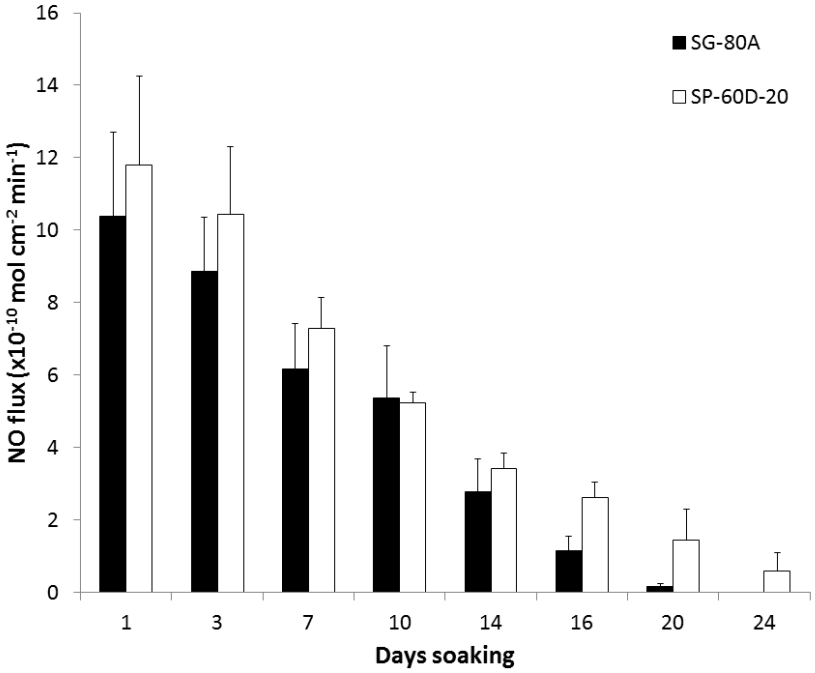

Figure 5.4. NO surface flux from SG-80A and SP-60D-20 films doped with 25 wt% DBHD/N_2O_2 and 10 wt% 6535DLG7E (3-4 month hydrolysis rate) PLGA additives. Films were incubated in PBS buffer at 37 ºC during the testing period. The data are means ± SEM (n=3).

Although these NO-releasing polymers have a wide variety of potential biomedical applications requiring various levels and duration of NO release,[38] in this study we examined their potential use to reduce infection in burn wounds. For wound healing applications, the NO release from patches can have short durations because new patches could be applied daily. To choose the appropriate polymer composition for the *in vivo* studies, patches were prepared with Tecoflex SG-80A as the base polymer (due to the lower initial burst observed on the first day of soaking) and doped with 25 wt% DBHD/N_2O_2 and 10 wt% PLGA (either 5050DLG1A or 5050DLG7E). In order to mimic the moist environment of the wounds, NO-releasing patches were wrapped with a moist Kim wipe and Tegaderm dressing, and tested at 37 ºC for their NO release. The patches doped with 5050DLG1A maintained a NO flux of approximately 13 x 10^{-10} mol cm^{-2} min^{-1} for the first 24 h under physiological conditions (**Figure 5.5**). In contrast, the patches doped with the 5050DLG7E exhibit a significantly lower flux of ~3 x 10^{-10} mol cm^{-2} min^{-1} under the same moist conditions and this flux is also sustained for the first 24 h. The NO release from both patches begins to diminish on the third day due to the

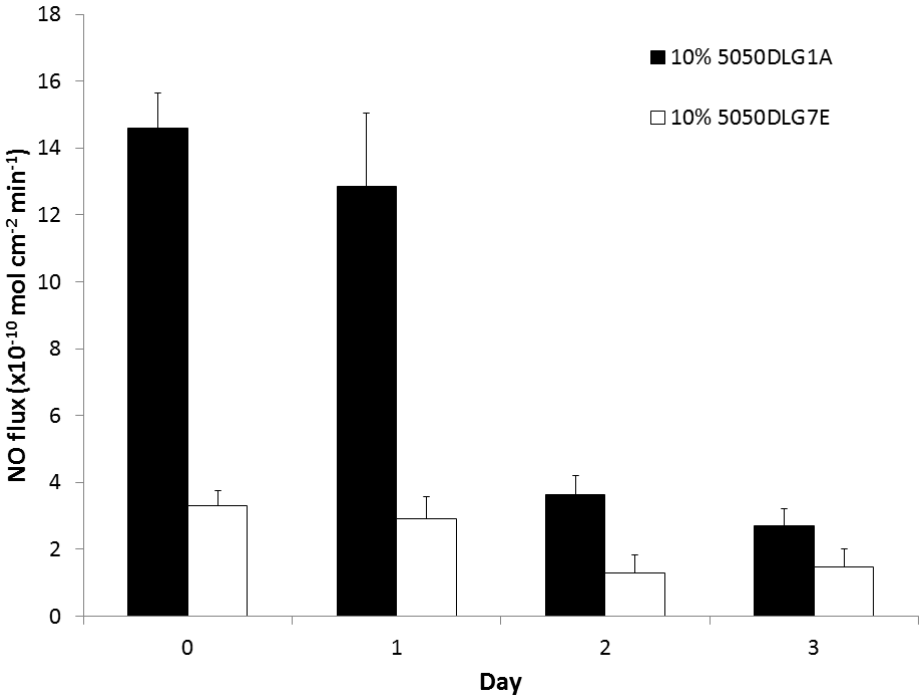

Figure 5.5. NO release from SG-80A patched doped with 25 wt% DBHD/N_2O_2 and 10 wt% of either 5050DLG1A (1-2 week hydrolysis rate) or 5050DLG7E (1-2 month hydrolysis rate) PLGA additives. Films were wrapped in moist Kim wipes and Tegederm dressing at 37 ºC during the testing period. The data are means ± SEM (n=3).

accumulation DBHD amine and the concomitant slower hydrolysis of the PLGA additive (from the reduced amount of water that diffuses into the polymer). For the *in vivo* studies, the SG-80A patch type doped with 25 wt% DBHD/N_2O_2 and 10 wt% 5050DLG1A was selected due to its higher NO release.

5.3.2 Effects of NO and Control Patches on Zone Inhibition

The NO-releasing (SG-80A doped with 25 wt% DBHD/N_2O_2 and 10 wt% 5050DLG1A) and control (SG-80A doped with 20 wt% DBHD amine and 10 wt% 5050DLG1A) used for the *in vitro* zone inhibition test and *in vivo* studies were prepared as described in Section 2.2. The control patches were prepared with equal moles of the DBHD amine, where the additional weight from the mass of the diaziniumdiolate NONO group was compensated by additional SG-80A, in order to observe the effects of the NO release vs. control. Prior to the *in vivo* experiments, the NO-releasing and control patches were tested *in vitro* for their zone of inhibition. *A. baumanii* was spread on agar plates and the patches (1 cm x 1 cm square) were placed in the center of the plate. After a 24 h

incubation at 37 ºC, the NO release patch created a zone of inhibition that had a diameter of ca. 4.3 ± 0.9 cm. The control patch showed no zone of inhibition, where only the bacteria underneath the patch were slightly suppressed. This zone of inhibition test mimics the nutrient environment of the wound and demonstrates that the NO released from patches has the potential to diffuse in and around the wound site, and ultimately reduce the bacteria and infection.

5.3.3 Effects of NO and Control Patches on Bacteria Counts and TGF-β mRNA in Mouse Burn Model

A mouse burn model was used to observe the effects of the NO-releasing patch on an infected wound. Partial thickness scald burn wounds on mice were inoculated with *A. baumannii* and covered with Tegaderm dressing. The bacteria were allowed to grow in the wound for 24 h prior to the application of NO release patches, control patches, or control (no patch). After 24 h of patch or control treatment, skin tissue was harvested, homogenized in PBS, and grown on agar plates to assess the effects of NO on bacterial growth in the wounds. As shown in **Figure 5.6**, the NO-releasing patches significantly reduced the amount of *A. baumannii* bacteria present in the wounds after 24 h application (~ 4 log reduction) in comparison to the control patches (which did not have NO release). The wounds that receive the control treatment of no patch (only Tegaderm dressing covering the wound) had similar bacteria counts as the other control patch group (data not shown). Part of the reduced bacteria counts can be attributed to neutrophil infiltration, which happens in the case of all treatment groups in this study. However, the additional NO that is supplied by the NO-releasing patches has the potential to improve the overall healing of the wound by reducing the infection and bacterial growth.

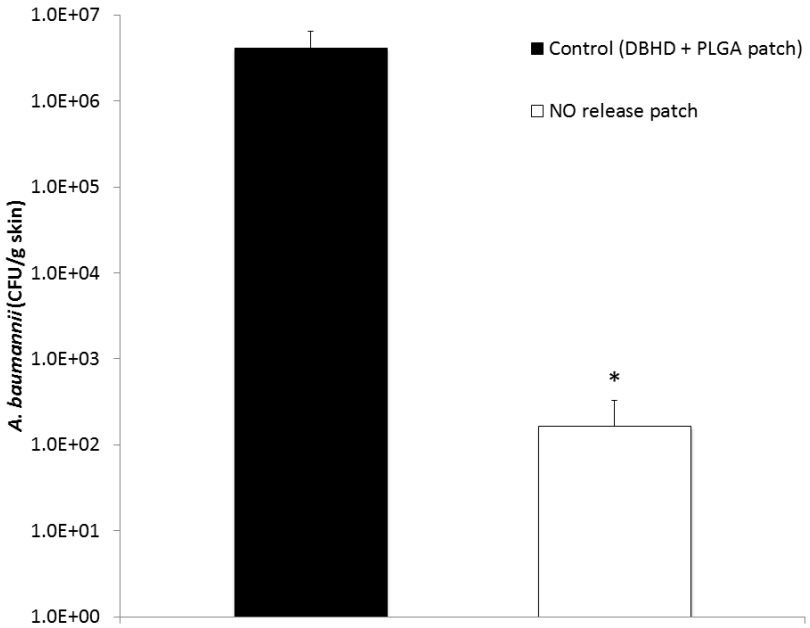

Figure 5.6. Plate counting of *A. baumannii* cells on the wounded skin of mice after 24 h application of SG-80A based NO-releasing and control patches. NO-releasing and control patches were applied to wounds 24 h after inoculation with *A. baumannii.* After 24 h, skin tissue was harvested, homogenized, serially diluted, and grown on agar plates. The data are means ± SEM (n=3). * = $p < 0.05$.

Burn wounds have been shown to have increased TGF-β mRNA levels, which contributes to immunosuppression,[54] impairs humoral immunity (antibody generation),[55] and contributes to scar formation.[56] In this study, the harvested skin tissue was also assessed for the expression of TGF-β mRNA levels using RT-PCR. The wounds with the NO-releasing patches created a significant reduction in TGF-β levels in comparison to the control patches (**Figure 5.7**). This reduction may be due to the inhibition of T cell proliferation by NO.[57] Further, it has been reported that NO regulates TGF-β expression transcriptionally, where inducible nitric oxide synthase (iNOS) expression is inversely proportional to TGF-β expression.[58] NO release from iNOS or NO donors (e.g., SNAP, GSNO) is known to downregulate TGF-β mRNA. Reduction of TGF-β has been shown to enhance reepithelialization, decrease post-burn scarring, and reduce trans-epithelial migration of bacteria.[59, 60] In addition to the promising bacteria and TGF-β results, the UM pathology report indicated that the NO-releasing patches did not worsen the injury and indicated that there was less overall damage in the wounds in comparison to the controls. Nitric oxide has many biological roles, including reducing bacterial infection

and decreasing TGF-β mRNA levels as addressed here, and both processes can be quite beneficial to the wound healing process.[38] The nitric oxide releasing patches used in this study could be replaced daily, in order to maintain consistent NO delivery to the wound site.

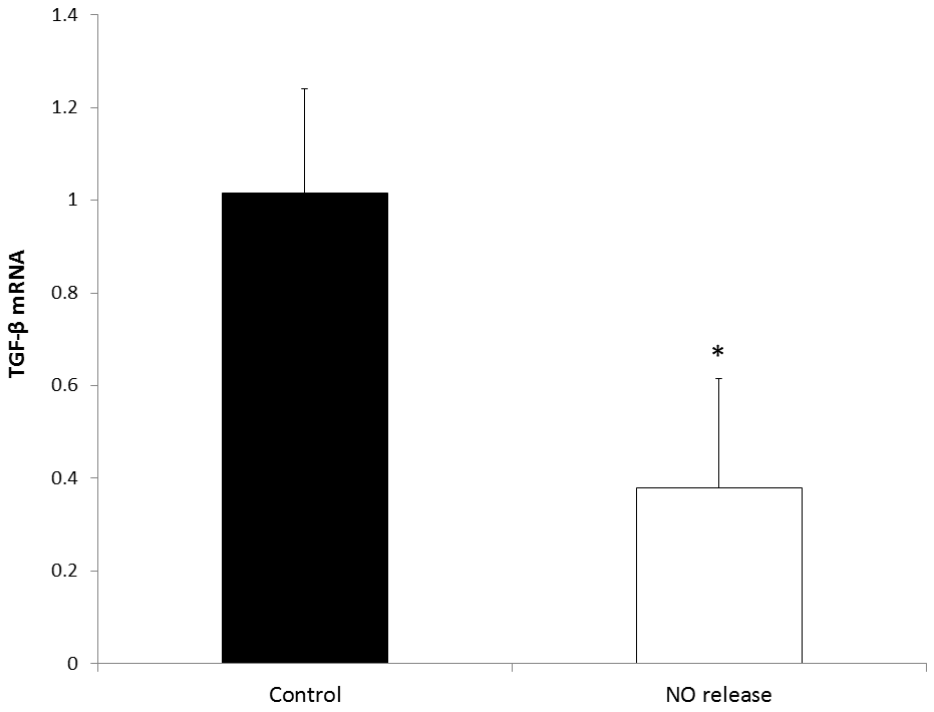

Figure 5.7. Expression of TGF-β mRNA after application of the SG-80A based NO-releasing and control patches. RNA was extracted from the homogenized skin tissue and the expression of TGF-β was determined using RT-PCR and expressed as the ratio to that of untreated mice. The data are means ± SEM (n=3). * = $p < 0.05$.

5.4 Conclusions

In summary, this study demonstrates that the water uptake properties of the base polymer can be used to further control the NO release rates from polymeric films/patches doped with DBHD/N_2O_2 and PLGA. Films prepared with a more hydrophobic polyurethane (SG-80A) exhibit NO release that is lower and shorter in duration than the polyurethane with 20% water uptake (SP-60D-20). The more hydrophilic base polymer increases the rate of hydrolysis of the PLGA additive, supplying more protons locally within the polymeric phase that thereby increase the NO release rate. These new DBHD/N_2O_2 and PLGA-doped SG-80A patches demonstrate the potential to improve the

healing of burn wounds by reducing the bacterial infection. Indeed, the NO released from the patches is clearly shown to be able to significantly reduce the *A. baumannii* infection (~4 log reduction) after 24 h application to scald burn wounds. The NO release patches are also shown to be able to reduce the TGF-β levels, in comparison to controls, and this species has been reported to enhance reepithelialization, decrease scarring, and reduce migration of bacteria. The novel NO-releasing patches developed here could be replaced frequently throughout the duration of the wound healing process in order to further promote and expedite the healthy wound healing process by maintaining exposure of the wound to a higher flux rate of NO.

5.5 References

1. G. M. Halpenny and P. K. Mascharak, *Anti-Infect Agents Med Chem*, **2010**, *9*, 187-197.

2. R. O. Darouiche, *New Engl J Med*, **2004**, *350*, 1422-1429.

3. R. M. Klevens, J. R. Edwards, C. L. Richards, T. C. Horan, R. P. Gaynes, D. A. Pollock and D. M. Cardo, *Public health reports*, **2007**, *122*, 160.

4. C. W. Runyan, C. Casteel, D. Perkis, C. Black, S. W. Marshall, R. M. Johnson, T. Coyne-Beasley, A. E. Waller and S. Viswanathan, *Am J Prev Med*, **2005**, *28*, 73-79.

5. J. M. Horan and S. Mallonee, *Epidemiol Rev*, **2003**, *25*, 24-42.

6. K. A. Moran, C. K. Murray and E. L. Anderson, *Infect Control Hosp Epidemiol*, **2008**, *29*, 981-984.

7. D. R. Hospenthal, C. K. Murray, R. C. Andersen, J. P. Blice, J. H. Calhoun, L. C. Cancio, K. K. Chung, N. G. Conger, H. K. Crouch and C. Laurie, *J Trauma Acute Care Surg*, **2008**, *64*, S211-S220.

8. M. A. Fischbach and C. T. Walsh, *Science*, **2009**, *325*, 1089-1093.

9. G. Taubes, *Science*, **2008**, *321*, 356.

10. B. S. Atiyeh, M. Costagliola, S. N. Hayek and S. A. Dibo, *Burns*, **2007**, *33*, 139-148.

11. S. F. Dallo and T. Weitao, *Adv Skin Wound Care*, **2010**, *23*, 169-174.

12. K. Towner, *J Hosp Infect*, **2009**, *73*, 355-363.

13. S. F. Beavers, D. B. Blossom, T. L. Wiemken, K. Y. Kawaoka, A. Wong, L. Goss, M. I. McCormick, D. Thoroughman and A. Srinivasan, *Public Health Rep*, **2009**, *124*, 868.

14. G. Vorgias, C. Iavazzo, E. Makarova, T. Akrivos and M. E. Falagas, *Int J Gynaecol Obstet*, **2009**, *105*, 264.

15. D. M. Supp, J. Gardner, J. M. Klingenberg and A. N. Neely, *Burns*, **2009**, *35*, 949-955.

16. H. Alişkan, S. Colakoğlu, T. Turunç, Y. Demiroğlu, F. Erdoğan, S. Akin and H. Arslan, *Mikrobiyol Nul*, **2008**, *42*, 321.

17. J. Babik, L. Bodnárová and K. Sopko, *Acta Chir Plast*, **2008**, *50*, 27-33.

18. J. H. Calhoun, C. K. Murray and M. FISDA, *Clin Orthop Relat Res*, **2008**, *466*, 1356-1362.

19. E. F. Keen, B. J. Robinson, D. R. Hospenthal, W. K. Aldous, S. E. Wolf, K. K. Chung and C. K. Murray, *Burns*, **2010**, *36*, 461-468.

20. F. C. Fang, *Nat Rev Micro*, **2004**, *2*, 820-832.

21. A. Denicola, B. A. Freeman, M. Trujillo and R. Radi, *Arch Biochem Biophys*, **1996**, *333*, 49-58.

22. D. A. Wink and J. B. Mitchell, *Free Radic Biol Med*, **1998**, *25*, 434-456.

23. F. C. Fang, *J Clin Invest*, **1997**, *99*, 2818-2825.

24. R. Raulli, G. McElhaney-Feser, J. Hrabie and R. Cihlar, *Recent Res Dev Microbiol*, **2002**, *6*, 177-183.

25. J. W. Costerton, Z. Lewandowski, D. E. Caldwell, D. R. Korber and H. M. Lappin-Scott, *Annu Rev Microbiol*, **1995**, *49*, 711-745.

26. L. Hall-Stoodley, J. W. Costerton and P. Stoodley, *Nature Rev Microbiol*, **2004**, *2*, 95-108.

27. M. R. Parsek and P. K. Singh, *Annu Rev Microbiol*, **2003**, *57*, 677-701.

28. G. O'Toole, H. B. Kaplan and R. Kolter, *Annu Rev Microbiol*, **2000**, *54*, 49-79.

29. C. Fux, J. Costerton, P. Stewart and P. Stoodley, *TIM*, **2005**, *13*, 34-40.

30. R. D. Wolcott and G. D. Ehrlich, *JAMA*, **2008**, *299*, 2682-2684.

31. D. McDougald, S. A. Rice, N. Barraud, P. D. Steinberg and S. Kjelleberg, *Nat Rev Micro*, **2011**, *10*, 39-50.

32. N. Barraud, M. V. Storey, Z. P. Moore, J. S. Webb, S. A. Rice and S. Kjelleberg, *J Microbial Biotech*, **2009**, *2*, 370-378.

33. I. Schmidt, P. J. Steenbakkers, H. J. op den Camp, K. Schmidt and M. S. Jetten, *J Bacteriol*, **2004**, *186*, 2781-2788.

34. W. Cai, J. Wu, C. Xi, A. J. Ashe Iii and M. E. Meyerhoff, *Biomaterials*, **2011**, *32*, 7774-7784.

35. B. J. Nablo, A. R. Rothrock and M. H. Schoenfisch, *Biomaterials*, **2005**, *26*, 917-924.

36. M. C. Jen, M. C. Serrano, R. van Lith and G. A. Ameer, *Adv Funct Mater*, **2012**, *22*, 239-260.

37. K. A. Wold, V. B. Damodaran, L. A. Suazo, R. A. Bowen and M. M. Reynolds, *ACS Appl Mater Interfaces*, **2012**, *4*, 3022-3030.

38. A. W. Carpenter and M. H. Schoenfisch, *Chem Soc Rev*, **2012**, *41*, 3742-3752.

39. P. Lopez-Jaramillo, C. Ruano, J. Rivera, E. Teran, R. Salazar-Irigoyen, J. V. Esplugues and S. Moncada, *Lancet*, **1998**, *351*, 1176-1177.

40. A. B. Seabra, E. Pankotai, M. Feher, A. Somlai, L. Kiss, L. Biro, C. Szabo, M. Kollai, M. G. de Oliveira and Z. Lacza, *Br J Dermatol*, **2007**, *156*, 814-818.

41. T. P. Amadeu, A. B. Seabra, M. G. De Oliveira and A. M. A. Costa, *J Eur Acad Dermatol*, **2007**, *21*, 629-637.

42. H. F. Zhu, X. F. Wei, K. Bian and F. Murad, *J Burn Care Res*, **2008**, *29*, 804-814.

43. A. B. Shekhter, V. A. Serezhenkov, T. G. Rudenko, A. V. Pekshev and A. F. Vanin, *Nitric Oxide*, **2005**, *12*, 210-219.

44. Y. Li and P. I. Lee, *Mol Pharm*, **2009**, *7*, 254-266.

45. M. M. Batchelor, S. L. Reoma, P. S. Fleser, V. K. Nuthakki, R. E. Callahan, C. J. Shanley, J. K. Politis, J. Elmore, S. I. Merz and M. E. Meyerhoff, *J Med Chem*, **2003**, *46*, 5153-5161.

46. T. C. Major, D. O. Brant, M. M. Reynolds, R. H. Bartlett, M. E. Meyerhoff, H. Handa and G. M. Annich, *Biomaterials*, **2010**, *31*, 2736-2745.

47. K. M. Davies, D. A. Wink, J. E. Saavedra and L. K. Keefer, *J Amer Chem Soc*, **2001**, *123*, 5473-5481.

48. H. Handa, E. J. Brisbois, T. C. Major, L. Refahiyat, K. A. Amoako, G. M. Annich, R. H. Bartlett and M. E. Meyerhoff, *J Mater Chem B*, **2013**, *1*, 3578-3587.

49. H. Handa, T. C. Major, E. J. Brisbois, K. A. Amoako, M. E. Meyerhoff and R. H. Bartlett, *J Mater Chem B*, **2014**, *2*, 1059-1067.

50. P. E. Porporato, V. L. Payen, C. J. De Saedeleer, V. Préat, J.-P. Thissen, O. Feron and P. Sonveaux, *Angiogenesis*, **2012**, *15*, 581-592.

51. D. Gilpin, *Burns*, **1996**, *22*, 607-611.

52. M. Menacho-Marquez, R. García-Escudero, V. Ojeda, A. Abad, P. Delgado, C. Costa, S. Ruiz, B. Alarcón, J. M. Paramio and X. R. Bustelo, *PLoS Biol*, **2013**, *11*, e1001615.

53. G. M. Risinger, D. L. Updike, E. C. Bullen, J. J. Tomasek and E. W. Howard, *Am J Physiol Cell Physiol*, **2010**, *298*, C191-C201.

54. M. Varedi, M. G. Jeschke, E. W. Englander, D. N. Herndon and R. E. Barrow, *Shock*, **2001**, *16*, 380-382.

55. K. Ishikawa, T. Nishimura and A. A. Meyer, *J Trauma Acute Care Surg*, **2004**, *57*, 529-536.

56. E. E. Tredget, H. A. Shankowsky, R. Pannu, B. Nedelec, T. Iwashina, A. Ghahary, T. V. Taerum and P. G. Scott, *Plast Reconstr Surg*, **1998**, *102*, 1317-1328.

57. R. C. van der Veen, *Int Immunopharmacol*, **2001**, *1*, 1491-1500.

58. D. Wang, S. Lu and Z. Dong, *The Prostate*, **2007**, *67*, 1825-1833.

59. C. Beisswenger, C. B. Coyne, M. Shchepetov and J. N. Weiser, *J Biol Chem*, **2007**, *282*, 28700-28708.

60. A. J. Singer, S. S. Huang, J. S. Huang, S. A. McClain, A. Romanov, J. Rooney and T. Zimmerman, *J Burn Care Res*, **2009**, *30*, 329-334.

CHAPTER 6

Conclusions and Future Directions

6.1 Conclusions

This dissertation research has focused on novel methods to achieve long-term nitric oxide (NO) release from polymers and their potential biomedical applications. These studied also attempted to overcome some of the challenges regarding clinical application of NO-releasing materials, including: 1) short durations of NO release (from a few hours to a few days); 2) the need for toxic additives to prolong the NO release; 3) prohibitive costs of the NO donor molecules; and 4) instability of the NO donor during storage and/or sterilization. Various NO-releasing polymers have been reported in the literature (representative examples listed in **Table 6.1**); however none have yet been clinically applied despite their potential benefits.

In Chapters 2 and 3, the *S*-nitroso-*N*-acetypenicillamine (SNAP)-doped polymers were studied for hemocompatibility applications. Polymers with low water uptake (silicone rubber, CarboSil, and Elast-eon E2As) were found to exhibit relatively low levels of SNAP leaching during the first 24 h soaking in buffer. The films were further studied for their long-term NO release and shelf-life stability. The SNAP-doped E2As creates an inexpensive homogeneous polymer that can locally deliver physiologically relevant levels of NO (via thermal and photochemical reactions) for up to 20 d. It was found that the SNAP is surprisingly stable in the E2As polymer, retaining 78% of the initial SNAP after 4 months storage at 37 ºC. The SNAP/E2As polymer was coated on the inner walls of extracorporeal circulation (ECC) circuits and exposed to 4 h blood flow in a rabbit model. The SNAP-doped E2As polymer preserved the blood platelet count at

Table 6.1. Examples of recently reported *S*-nitrosothiol (RSNO)- and diazeniumdiolate-based NO releasing polymers, the duration of NO release, and additional noted properties (e.g., stability in terms of % loss of the NO donor after dry storage, leaching of NO donor molecules, etc.).

NO-Releasing Polymer	NO Release (at 37 °C)	Other Properties (e.g., stability, leaching)	Ref.
RSNO-modified xerogels	14 d	~30-50% loss after 30 d at room temperature	1, 2
RSNO-modified polyester/poly(methyl methacrylate)	25 h	Initial burst of NO	3
GSNO-doped poly(vinyl alcohol)/poly(vinyl pyrrolidone)	12 h	~33% loss after 30 d at 25 ºC Leaching of GSNO	4, 5
GSNO-doped poly(ethylene glycol)	16 h	~87% loss after 65 d at 8 ºC	7
RSNO-modified polyurethanes	1-3 d	Initial burst and low flux of NO	8
RSNO-modified poly(sulfhydrylated polyester) and poly(methyl methacrylate)	1-3 d	60% loss during EO sterilization	9
SNAP covalently bound to polydimethylsiloxane	1 d	50% loss after 57 d at 4 ºC	10
SNAP-doped Elast-eon E2As	**20 d**	**~20% loss after 4 mo at 37 ºC**	**13**
DMHD/N_2O_2 and LPEI/N_2O_2-doped PU and PVC	3-4 d	Leaching of NO donors	14
DBHD/N_2O_2-doped PVC/DOS with borate additive	1-3 d	Initial burst of NO	6
DACA/N_2O_2-modified silicone rubber	20 d	>50% loss after 45 d at 23 ºC	17
RSNO- and Diazeniumdiolate-modified silica particles dispersed within polyurethane or SR	1-2 d	Initial burst of NO; leaching of particles	18-20
Diazeniumdiolate-modified sol-gels	1-6 d	99% loss during autoclaving 10% loss after UV sterilization	16, 21
DBHD/N_2O_2-doped polyurethanes with PLGA additive	**14-24 d**	**NO release profile tailored with PLGA additive**	**22, 23**

100 ± 7% of baseline (compared to 60 ± 6% for E2As control circuits) and also reduced the thrombus area.

In Chapter 3, the SNAP/E2As polymer was used to fabricate NO-releasing intravascular catheters. These catheters were found to release NO (> 0.5 x 10^{-10} mol cm^{-2} min^{-1}) for up to 20 d under physiological conditions. In addition, the new SNAP/E2As catheters were able to retain 89% of the SNAP after ethylene oxide sterilization. SNAP/E2As and E2As control catheters were implanted in sheep veins for 7 d. The SNAP/E2As catheters were able to significantly reduce the amount of thrombus and bacterial adhesion after 7 d implantation compared to the controls. These *in vivo* studies demonstrate the great potential of the SNAP/E2As polymer to improve the hemocompatibility and bactericidal activity of catheters and other blood-contacting devices for short- and long-term applications (vascular grafts, stents, extracorporeal circuits, etc.).

In Chapters 4 and 5, the NO release properties from diazeniumdiolated dibutylhexanediamine (DBHD/N_2O_2)-doped polymers was significantly improved using various poly(lactic-*co*-glycolic acid) (PLGA) additives. The PLGA additives are a safer alternative to the toxic tetraphenylborate species that was previously used[6] and significantly improve the durations of the NO release. High initial bursts of NO release were observed when using acid-capped PLGAs as an additive, due to the higher residual acid content and faster hydrolysis rate of such PLGAs. The NO release from DBHD/N_2O_2-doped PVC and E2As was extended to 14 d by using ester-capped PLGAs. The pH changes corresponding to the NO release profiles from these films were visualized by doping films with appropriate pH indicator dyes. The hemocompatibility of biomedical grade base polymers (plasticized PVC and Elast-eon E2As) was compared in the rabbit thrombogenicity model. The Elast-eon E2As was found to have superior hemocompatibility properties, in terms of platelet preservation and reduced thrombus area, as compared to the other polymers. NO-releasing (NOrel) circuits were prepared using the plasticized PVC and E2As as the base polymers and tested in the rabbit model. The E2As-based NOrel circuits preserved platelets at a higher level than PVC-based NOrel circuits (97% and 80% of baseline, respectively). After 4 h of blood flow, the E2As-based NOrel circuits also had a significantly lower thrombus area than the PVC-

based NOrel circuits. This study demonstrated that the inherent hemocompatibility properties of the base polymer can also influence the efficiency of the NO release coatings.

In Chapter 5, the DBHD/N_2O_2 and PLGA-doped polymers were optimized using two polyurethanes with different water uptakes (Tecoflex SG-80A (6.2 ± 0.7 wt %) and Tecophillic SP-60D-20 (22.5 ± 1.1 wt%)). Films prepared with the polymer that has the higher water uptake (SP-60D-20) were found to have higher NO release and for a longer duration than the polyurethane with lower water uptake (SG-80A). The more hydrophilic polymer enhances the hydrolysis rate of the PLGA additive, thereby providing a more acidic environment that increases the rate of NO release from the NO donor. The optimal SG-80A-based NO-releasing and control polymer patches were applied to scald burn wounds in mice infected with *Acinetobacter baumannii*. The NO released from these patches applied to the wounds is shown to significantly reduce the degree of *A. baumannii* infection after 24 h (~4 log reduction). The NO release patches are also able to reduce the TGF-β levels, in comparison to controls, which can enhance reepithelialization, decrease scarring, and reduce migration of bacteria. The combined DBHD/N_2O_2 and PLGA-doped polymer patches, which could be replaced periodically throughout the wound healing process, demonstrate the potential to reduce risk of bacterial infection and promote the overall wound healing process.

In this dissertation work two novel strategies to achieving long-term NO-release from polymers, SNAP-doped and DBHD/N_2O_2-doped polymers, were examined for their potential to improve hemocompatibility and reduce infection. For example, NO released from Elast-eon E2As polymer (which was found to have superior intrinsic hemocompatibility properties) is effective at preserving platelets and reducing thrombus when tested in the ECC model. The inner surfaces of ECC loops coated with E2As doped with DBHD/N_2O_2-doped E2As had higher NO release than loops coated with SNAP-doped E2As, which was able to preserve platelets and reduce thrombus to a greater extent. The SNAP-doped E2As polymer is advantageous for potential clinical applications due to the inexpensive costs of SNAP, low toxicity concerns (NAP is already a clinically used drug), excellent stability of SNAP during shelf storage and sterilization, and long-term NO release (up to 20 d). However, the SNAP-doped E2As polymer used

in these studies had NO fluxes that mimicked the lower range of the endothelium, so strategies to increase the NO flux are needed to further improve the biocompatibility properties of this new material (see Section 6.2). The DBHD/N_2O_2-based polymers have the advantage that the NO release profile can be well controlled, using various PLGA additives and the water uptake properties of the base polymer, allowing the NO release to be tailored for specific biomedical applications (up to 24 d NO release). Some disadvantages of the DBHD/N_2O_2 molecule that could hinder potential clinical applications might be the expensive synthesis costs, potential toxicity concerns (nitrosamine formation), and heat/moisture sensitivity. Strategies for improving both the SNAP- and DBHD/N_2O_2-based polymers systems are described below (Section 6.2).

6.2 Future Directions

6.2.1 SNAP-Based Polymers

Although SNAP-doped E2As polymer has very encouraging properties, as reported thus far in this thesis work, there are several directions that could potentially improve the SNAP-doping approach. The SNAP-doped E2As films leach ~10% of the SNAP during the first day of soaking. This leaching can be attributed to the initial water uptake of the polymer as well as any residual SNAP that is on the outermost polymer surface. Leaching of the NO donor species is not ideal (even though SNAP and its byproducts have low toxicity concerns) because the NO release can occur downstream, rather than being localized at the polymer/blood or polymer/tissue interface. One approach to reduce or eliminate this leaching could be adding a thin top-coat of a cross-linked polymer (e.g., silicone rubber or cross-linked polyurethanes). SNAP-doped silicone rubber and CarboSil (which were also found to have low levels of SNAP leaching) could also be further characterized for their NO release and stability, and evaluated for potential biomedical applications.

Synthesizing derivatives of SNAP that are more lipophilic may reduce the leaching of the NO donor, since these molecules should have a greater preference for remaining in the polymer phase. Lipophilic derivatives of SNAP have been studied and are also reported to have increased stability in comparison to SNAP.[11, 12] The

SNAP/E2As films and catheters had NO release 0.5 ~1 x 10^{-10} mol cm^{-2} min^{-1} (after the first day) that mimics the lower end of the endothelial release. One simple method to increase the NO flux from SNAP-doped E2As is to shine light on the polymer (corresponding to the wavelengths responsible for RSNO decomposition: 340 or 590 nm). Various intensities of light could be used to tailor the NO release to specific flux levels (as shown in **Figure 6.1**, where the light intensity corresponds to the distance between the light and SNAP/E2As). This method could be easily applied for extracorporeal circulation

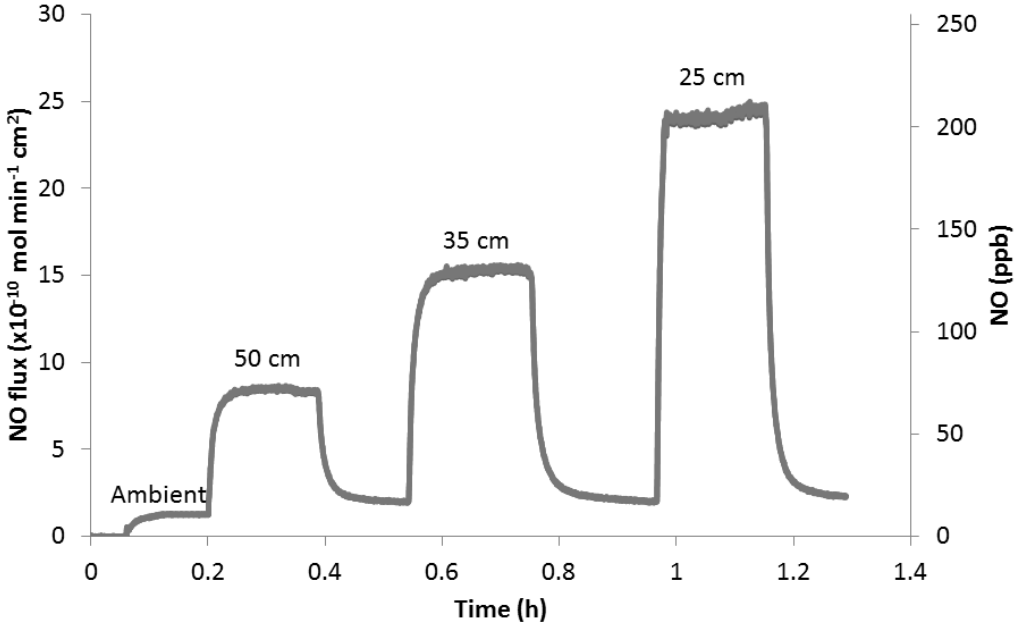

Figure 6.1. Effect of light intensity (in terms of distance between 100W light and polymer) on the NO release from SNAP-doped E2As.

situations (e.g., dialysis treatments or open heart surgery), but would not work as well for indwelling devices. Another method to increase NO release from SNAP/E2As might include adding hydrophilic polymers to the SNAP-doped layer, which will help draw water into the innermost regions of the polymer to initiate NO release. New polymer compositions with NO fluxes between 2~4 x 10^{-10} mol cm^{-2} min^{-1} may further improve the hemocompatibility properties of the SNAP/E2As polymer.

Further studies to better understand the mechanisms of NO release and enhanced stability of the SNAP/E2A polymer are also important. One observation in this thesis work is that increasing the thickness of the SNAP/E2As (thin films studies in Chapter 2 vs. the thick walls of the catheters in Chapter 3) does not significantly increase the NO flux. One explanation for this is that the SNAP molecules need to diffuse to the outer water-rich regions in the polymer matrix (closest to the water/polymer interface) in order to initiate NO release. Studies to correlate the diffusion of SNAP through E2As, or other polymers, with the rate of NO release should be conducted. Further, in this thesis work, the shelf-life stability study demonstrates that SNAP is stable in the E2As polymer matrix (in dry state), even during storage at elevated temperatures. However, exposure to humidity initiates NO release (as shown in Chapter 3). One potential theory to explain these phenomena is the formation of a hydrogen bonding network (between SNAP and the E2As polymer, as well as between SNAP molecules) that stabilizes SNAP in the dry state. Upon exposure to humidity, this hydrogen bonding network could be disrupted, resulting in the NO release that is observed. It has been previously reported that intramolecular hydrogen bonding occurs in SNAP, which results in a stabilization effect on the S—NO bond.[15, 16] Therefore a similar stabilization effect can occur if intermolecular hydrogen bonds form between SNAP and the polymer backbone, or neighboring SNAP molecules (examples shown in **Figure 6.2**). Further studies, using techniques such as FTIR or solid state NMR, are critical to fully understand the role of

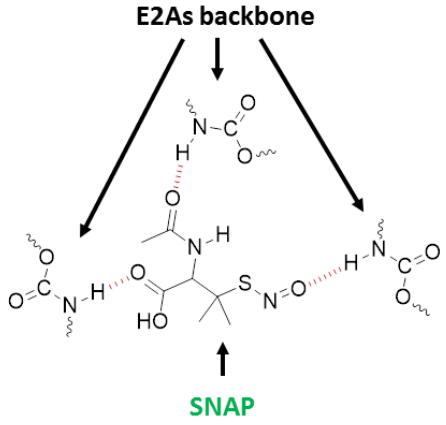

Figure 6.2. Proposed hydrogen bonding between urethane groups of the E2As backbone and SNAP.

hydrogen bonding on the stability of SNAP in E2As and other polymers. These studies may provide valuable information that will help improve and design other NO-releasing materials using the SNAP-doping approach.

The SNAP-doped E2As may also face challenges in potential clinical applications (e.g., catheter applications) because the thermal stability of SNAP may not be able to withstand the high temperatures used during conventional extrusion and manufacturing processes. One approach to overcome this issue might be a solvent swelling/impregnation method that could load existing commercial catheters with SNAP. This solvent swelling/impregnation method has been previously used to load ionophores into catheters for sensor applications,[24] but a similar methodology could be applied for SNAP loading. In this method, existing catheters or biomedical grade tubing could be swelled in an organic solvent containing SNAP. The degree of solvent swelling of the polymer tubing and the concentration of SNAP in the swelling solvent will directly affect the amount of SNAP loading that is achievable. Another approach might be to dedicate one lumen of a multi-lumen catheter to the NO release chemistry (**Figure 6.3)**. Viscous

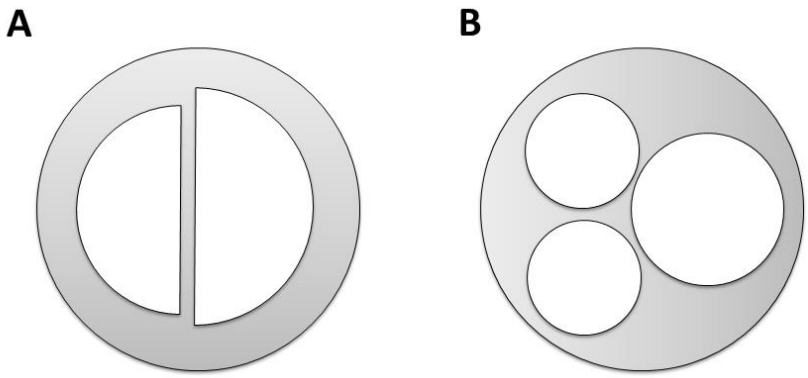

Figure 6.3. Example cross sections of dual lumen (A) and triple lumen (B) catheters, where one lumen could be dedicated to the NO-releasing polymer.

SNAP-doped polymer solutions could be used to fill one lumen of the commercial catheter, while the other lumen(s) would still be available for clinical use. The residual solvent would evaporate and create a catheter that could release NO upon exposure to physiological conditions. Nitric oxide has a greater solubility in silicone rubber than in aqueous phase,[16, 25] so this should help reduce any asymmetry in the NO release distribution. In all of these new directions, the properties (in terms of NO release

kinetics, leaching studies, stability, and potential biomedical applications) will need to be evaluated.

6.2.2 Diazeniumdiolate-Based Polymers

One concern with diazeniumdiolates, such as DBHD/N_2O_2, is the formation and leaching of some potentially carcinogenic decomposition products (e.g., *N*-nitrosamines).[14, 26] Therefore further research should include toxicity studies and monitoring any leaching of the DBHD/N_2O_2 or diamine species, as well as nitrosamine formation. Leaching of DBHD/N_2O_2 or the decomposition products should be minimal from the Elast-eon E2As polymer, due to its lipophilic nature and the low water uptake of E2As. However, if leaching is a concern with the DBHD/N_2O_2–based materials, the PLGA additives could be used along with immobilized diazeniumdiolated species, such as diazeniumdiolated diaminoalkyltrimethoxysilane cross-linked to silicone rubber (DACA-SR).[17] Other PLGAs with various hydrolysis rates could be used to further tune the NO release profiles. The stability of these polymer formulations during storage and/or sterilization should be evaluated for potential clinical applications. Long-term studies to further evaluate the hemocompatibility (e.g., catheters) and wound healing properties could then be conducted. In this dissertation work, the NO-releasing patches were applied to the infected scald burn wounds for only 1 d to observe the initial effects of NO on the infection. Further long-term studies with this burn wound model could be conducted to determine the effects of NO release on the entire wound healing process. *In vitro* biofilm studies, using a CDC flow bioreactor,[27] could also be conducted to observe the effects of NO on various bacteria strains over a 1-2 week period.

Overall, there are many opportunities to explore with respect to using and optimizing the novel SNAP- and DBHD/N_2O_2-doped polymeric materials developed in this thesis research. The NO release from these materials has the potential to improve the biocompatibility of a wide variety of biomedical devices by reducing thrombosis- and infection-related complications. Clinical application of these NO-releasing materials will have a positive impact on patients, especially in terms of reducing medical costs and saving lives.

6.3 References

1. D. A. Riccio, P. N. Coneski, S. P. Nichols, A. D. Broadnax and M. H. Schoenfisch, *ACS Appl Mater Interfaces*, **2012**, *4*, 796-804.

2. D. A. Riccio, K. P. Dobmeier, E. M. Hetrick, B. J. Privett, H. S. Paul and M. H. Schoenfisch, *Biomaterials*, **2009**, *30*, 4494-4502.

3. A. B. Seabra, R. Da Silva, G. F. P. De Souza and M. G. De Oliveira, *Artif Organs*, **2008**, *32*, 262-267.

4. A. B. Seabra, L. L. Da Rocha, M. N. Eberlin and M. G. De Oliveira, *J Pharm Sci*, **2005**, *94*, 994-1003.

5. A. B. Seabra and M. G. de Oliveira, *Biomaterials*, **2004**, *25*, 3773-3782.

6. M. M. Batchelor, S. L. Reoma, P. S. Fleser, V. K. Nuthakki, R. E. Callahan, C. J. Shanley, J. K. Politis, J. Elmore, S. I. Merz and M. E. Meyerhoff, *J Med Chem*, **2003**, *46*, 5153-5161.

7. A. B. Seabra, G. F. P. de Souza, L. L. da Rocha, M. N. Eberlin and M. G. de Oliveira, *Nitric Oxide-Biology and Chemistry*, **2004**, *11*, 263-272.

8. P. N. Coneski and M. H. Schoenfisch, *Polym Chem*, **2011**, *2*, 906-913.

9. A. B. Seabra, D. Martins, M. Simoes, R. da Silva, M. Brocchi and M. G. de Oliveira, *Artif Organs*, **2010**, *34*, E204-E214.

10. G. E. Gierke, M. Nielsen and M. C. Frost, *Sci Technol Adv Mat*, **2011**, *12*, 055007.

11. I. L. Megson, *Drug Future*, **2002**, *27*, 777-784.

12. I. L. Megson, S. Morton, I. R. Greig, F. A. Mazzei, R. A. Field, A. R. Butler, G. Caron, A. Gasco, R. Fruttero and D. J. Webb, *Br J Pharmacol*, **1999**, *126*, 639-648.

13. E. J. Brisbois, H. Handa, T. C. Major, R. H. Bartlett and M. E. Meyerhoff, *Biomaterials*, **2013**, *34*, 6957-6966.

14. K. A. Mowery, M. H. Schoenfisch, J. E. Saavedra, L. K. Keefer and M. E. Meyerhoff, *Biomaterials*, **2000**, *21*, 9-21.

15. M. G. de Oliveira, S. M. Shishido, A. B. Seabra and N. H. Morgon, *J Phys Chem A*, **2002**, *106*, 8963-8970.

16. B. J. Nablo and M. H. Schoenfisch, *Biomaterials*, **2005**, *26*, 4405-4415.

17. H. Zhang, G. M. Annich, J. Miskulin, K. Osterholzer, S. I. Merz, R. H. Bartlett and M. E. Meyerhoff, *Biomaterials*, **2002**, *23*, 1485-1494.

18. A. Koh, D. A. Riccio, B. Sun, A. W. Carpenter, S. P. Nichols and M. H. Schoenfisch, *Biosens Bioelectron*, **2011**, *28*, 17-24.

19. A. Koh, A. W. Carpenter, D. L. Slomberg and M. H. Schoenfisch, *ACS Appl Mater Interfaces*, **2013**, *5*, 7956-7964.

20. J. H. Shin, S. K. Metzger and M. H. Schoenfisch, *J Am Chem Soc*, **2007**, *129*, 4612-4619.

21. S. M. Marxer, A. R. Rothrock, B. J. Nablo, M. E. Robbins and M. H. Schoenfisch, *Chem Mater*, **2003**, *15*, 4193-4199.

22. H. Handa, E. J. Brisbois, T. C. Major, L. Refahiyat, K. A. Amoako, G. M. Annich, R. H. Bartlett and M. E. Meyerhoff, *J Mater Chem B Mater Biol Med*, **2013**, *1*, 3578-3587.

23. H. Handa, T. C. Major, E. J. Brisbois, K. A. Amoako, M. E. Meyerhoff and R. H. Bartlett, *J Mater Chem B Mater Biol Med*, **2014**, *2*, 1059-1067.

24. E. J. Fogt, P. T. Cahalan, A. Jevne and M. A. Schwinghammer, *Anal Chem*, **1985**, *57*, 1155-1157.

25. K. A. Mowery and M. E. Meyerhoff, *Polymer*, **1999**, *40*, 6203-6207.

26. G. M. Annich, J. P. Meinhardt, K. A. Mowery, B. A. Ashton, S. I. Merz, R. B. Hirschl, M. E. Meyerhoff and R. H. Bartlett, *Crit Care Med*, **2000**, *28*, 915-920.

27. W. Cai, J. Wu, C. Xi and M. E. Meyerhoff, *Biomaterials*, **2012**, *33*, 7933-7944.